

**A NEW SERIES OF RATE DECLINE RELATIONS BASED ON THE
DIAGNOSIS OF RATE-TIME DATA**

A Thesis

by

ANASTASIOS S. BOULIS

Submitted to the Office of Graduate Studies of
Texas A&M University
in partial fulfillment of the requirements for the degree of
MASTER OF SCIENCE

August 2009

Major Subject: Petroleum Engineering

**A NEW SERIES OF RATE DECLINE RELATIONS BASED ON THE
DIAGNOSIS OF RATE-TIME DATA**

A Thesis

by

ANASTASIOS S. BOULIS

Submitted to the Office of Graduate Studies of
Texas A&M University
in partial fulfillment of the requirements for the degree of

MASTER OF SCIENCE

Approved by:

Co-Chairs of Committee,	Thomas A. Blasingame
	George J. Moridis
Committee Members,	Maria A. Barrufet
	Peter P. Valko
Head of Department,	Stephen A. Holditch

August 2009

Major Subject: Petroleum Engineering

ABSTRACT

A New Series of Rate Decline Relations Based on the Diagnosis of Rate-Time Data. (August 2009)

Anastasios S. Boulis, B.E., National Technical University of Athens

Co-Chairs of Advisory Committee: Dr. Thomas A. Blasingame
Dr. George J. Moridis

The so-called "Arps" rate decline relations are by far the most widely used tool for assessing oil and gas reserves from rate performance. These relations (*i.e.*, the exponential and hyperbolic decline relations) are empirical where the starting point for their derivation is given by the definitions of the "loss ratio" and the "derivative of the loss ratio", where the "loss ratio" is the ratio of rate data to derivative of rate data, and the "derivative of the loss ratio" is the "*b*-parameter" as defined by Arps [1945].

The primary goal of this work is the interpretation of the *b*-parameter continuously over time and thus the better understanding of its character. As is shown below we propose "monotonically decreasing functional forms" for the characterization of the *b*-parameter, in addition to the exponential and hyperbolic rate decline relations, where the *b*-parameter is assumed to be zero and constant, respectively. The proposed equations are as follow: $b(t)=\text{constant}$ (Arps' hyperbolic rate-decline relation), $b(t)=b_0 \exp[-b_1 t]$ (exponential function), $b(t)=b_0 t^{-b_1}$ (power-law function), $b(t)=1/(b_0 + b_1 t)$ (rational function).

The corresponding rate decline relation for each case is obtained by solving the differential equation associated with the selected functional for the *b*-parameter. The next step of this procedure is to test and validate each of the rate decline relations by applying them to various numerical simulation cases (for gas), as well as for field data cases obtained from tight/shale gas reservoirs.

Our results indicate that *b*-parameter is never constant but it changes continuously with time. The ultimate objective of this work is to establish each model as a potential analysis/diagnostic relation. Most of the proposed models yield more realistic estimations of gas reserves in comparison to the traditional Arps' rate decline relations (*i.e.*, the hyperbolic decline) where the reserves estimates are inconsistent and over-estimated. As an example, the rational *b*-parameter model seems to be the most accurate model in terms of representing the character of rate data; and therefore, should yield more realistic reserves estimates. Illustrative examples are provided for better understanding of each *b*-parameter rate decline model.

The proposed family of rate decline relations was based on the character of the *b*-parameter computed from the rate-time data and they can be applied to a wide range of data sets, as dictated by the character of rate data.

DEDICATION

This thesis is dedicated to the memory of my grandfathers Anastasios S. Boulis and Konstantinos O.Papanikolaou as a small piece of appreciation for everything they taught me.

The roots of education are bitter, but the fruit is sweet.

— Aristotle

In the world of knowledge the idea of the good appears last of all, and is seen only with effort.

— Socrates

ACKNOWLEDGEMENTS

I want to express thanks to Dr. Tom Blasingame and Dr. George Moridis for their support and guidance during my research and graduate studies. Moreover, I would like to express my deep appreciation to Dr. Maria Barrufet and Dr. Peter Valko for serving as members of my advisory committee.

TABLE OF CONTENTS

	Page
ABSTRACT	iii
DEDICATION	v
ACKNOWLEDGEMENTS.....	vi
TABLE OF CONTENTS	vii
LIST OF FIGURES.....	x
LIST OF TABLES	xiv
 CHAPTER	
I INTRODUCTION	1
1.1 Statement of the Problem	1
1.2 Objectives.....	2
1.3 Validation.....	3
1.4 Summary and Conclusion	3
II LITERATURE REVIEW	4
III A NEW SERIES OF RATE DECLINE RELATIONS.....	5
3.1 Development of New Series of Rate Decline Relations.....	5
3.2 Validation of the New Series of Rate Decline Relations.....	6
IV SUMMARY, CONCLUSIONS, AND RECOMMENDATIONS FOR FUTURE WORK	67
4.1 Summary	67
4.2 Conclusions	67
4.3 Recommendations, Comments and Future Work.....	68
NOMENCLATURE.....	69
REFERENCES.....	71

	Page
APPENDIX A — DERIVATION OF THE RATE-DECLINE RELATIONS	74
APPENDIX B — BEHAVIOR OF THE COMPUTED b -PARAMETER FOR THE FIELD CASE EXAMPLES	84
APPENDIX C — SUMMARY OF THE b -PARAMETER MODEL RESULTS FOR THE FIELD CASE EXAMPLES	93
VITA.....	97

LIST OF FIGURES

FIGURE	Page
3.1 Numerical Simulation Case 1: History (Semi-Log) plot — Horizontal gas well with multiple transverse fractures.	7
3.2 Numerical Simulation Case 1: " q - D - b " Log-Log plot — Horizontal gas well with multiple transverse fractures — definition of the " D - and b -" parameters, b -constant case (Arps' hyperbolic rate-decline relation).....	9
3.3 Numerical Simulation Case 1: " q - D - b " Log-Log plot — Horizontal gas well with multiple transverse fractures — definition of the " D - and b -" parameters, exponential b -parameter model.	10
3.4 Numerical Simulation Case 1: " q - D - b " Log-Log plot — Horizontal gas well with multiple transverse fractures — definition of the " D - and b -" parameters, power-law b -parameter model.	11
3.5 Numerical Simulation Case 1: " q - D - b " Log-Log plot — Horizontal gas well with multiple transverse fractures — definition of the " D - and b -" parameters, rational b -parameter model.	12
3.6 Numerical Simulation Case 1: Production forecast (Semi-Log) plot — Horizontal gas well with multiple transverse fractures (all models are shown).....	14
3.7 Numerical Simulation Case 1: Production forecast (Log-Log) plot — Horizontal gas well with multiple transverse fractures (all models are shown).....	14
3.8 Numerical Simulation Case 2: History (Semi-Log) plot — Horizontal gas well.....	16
3.9 Numerical Simulation Case 2: " q - D - b " Log-Log plot — Horizontal gas well — definition of the " D - and b -" parameters, b -constant case (Arps' hyperbolic rate-decline relation).	17
3.10 Numerical Simulation Case 2: " q - D - b " Log-Log plot — Horizontal gas well — definition of the " D - and b -" parameters, exponential b -parameter model.	18
3.11 Numerical Simulation Case 2: " q - D - b " Log-Log plot — Horizontal gas well — definition of the " D - and b -" parameters, power-law b -parameter model.....	19

FIGURE	Page
3.12 Numerical Simulation Case 2: " q - D - b " Log-Log plot — Horizontal gas well — definition of the " D - and b -" parameters, rational b -parameter model.....	20
3.13 Numerical Simulation Case 2: Production forecast (Semi-Log) plot — Horizontal gas well (all models are shown).....	22
3.14 Numerical Simulation Case 2: Production forecast (Log-Log) plot — Horizontal gas well (all models are shown).	22
3.15 Numerical Simulation Case 3: History (Semi-Log) plot — Vertical unfractured gas well in a cylindrical bounded reservoir — True Radial Flow.	23
3.16 Numerical Simulation Case 3: " q - D - b " Log-Log plot — Vertical unfractured gas well in a cylindrical bounded reservoir — True Radial Flow — definition of the " D - and b -" parameters, b -constant case (Arps' hyperbolic rate-decline relation).	25
3.17 Numerical Simulation Case 3: " q - D - b " Log-Log plot — Vertical unfractured gas well in a cylindrical bounded reservoir — True Radial Flow — definition of the " D - and b -" parameters, exponential b -parameter model.....	26
3.18 Numerical Simulation Case 3: " q - D - b " Log-Log plot — Vertical unfractured gas well in a cylindrical bounded reservoir — True Radial Flow— definition of the " D - and b -" parameters, power-law b -parameter model.	27
3.19 Numerical Simulation Case 3: " q - D - b " Log-Log plot — Vertical unfractured gas well in a cylindrical bounded reservoir — True Radial Flow — definition of the " D - and b -" parameters, rational b -parameter model.	28
3.20 Numerical Simulation Case 3: Production forecast (Semi-Log) plot — Vertical unfractured gas well in a cylindrical bounded reservoir — True Radial Flow (all models are shown).	30
3.21 Numerical Simulation Case 3: Production forecast (Log-Log) plot — Vertical unfractured gas well in a cylindrical bounded reservoir — True Radial Flow (all models are shown).	30
3.22 Numerical Simulation Case 4: History (Semi-Log) plot — Vertical fractured tight gas Well (East TX).....	31

FIGURE	Page
3.23 Numerical Simulation Case 4: " q - D - b " Log-Log plot — Vertical fractured tight gas Well (East TX) — definition of the " D - and b -" parameters, b -constant case (Arps' hyperbolic rate-decline relation).	33
3.24 Numerical Simulation Case 4: " q - D - b " Log-Log plot — Vertical fractured tight gas Well (East TX) — definition of the " D - and b -" parameters, exponential b -parameter model.	34
3.25 Numerical Simulation Case 4: " q - D - b " Log-Log plot — Vertical fractured tight gas Well (East TX) — definition of the " D - and b -" parameters, power-law b -parameter model.	35
3.26 Numerical Simulation Case 4: " q - D - b " Log-Log plot — Vertical fractured tight gas Well (East TX) — definition of the " D - and b -" parameters, rational b -parameter model.	36
3.27 Numerical Simulation Case 4: " q - D - b " Log-Log plot — Vertical fractured tight gas Well (East TX) — (all models are shown).....	38
3.28 Numerical Simulation Case 4: " q - D - b " Log-Log plot — Vertical fractured tight gas Well (East TX) — (all models are shown).....	38
3.29 Field Example Case 1: History (Semi-Log) plot — Fractured well in a tight gas reservoir (LWF1 – 20/40 Proppant) (ref. Ilk <i>et al</i> [2008c]).	39
3.30 Field Example Case 1: " q - D - b " Log-Log plot — Fractured well in a tight gas reservoir (LWF1 – 20/40 Proppant) (ref. Ilk <i>et al</i> [2008c]). — definition of the " D and b " parameters, b -constant case (Arps' hyperbolic rate-decline relation).	40
3.31 Field Example Case 1: " q - D - b " Log-Log plot — Fractured well in a tight gas reservoir (LWF1 – 20/40 Proppant) (ref. Ilk <i>et al</i> [2008c]). — definition of the " D and b " parameters, exponential b -parameter model.	41
3.32 Field Example Case 1: " q - D - b " Log-Log plot — Fractured well in a tight gas reservoir (LWF1 – 20/40 Proppant) (ref. Ilk <i>et al</i> [2008c]). — definition of the " D and b " parameters, power-law b -parameter model.	42

FIGURE	Page
3.33 Field Example Case 1: " q - D - b " Log-Log plot — Fractured well in a tight gas reservoir (LWF1 – 20/40 Proppant) (ref. Ilk <i>et al</i> [2008c]). — definition of the " D and b " parameters, rational b -parameter model.	43
3.34 Field Example Case 1: Production forecast (Semi-Log) plot — Fractured well in a tight gas reservoir (LWF1 – 20/40 Proppant) (ref. Ilk <i>et al</i> [2008c]) — (all models are shown).....	45
3.35 Field Example Case 1: Production forecast (Log-Log) plot — Fractured well in a tight gas reservoir (LWF1 – 20/40 Proppant) (ref. Ilk <i>et al</i> [2008c]) — (all models are shown).....	45
3.36 Field Example Case 2: History (Semi-Log) plot — Shale gas well 1 — (ref. Mattar <i>et al</i> [2008]).	46
3.37 Field Example Case 2: " q - D - b " Log-Log plot — Shale gas well 1 — (ref. Mattar <i>et al</i> [2008]) — definition of the " D and b " parameters, b -constant case (Arps' hyperbolic rate-decline relation).	47
3.38 Field Example Case 2: " q - D - b " Log-Log plot — Shale gas well 1 — (ref. Mattar <i>et al</i> [2008]) — definition of the " D and b " parameters, exponential b -parameter model.	48
3.39 Field Example Case 2: " q - D - b " Log-Log plot — Shale gas well 1 — (ref. Mattar <i>et al</i> [2008]) — definition of the " D and b " parameters, power-law b -parameter model.....	49
3.40 Field Example Case 2: " q - D - b " Log-Log plot — Shale gas well 1 — (ref. Mattar <i>et al</i> [2008]) — definition of the " D and b " parameters, rational b -parameter model.	50
3.41 Field Example Case 2: Production forecast (Semi-Log) plot — Shale gas well 1 — (ref. Mattar <i>et al</i> [2008]) — (all models are shown).....	52
3.42 Field Example Case 2: Production forecast (Log-Log) plot — Shale gas well 1 — (ref. Mattar <i>et al</i> [2008]) — (all models are shown).....	52
3.43 Field Example Case 3: History (Semi-Log) plot — Fractured well in a tight gas reservoir (LWF2 – 40/70 Proppant) (ref. Ilk <i>et al</i> [2008c]).	53
3.44 Field Example Case 3: " q - D - b " Log-Log plot — Fractured well in a tight gas reservoir (LWF2 – 40/70 Proppant) (ref. Ilk <i>et al</i> [2008c]). — definition of the " D and b " parameters, b -constant case (Arps' hyperbolic rate-decline relation).	54

FIGURE	Page
3.45 Field Example Case 3: " q - D - b " Log-Log plot — Fractured well in a tight gas reservoir (LWF2 – 40/70 Proppant) (ref. Ilk <i>et al</i> [2008c]). — definition of the " D and b " parameters, exponential b -parameter model.	55
3.46 Field Example Case 3: " q - D - b " Log-Log plot — Fractured well in a tight gas reservoir (LWF2 – 40/70 Proppant) (ref. Ilk <i>et al</i> [2008c]). — definition of the " D and b " parameters, power-law b -parameter model.	56
3.47 Field Example Case 3: " q - D - b " Log-Log plot — Fractured well in a tight gas reservoir (LWF2 – 40/70 Proppant) (ref. Ilk <i>et al</i> [2008c]). — definition of the " D and b " parameters, rational b -parameter model.	57
3.48 Field Example Case 3: Production forecast (Semi-Log) plot — Fractured well in a tight gas reservoir (LWF2 – 40/70 Proppant) (ref. Ilk <i>et al</i> [2008c]) — (all models are shown).	59
3.49 Field Example Case 3: Production forecast (Log-Log) plot — Fractured well in a tight gas reservoir (LWF2 – 40/70 Proppant) (ref. Ilk <i>et al</i> [2008c]) — (all models are shown).	59
3.50 Field Example Case 4: History (Semi-Log) plot — Shale gas well 2 — (ref. Mattar <i>et al</i> [2008]).	60
3.51 Field Example Case 4: " q - D - b " Log-Log plot — Shale gas well 2 — (ref. Mattar <i>et al</i> [2008]) — definition of the " D and b " parameters, b -constant case (Arps' hyperbolic rate-decline relation).	61
3.52 Field Example Case 4: " q - D - b " Log-Log plot — Shale gas well 2 — (ref. Mattar <i>et al</i> [2008]) — definition of the " D and b " parameters, exponential b -parameter model.	62
3.53 Field Example Case 4: " q - D - b " Log-Log plot — Shale gas well 2 — (ref. Mattar <i>et al</i> [2008]) — definition of the " D and b " parameters, power-law b -parameter model.	63
3.54 Field Example Case 4: " q - D - b " Log-Log plot — Shale gas well 2 — (ref. Mattar <i>et al</i> [2008]) — definition of the " D and b " parameters, rational b -parameter model.	64
3.55 Field Example Case 4: Production forecast (Semi-Log) plot — Shale gas well 2 — (ref. Mattar <i>et al</i> [2008]) — (all models are shown).	66

FIGURE	Page
3.56 Field Example Case 4: Production forecast (Log-Log) plot — Shale gas well 2 — (ref. Mattar <i>et al</i> [2008]) — (all models are shown).....	66

LIST OF TABLES

TABLE	Page
3.1 Reservoir and fluid properties for the Numerical Simulation Case 1 — Horizontal gas well with multiple transverse fractures in a rectangular-bounded gas reservoir (SPE 119897 Data).	8
3.2 Production forecasts of the Numerical Simulation Case 1 — Horizontal gas well with multiple transverse fractures (SPE 119897 Data).	13
3.3 Reservoir and fluid properties for the Numerical Simulation Case 2 — Horizontal gas well.	15
3.4 Production forecasts of the Numerical Simulation Case 2 — Horizontal gas well.....	21
3.5 Reservoir and fluid properties for the Numerical Simulation Case 3 — Vertical unfractured gas well in a cylindrical bounded reservoir — True Radial Flow.	24
3.6 Production forecasts of the Numerical Simulation Case 3 — Vertical unfractured gas well in a cylindrical bounded reservoir — True Radial Flow.	29
3.7 Reservoir and fluid properties for the Numerical Simulation Case 4 — Vertical fractured tight gas well (East TX).....	32
3.8 Production forecasts of the Numerical Simulation Case 4 — Vertical fractured tight gas well (East TX).	37
3.9 Production forecasts of the Field Case 1 — Fractured well in a tight gas reservoir (LWF1 – 20/40 Proppant) (ref. Ilk <i>et al</i> [2008c]).	44
3.10 Production forecasts of the Field Case 2 — Shale gas well 1 — (ref. Mattar <i>et al</i> [2008]).	51
3.11 Production forecasts of the Field Case 3 — Fractured well in a tight gas reservoir (LWF2 – 40/70 Proppant) (ref. Ilk <i>et al</i> [2008c]).	58
3.12 Production forecasts of the Field Case 4 — Shale gas well 2 (Mattar <i>et al</i> [2008]).	65

CHAPTER I

INTRODUCTION

1.1. Statement of the Problem

Decline curve analysis is one of the primary tools, which is practiced by the petroleum engineers to estimate reserves in oil and gas wells. The widespread use of decline curve analysis is due to the simplicity of the exponential and hyperbolic rate-decline equations as introduced by Arps (Arps [1945]). Exponential and hyperbolic rate-decline equations are empirical relations based on observations of the well performance data and are only applicable for the boundary-dominated flow. These relations can be derived by using the so-called "loss-ratio" and the "derivative of the loss-ratio" definitions as proposed by Johnson and Bollens [1928] and later by Arps [1945].

Definition of the Loss-Ratio:

$$a \equiv \frac{1}{D} \equiv -\frac{q}{dq/dt} \dots\dots\dots (1.1)$$

Derivative of the Loss Ratio:

$$b \equiv \frac{d}{dt} [a] \equiv \frac{d}{dt} \left[\frac{1}{D} \right] \equiv -\frac{d}{dt} \left[\frac{q}{dq/dt} \right] \dots\dots\dots (1.2)$$

For reference, we present the derivations for the exponential and hyperbolic rate-decline cases in **Appendix A**. As mentioned earlier, exponential rate-decline case can be derived theoretically; for the case of constant compressibility liquid in a closed reservoir flowing at a constant wellbore flowing pressure during boundary-dominated flow conditions. To our knowledge there is no "theoretical" derivation for the hyperbolic rate-decline case. The hyperbolic rate-decline relation is obtained by assuming a constant value for the b -parameter in **Eq. 1.2** and solving the associated differential equations.

In this work, we focus on the estimation of reserves in gas wells using only rate-time data. The common practice in the industry for reserves estimation is to use the hyperbolic rate-decline relation. However, our observations indicate that gas well performance behavior does not exhibit a constant b -parameter data trend when b -parameter is computed using rate-time data as dictated by **Eq. 1.2**. Despite this observation, it is still possible to use the hyperbolic rate-decline relation by using conservative values for the b -parameter ($0 < b < 1$) or using variations of hyperbolic rate decline relations (see Kupchenko *et al* [2008]).

The main issue is that the use of hyperbolic rate-decline relation could be applicable for conventional gas reservoirs. But, when production data from tight gas sand and shale gas wells are assessed using the hyperbolic rate-decline relation, the identification of a "reasonable" b -parameter is in fact really difficult due to the very long transient period. In practice we often observe b -parameter values higher than 1.0 — particularly, to the onset of true boundary-dominated flow. This situation results in the over-estimation of reserves by errors more than 100 percent (see the recent study by Rushing *et al* [2007] on assessing the validity of using Arps' hyperbolic rate-decline relation).

There are also other methodologies which require flowing bottom-hole pressure data in addition to flowrate data for analyzing well performance to estimate reservoir properties and obtain gas-in-place. These methodologies are classified as the "modern decline analysis (decline type curves)" or "rate-transient analysis" techniques and they are based on the analytical solutions for several well/reservoir configurations (see Fetkovich [1980], Palacio and Blasingame [1993], Doublet *et al* [1994], Agarwal [1998], and Amini *et al* [2007] for details). Although, using "modern decline analysis" is more favorable, the flowing bottomhole pressure data may not available for every case and also for complex well/reservoir configurations (*e.g.*, horizontal wells with multiple transverse fractures) the analytical solution may not be available. Under these circumstances the need for a practical method in addition to hyperbolic rate-decline is obvious to estimate reserves in tight gas sand and shale gas reservoirs. In this work, we propose to model the computed b -parameter trend from rate-time data according to **Eq. 1.2** using several (continuous) functions. The solution of each corresponding differential equation yields the "empirical" rate-decline relation for each case and we test the performance of each rate-decline relation using simulated data and field data obtained from tight gas and shale gas wells.

1.2. Objectives

The objectives of this work are:

- To *prove* that the b -parameter is not constant (contrary to the hyperbolic rate-decline relation), but changes as a function of time.
- To *provide* a diagnostic understanding of the b -parameter (*i.e.*, the behavior of the computed b -parameter data trend for several different cases).
- To *propose* a series of new rate-decline relations based on the characterization of the computed b -parameter trend.
- To *demonstrate* the applicability of our new rate decline relations using both synthetic and field data.

1.3. Validation

To validate the models we have used data sets generated by numerical simulations covering a satisfactory range of different gas reservoir/well cases. In particular the simulation cases that have been used for the validation of the new rate-decline relations are the following:

- Horizontal Gas Well with Multiple Transverse Fractures (SPE 119897 Data).
- Horizontal Gas Well.
- Vertical Unfractured Gas Well in a Cylindrical Bounded Reservoir — True Radial Flow
- Vertical Fractured Tight Gas Well (East TX) (Ilk *et al* [2008a])

Moreover, we demonstrate the application of the new rate-decline relations to field case data. In this work the data was obtained from the following gas wells:

- Fractured Gas Well in a Tight Gas Sand Reservoir (LWF1 — 20/40 Proppant) (Ilk *et al* [2008c]).
- Shale Gas Well (Gas Well 1 — Barnett Shale) (Mattar *et al* [2008]).
- Fractured Gas Well in a Tight Gas Sand Reservoir (LWF2 — 40/70 Proppant) (Ilk *et al* [2008c])
- Shale Gas Well (Gas Well 2 — Barnett Shale) (Mattar *et al* [2008])

1.4 Summary and Conclusion

This study documents the evaluation of the computed b -parameter as a continuous function of time using several models. We propose three new models in addition to the Arps' rate decline relation and evaluate the performance of the models using synthetic and field cases. We present four synthetic and four field examples to achieve our objective.

First and foremost, the computation of the b -parameter indicates that the b -parameter is not constant as opposed to Arps' rate decline relation. Therefore, from an empirical standpoint we conclude that the computed b -parameter could be modeled by continuous functions. We explore the use of the three models and show in this work that each model has certain characteristics and applicable to a variety of conditions.

It is worth to mention that each model has advantages and disadvantages and the performance of the models vary under specific circumstances. We conclude that all models should be used in conjunction to yield better resolution and to decrease the uncertainty.

CHAPTER II

LITERATURE REVIEW

Analysis of production data can be categorized into the following: empirical methods and semi-analytical/analytical methods. In this section we will only discuss the empirical methods which make use of rate-time data to estimate gas reserves. The definition of the "loss-ratio" by Johnson and Bollens [1928] and later by Arps [1945] lays the foundation for the traditional decline curve analysis (*i.e.*, empirical exponential and hyperbolic rate-decline relations). Arps suggested that the values for the b -parameter should fall between zero and one for the hyperbolic rate-decline relation but did not discuss the possibility of the value of the b -parameter for greater than one. Fetkovich *et al* (Fetkovich *et al* [1996]) discussed the relationships between the b -parameter and various kinds of reservoir heterogeneities and drive mechanisms. However, the work by Fetkovich *et al* did not indicate a b -parameter value greater than one.

As mentioned earlier for unconventional gas reservoirs the value of the b -parameter could exceed one when hyperbolic rate-decline relation is applied. Maley (Maley [1985]) investigated the application of traditional decline curve analysis to tight gas reservoirs and documented cases from the Lower Cotton Valley tight gas sands with b -parameter values greater than one. In a recent study by Rushing *et al* (Rushing *et al* [2007]), it was indicated that the value of the b -parameter would generally fall between 0.5 and 1 for various reservoir and hydraulic fracture heterogeneities. It was also observed that the values of the b -parameter greater than one indicated transient or transitional flow rather than true boundary-dominated flow regime. Kupchenko *et al* (Kupchenko *et al* [2008]) discussed the application of a piecewise hyperbolic rate-decline relation to take the transient/transitional flow regimes into account and to prevent the over-estimation of reserves.

Recently Ilk *et al* (Ilk *et al* [2008a] and Ilk *et al* [2008b]) introduced the "power-law exponential" rate-decline model to estimate gas reserves. The basis of this model is to compute the D -parameter according to **Eq. 1.1** and to model the computed D -parameter trend with a power-law equation with a constant at late times. The work by Mattar *et al* (Mattar *et al* [2008]) considered the application of the power-law exponential rate-decline model to shale gas wells. The results verified that not only the power-law exponential rate-decline model was very flexible enough to match transient, transition, and boundary-dominated flow data, but also it yielded consistent and reasonable reserves estimates. To our knowledge, this is a new attempt to model/characterize the loss-ratio and consequently the derivative of the loss-ratio with a continuous function rather than a constant. In addition to the work by Ilk *et al*, Valko (Valko [2008]) presented another form of power-law exponential model to forecast the production of unconventional gas reservoirs.

CHAPTER III

A NEW SERIES OF RATE-DECLINE RELATIONS

3.1. Development of New Series of Rate Decline Relations

As mentioned earlier our primary objective in this work is to characterize the computed b -parameter trend and develop the corresponding the rate-decline relation according to each b -parameter model. In addition to constant b -parameter model — yielding the hyperbolic rate-decline relation — we propose three "continuous" functions to model the b -parameter trend. Our rationale behind developing various models is that we believe that only one model for the b -parameter is not enough to characterize the b -parameter for different conditions (*e.g.* different well/reservoir configurations). We note that the models we are proposing are empirical based on our observations of rate-time data.

The models for characterizing the b -parameter are:

- $b(t) = \text{constant}$ (Arps' hyperbolic rate-decline relation)
- $b(t) = b_0 \exp[-b_1 t]$ (exponential function)
- $b(t) = b_0 t^{-b_1}$ (power-law function)
- $b(t) = 1/(b_0 + b_1 t)$ (rational function)

We derive the corresponding rate-decline relation associated with each model in **Appendix A**. For orientation, we present the rate-decline relations for each model as follows:

- $b(t) = \text{constant}$ (this yields the hyperbolic rate-decline relation.)

$$q = q_i \frac{1}{[1 + bD_i t]^{1/b}} \dots\dots\dots (3.1)$$

- $b(t) = b_0 \exp[-b_1 t]$

$$q(t) = q_i \left[-b_0 D_i + (b_1 + b_0 D_i) e^{b_1 t} \right]^{\frac{-D_i}{b_1 + b_0 D_i}} \frac{D_i}{b_1} \frac{1}{b_1 + b_0 D_i} \dots\dots\dots (3.2)$$

- $b(t) = b_0 t^{-b_1}$

$$q(t) = q_i \exp \left[\frac{(-1 + b_1)(b_1 - D_i) t^{b_1}}{b_0 b_1^2} \right] \dots\dots\dots (3.3)$$

- $b(t) = 1/(b_0 + b_1 t)$

$$q(t) = q_i \frac{\exp\left[-\exp\left[-b_1\left[-\frac{\ln(b_0)}{b_1} + \frac{1}{D_i}\right]\right] E_1\left[b_1\left[-\frac{\ln(b_0)}{b_1} + \frac{1}{D_i}\right] + \ln(b_0 + b_1 t)\right]\right]}{\exp\left[-\exp\left[-b_1\left[-\frac{\ln(b_0)}{b_1} + \frac{1}{D_i}\right]\right] E_1\left[b_1\left[-\frac{\ln(b_0)}{b_1} + \frac{1}{D_i}\right] + \ln(b_0)\right]\right]} \dots\dots\dots (3.4)$$

In the equations above, b , b_0 , b_1 are model parameters defined in each b -parameter model and D_i , q_i are the model parameters obtained from the solution of the corresponding differential equation for the rate function. We present the application and performance of each model in the next sections. We note the performance of each model can vary according to different well performance data. Therefore, it is our contention that all the proposed models should be applied at the same time. We also develop a step by step procedure for the application of the models. The procedure is given as:

1. Collect rate-time data.
2. Carefully edit the spurious data from the dataset.
3. Compute the D - and b -parameters by numerical differentiation according to **Eqs. 1.1** and **1.2**. We use the "Bourdet algorithm" (Bourdet [1989]) for numerical differentiation.
4. We also compute the D - and b -parameters by using rate-cumulative data according to the equations given below.

$$\frac{1}{D} \equiv -\frac{dq}{dQ} \dots\dots\dots (3.5)$$

$$b \equiv q \frac{d}{dQ} \left[\frac{1}{D} \right] \dots\dots\dots (3.6)$$

5. Plot the " q - D - b " data and apply each b -parameter model to data set. We do not recommend a statistical approach (*i.e.*, regression) to find the model parameters. Instead, we visually obtain the optimum matches for each model.
6. Compute the cumulative production as depicted by the model (this is done numerically for the proposed models) and forecast the production.

3.2. Validation of the New Series of Rate Decline Relations

In this section, as a mechanism for validation, we validate our proposed models for the b -parameter by making use of data sets generated by numerical simulation. We note that we use different reservoir configurations and reservoir fluid characteristics for our simulations.

Numerical Simulation Cases

Case 1: Horizontal Gas Well with Multiple Transverse Fractures (SPE 119897 Data)

This case considers a horizontal gas well having multiple transverse fractures (see **Fig. 3.1** for rate and cumulative gas production versus time). The original data was earlier analyzed using the "power-law exponential" rate-decline model in the work by Mattar *et al* (Mattar *et al* [2008]).

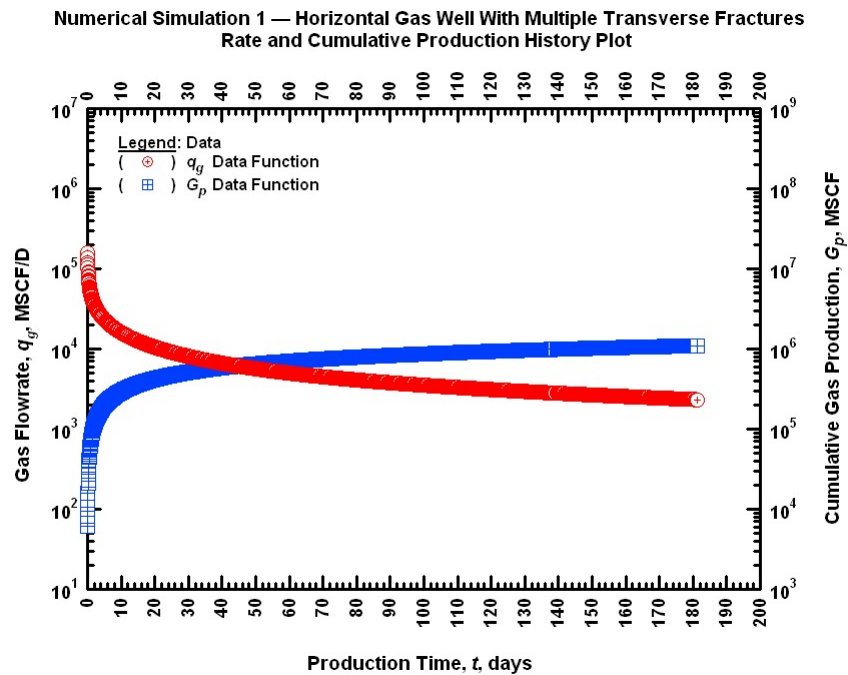


Figure 3.1 — Numerical Simulation Case 1: History (Semi-Log) plot — Horizontal gas well with multiple transverse fractures.

The model parameters and reservoir/fluid properties are provided in **Table 3.1**. It should be noted that this well is producing in a (bounded) rectangular reservoir and boundary effects are observed during late times of the production.

Table 3.1 — Reservoir and fluid properties for the numerical simulation case 1 — Horizontal gas well with multiple transverse fractures in a rectangular-bounded gas reservoir (SPE 119897 Data).

<i>Reservoir Properties:</i>	
Net pay thickness, h	= 30 ft
Permeability in x -direction, k_x	= 0.1 md
Permeability in y -direction, k_y	= 0.1 md
Permeability in z -direction, k_z	= 0.1 md
Wellbore radius, r_w	= 0.30 ft
Formation compressibility, c_f	= 1×10^{-9} 1/psi
Porosity, ϕ	= 0.1 (fraction)
Initial reservoir pressure, p_i	= 5000 psia
Wellbore storage coefficient, C_D	= 0 (dimensionless)
Gas saturation, S_g	= 1.0 (fraction)
Skin factor, s	= 0 (dimensionless)
Reservoir temperature, T_r	= 212 °F
Drainage area (2x1 Rect.), A	= 184 acres
<i>Fluid Properties:</i>	
Gas specific gravity, γ_g	= 0.65 (air = 1)
<i>Horizontal Well Model Parameters:</i>	
Horizontal well length, L_h	= 2500 ft
Position of horizontal well, z_w	= 15 ft
<i>Hydraulically Fracture Model Parameters:</i>	
Number of fractures	= 4
Fracture half-length, x_f	= 500 ft
Fracture width, w_f	= 0.79 inches
Fracture conductivity, F_{cD}	= Infinite (dimensionless)
Fracture spacing	= 500 ft
<i>Production Parameters:</i>	
Flowing pressure, p_{wf}	= 1000 psia
Producing time, t	= 700 days

We start by applying the hyperbolic rate-decline relation to data (Arps' equation, b =constant model). But, before the application we emphasize the end-point effects caused by the numerical differentiation algorithm at late times — therefore, the end-point effects should not be seen as a feature exhibited by data. We also note that the computed b -parameter data trend exhibits a declining behavior (as opposed to constant) and the computed D -parameter trend exhibits a straight line behavior (on log-log scale).

Our objective is not to find the "best-fit" according to each model. But, rather we use the three models in conjunction and force the same maximum cumulative production value for each case. For the hyperbolic rate-decline case we usually set the b value to an average value of the data trend (for this specific case, this value is set to 0.99 as depicted by data trend at late times).

For this case we set $b=0.99$, this gives us a fair match with the rate data and the hyperbolic rate-decline relation. **Fig. 3.2** presents the q - D - b plot for the constant b case. It can be clearly seen from the plot that the constant b -parameter model has provided us with poor matches especially for the transient and transitional flow regimes. Satisfactory matches are obtaining for the case of the D -parameter and the production rate in the boundary dominated flow regime. Overall, we can conclude that this model can be applicable only for the boundary dominated flow and as we will present below, it will eventually over-estimate the actual reserves. Our next task is to apply the exponential b -parameter trend to the computed b -parameter data.

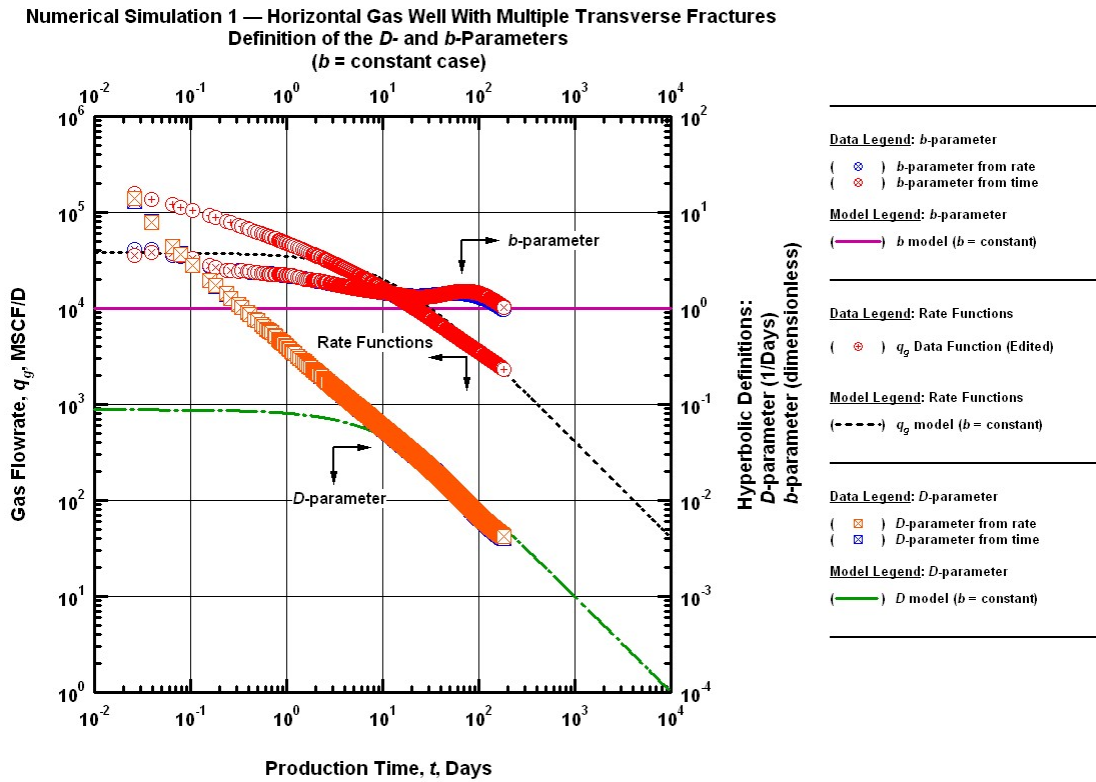


Figure 3.2 — Numerical Simulation Case 1: " q - D - b " Log-Log plot — Horizontal gas well with multiple transverse fractures — definition of the " D - and b -" parameters, b -constant case (Arps' hyperbolic rate-decline relation).

The exponential b -parameter model can be more useful than the constant b model as the model indicates that at late times the decline trend is exponential. In fact it might be reasonable to assume to use an exponential decline when boundary-dominated flow regime is reached. The issue with the exponential b -parameter model is that at early/middle times, this relation is not sufficient to model transient/transitional flow. Therefore, the match of the rate data model with the exponential b -parameter model may not be adequate for all cases. **Fig. 3.3** presents the q - D - b plot for the exponential b -parameter model case. We note the early time data are not modeled by the relation. However, the overall match of the rate data with the model is good not only for the boundary dominated flow but for the transitional flow regime as well. The next model that we applied is the power-law model.

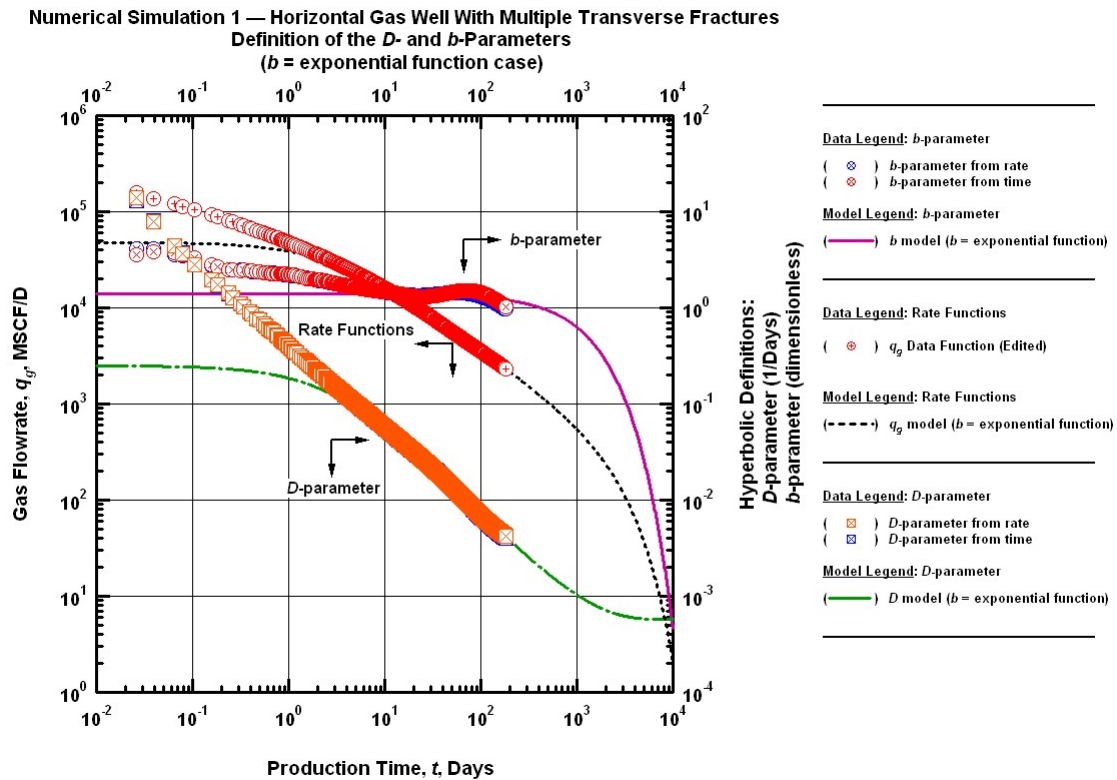


Figure 3.3 — Numerical Simulation Case 1: " q - D - b " Log-Log plot — Horizontal gas well with multiple transverse fractures — definition of the " D - and " b -" parameters, exponential b -parameter model.

Our next step is to apply the power-law b -parameter model. The computed b -parameter data trend indicates a straight line behavior on the log-log scale (see the q - D - b plot, **Fig. 3.4**). As a result, the power-law b -parameter model should be a good candidate for estimating reserves in this case. We match the computed b -parameter data with the power-law model and observe a very good match. Consequently, D -parameter data and rate data matches are excellent (except for the early and late times — end point effects). Moreover, we expect satisfactory matches with the production rate/cumulative data and thus very accurate production forecasts.

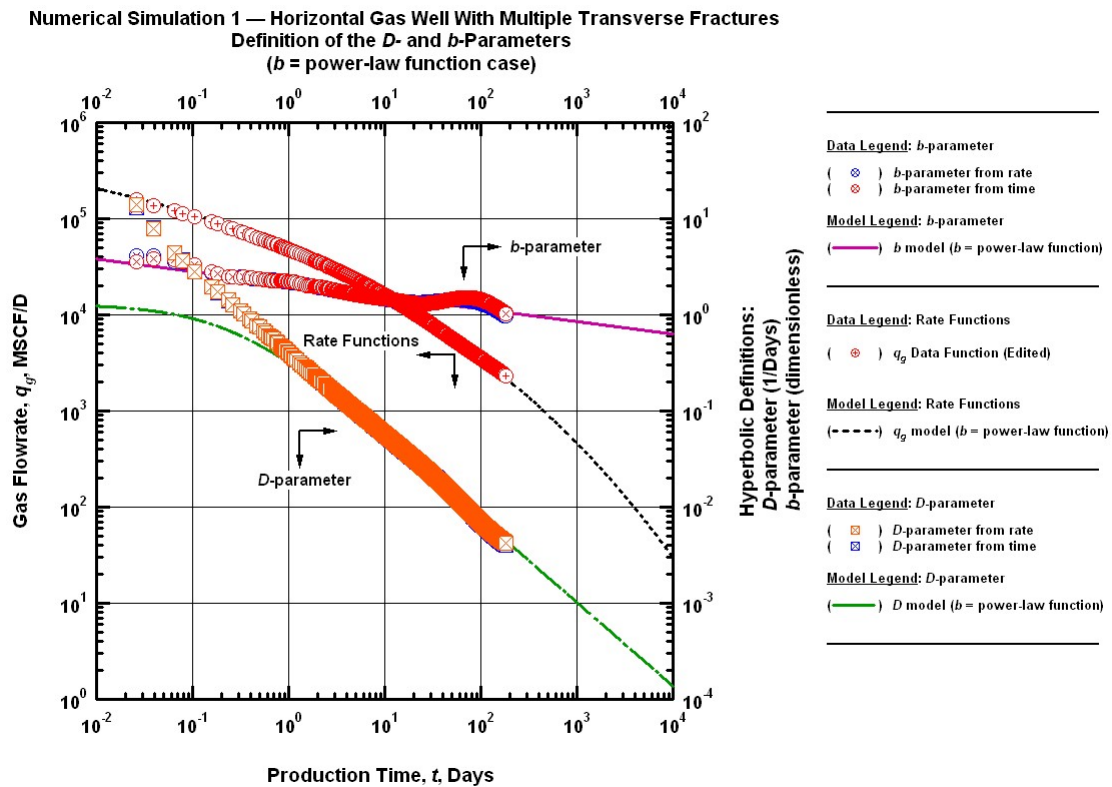


Figure 3.4 — Numerical Simulation Case 1: " q - D - b " Log-Log plot — Horizontal gas well with multiple transverse fractures — definition of the " D - and b -" parameters, power-law b -parameter model.

Finally we apply the rational b -parameter model to the computed b -parameter data trend. The rational b -parameter model is similar to the exponential b -parameter model in terms of modeling the b -parameter data (i.e., constant b at early times followed by a decline). We also note that the declining part of the b -parameter data trend can easily be modeled by the exponential and rational models. However, these models can not capture the early-time part of the data due to their nature. It can also be mentioned that the rational b -parameter model is more flexible than the exponential b -parameter model. For this case, we have a fair match of the computed b -parameter data trend with the model. The matches of D -parameter and rate data with the model are also similar to the exponential b -parameter case. **Fig. 3.5** illustrates the application of the rational b -parameter model for this case.

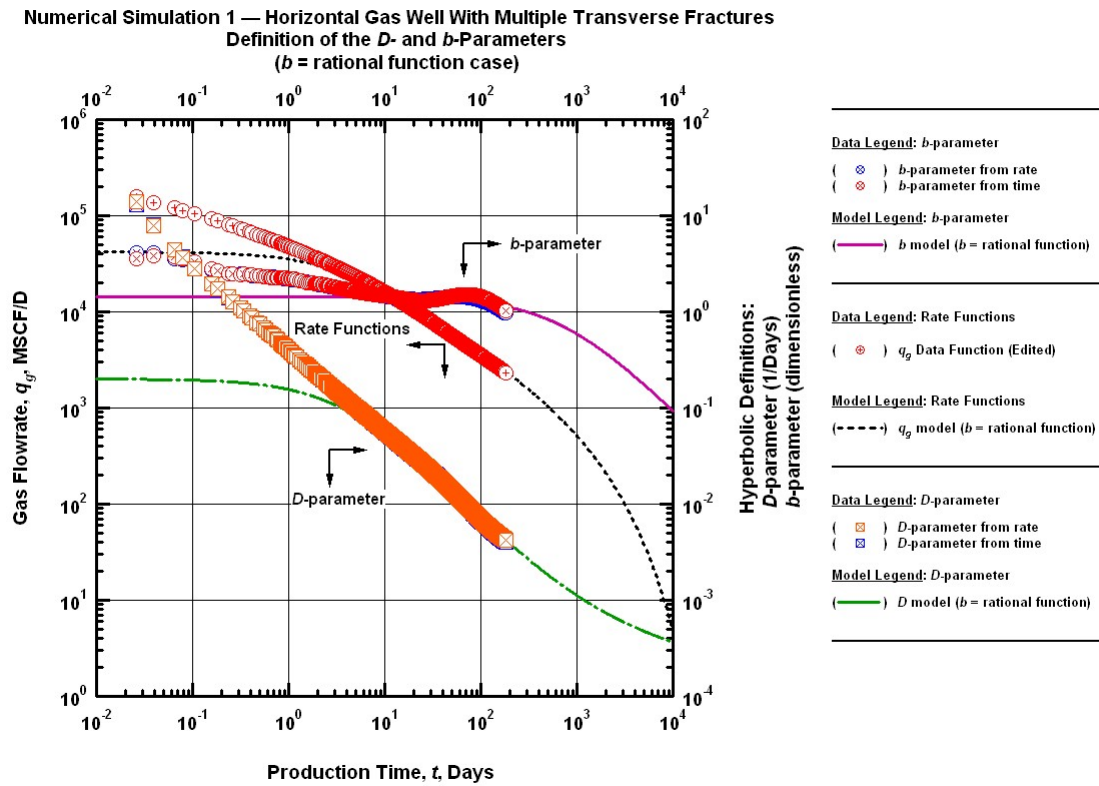


Figure 3.5 — Numerical Simulation Case 1: " q - D - b " Log-Log plot — Horizontal gas well with multiple transverse fractures — definition of the " D - and b -" parameters, rational b -parameter model.

Application of the New Rate Decline Relations — Production Forecasts

In the section that follows, we provide a diagnostic validation of the new rate decline relations that we have demonstrated above in terms of production forecasts. The two illustrative examples which are provided below represent the production rate/cumulative forecasts presented in log- and semi-log plots. The cumulative production was calculated numerically.

In **Figs. 3.6** and **3.7** below we present the schematic plots of the production rate (q) and the cumulative production (G_p) with time in a log-log and semi-log plot respectively for the numerical simulation case 1 (Horizontal Well with Multiple Transverse Fractures). The dotted lines represent the performance of the newly proposed models as well as the classical Arps' hyperbolic rate decline relation. By observing the log-log plot (**Fig. 3.7**), we immediately note that the typical and widely used, hyperbolic rate decline relation of Arps yields highest estimates of gas reserves. More specifically, as it is shown in the **Table 3.2** of the production forecasts below, we can see that Arps' model overestimates more than two times the original gas in place, while the new models give remarkable results and extremely consistent forecasts (see **Table 3.2**).

Table 3.2 — Production forecasts of the Numerical Simulation Case 1: Horizontal gas well with multiple transverse fractures (SPE 119897 Data).

Production Forecasts:

$b(t)=\text{constant (base)}$	=	6.40 BSCF
$b(t)=\text{exponential function}$	=	2.67 BSCF
$b(t)=\text{power law function}$	=	2.67 BSCF
$b(t)=\text{rational function}$	=	2.67 BSCF

Original Gas In Place (OGIP): 2.67 BSCF

Although all of the new models give more accurate estimates than the classical b -constant model, it is clear by observing the log-log plot (**Fig. 3.7**) that only the power-law model can totally capture the production trend throughout the flow regimes, since it is the only model which provided us such an exceptional match with the computed b -parameter data. The rest of the models have failed to match with the production data especially at the early times of the transient flow as a result of the poor matches with the computed data. This fact can be used in order to show the importance of the correct evaluation of the b -parameter and the huge impact that has on the production forecasts.

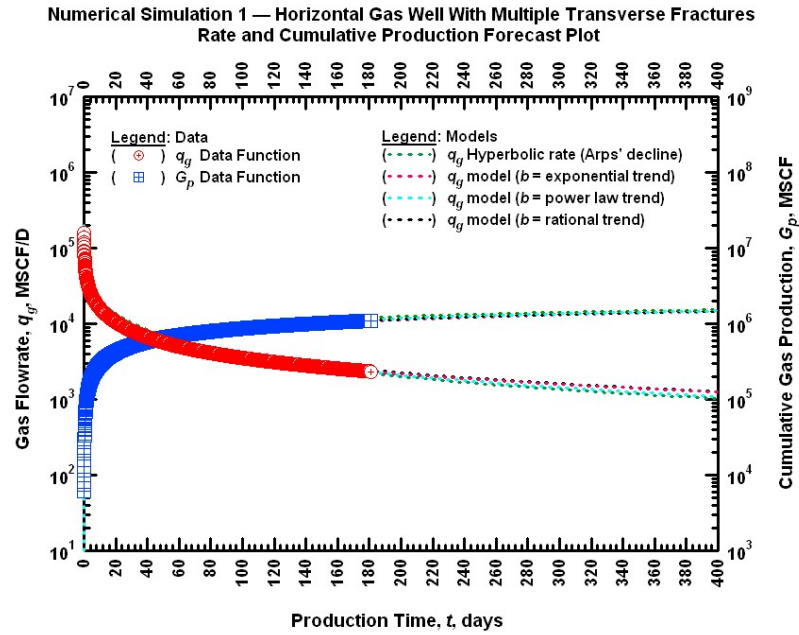


Figure 3.6 — Numerical Simulation Case 1: Production forecast (Semi-Log) plot — Horizontal gas well with multiple transverse fractures (all models are shown).

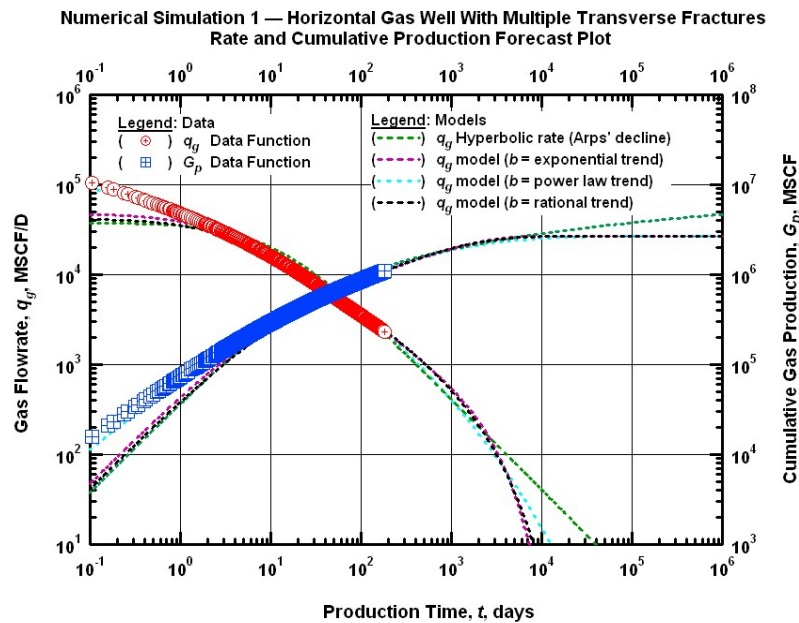


Figure 3.7 — Numerical Simulation Case 1: Production forecast (Log-Log) plot — Horizontal gas well with multiple transverse fractures (all models are shown).

Case 2: Horizontal Gas Well

In this case we consider a horizontal gas well. We generate the synthetic rate performance using a numerical simulator. The model parameters and reservoir/fluid properties are provided in **Table 3.3**. It should be noted that this well is producing in a (bounded) rectangular reservoir and boundary effects are observed during late times of the production. **Fig. 3.8** presents the summary history plot for this case (rate and cumulative gas production versus time). A visual inspection of the data suggests that boundary-dominated flow has been established (*i.e.*, straight line rate data behavior at late times on semi-log scale).

Table 3.3 — Reservoir and fluid properties for the numerical simulation case 2 — Horizontal gas well.

<i>Reservoir Properties:</i>	
Net pay thickness, h	= 100 ft
Permeability in x -direction, k_x	= 0.295 md
Permeability in y -direction, k_y	= 0.295 md
Permeability in z -direction, k_z	= 0.295 md
Wellbore radius, r_w	= 0.30 ft
Formation compressibility, c_f	= 4×10^{-6} 1/psi
Porosity, ϕ	= 0.1 (fraction)
Initial reservoir pressure, p_i	= 5000 psia
Wellbore storage coefficient, C_D	= 0 (dimensionless)
Gas saturation, S_g	= 1.0 (fraction)
Skin factor, s	= 0 (dimensionless)
Reservoir temperature, T_r	= 300 °F
Drainage area (1x1 Square), A	= 23 acres
<i>Fluid Properties:</i>	
Gas specific gravity, γ_g	= 0.7 (air = 1)
<i>Horizontal Well Model Parameters:</i>	
Horizontal well length, L_h	= 500 ft
Position of horizontal well, z_w	= 25 ft
<i>Production Parameters:</i>	
Flowing pressure, p_{wf}	= 100 psia
Producing time, t	= 3650 days

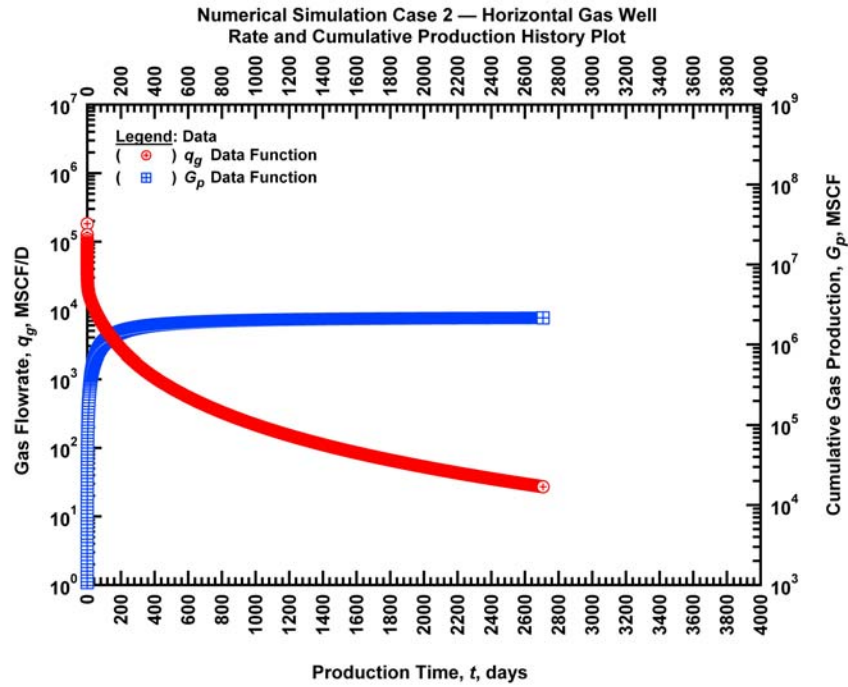


Figure 3.8 — Numerical Simulation Case 2: History (Semi-Log) plot — Horizontal gas well.

Before applying the proposed models to the data set, we inspect the computed b -parameter data trend. In this case the computed b -parameter data indicates a different behavior — at very early times b -parameter data trend exhibits an increasing trend then starts to decline and later stabilizes, then again shows a decreasing trend and finally stabilizes during complete boundary-dominated flow regime (end-point effects are not taken into account). We attribute these changes to the various flow regimes encountered in the case of a horizontal well.

At late times the computed b -parameter data trend stabilizes at approximately 0.4 (see **Fig. 3.9**). Therefore, we use this value in the application of the Arps' hyperbolic rate-decline relation (constant b -parameter case). It is apparent that there is a very good match for the boundary-dominated flow data with the hyperbolic rate-decline relation (after 100 days). This case suggests that if the complete boundary-dominated flow regime is reached, then it is possible to estimate the reserves with the hyperbolic rate-decline relation by computing the b -parameter using rate-time data. On the other hand, we acknowledge that this is a special case and for most of the unconventional gas reservoir applications it is very difficult to identify the onset of the boundary-dominated flow regime. In this case as well we observe the weakness of this model to fully capture the trend of the computed data at the transient/transitional flow regimes.

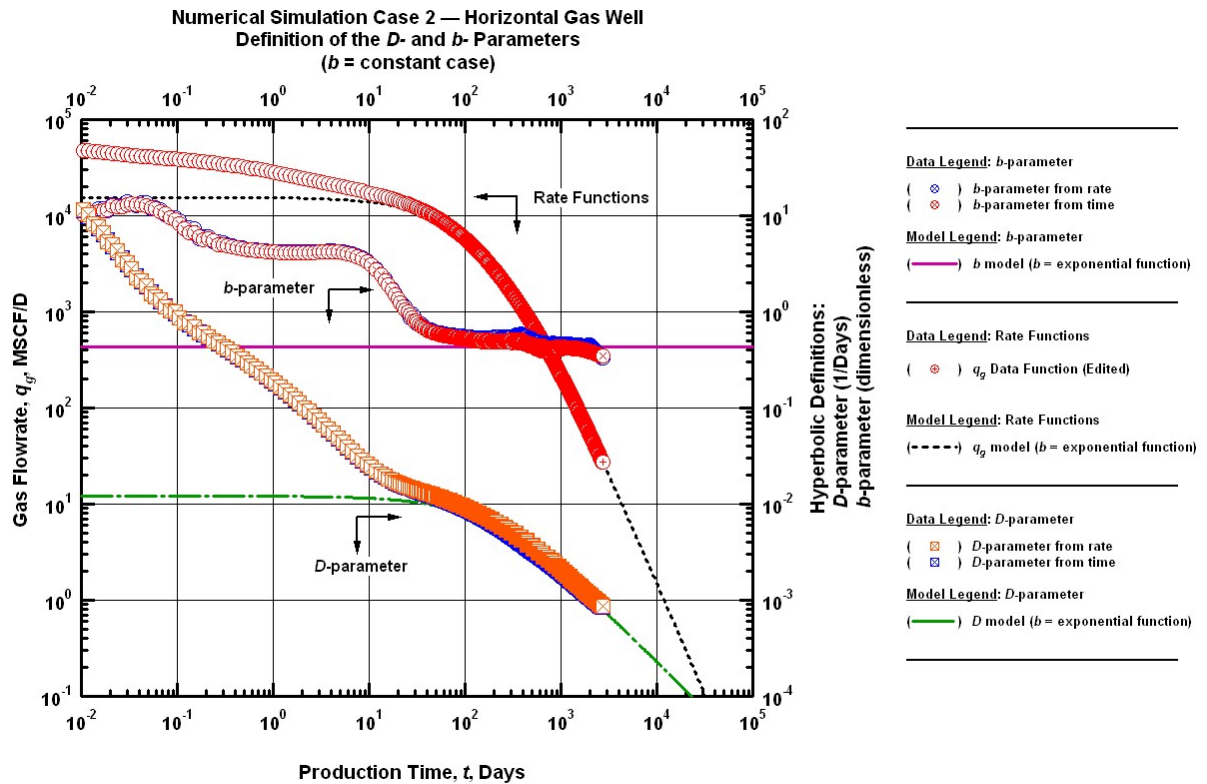


Figure 3.9 — Numerical Simulation Case 2: " q - D - b " Log-Log plot — Horizontal gas well — definition of the " D - and b -" parameters, b -constant case (Arps' hyperbolic rate-decline relation).

Next, we apply the exponential b -parameter model to the data set. We use the stabilized b -parameter value (approximately 0.4) for the b_0 model parameter which actually dominates the early/middle time behavior. At late times the b_1 model parameter starts to dominate and this defines the decline behavior of the model. **Fig. 3.10** presents our matches for the exponential b -parameter model case with the data. We note that exponential b -parameter model performs slightly better than the Arps' hyperbolic rate-decline relation in terms of matching the rate data and capturing the declining trend of the end effects of the computed b -parameter.

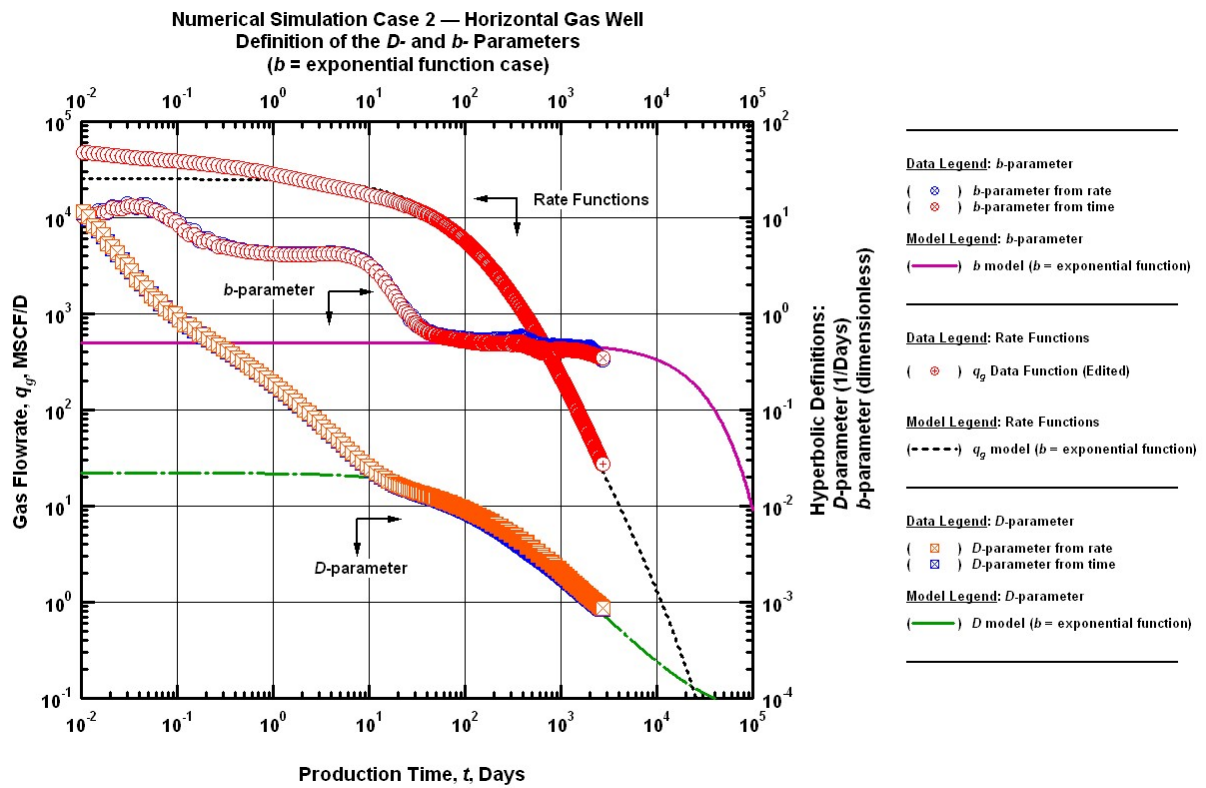


Figure 3.10 — Numerical Simulation Case 2: " q - D - b " Log-Log plot — Horizontal gas well — definition of the " D - and b -" parameters, exponential b -parameter model.

For the power-law b -parameter model, the computed b -parameter data trend implies that this model should not be applicable for this case. This situation clearly explains why we need more than one b -parameter models — each proposed model might work better for a particular case. Our strategy for applying the power-law b -parameter model is to find an average straight line which passes through the computed b -parameter data trend. By doing so, we obtain the matches in **Fig. 3.11**. We note that the match of the rate data with the power-law b -parameter model is good (perhaps the best among all models) confirming our strategy to use an average straight line for the computed b -parameter data. Furthermore, a satisfactory match with the computed D -parameter in the boundary dominated flow has obtained.

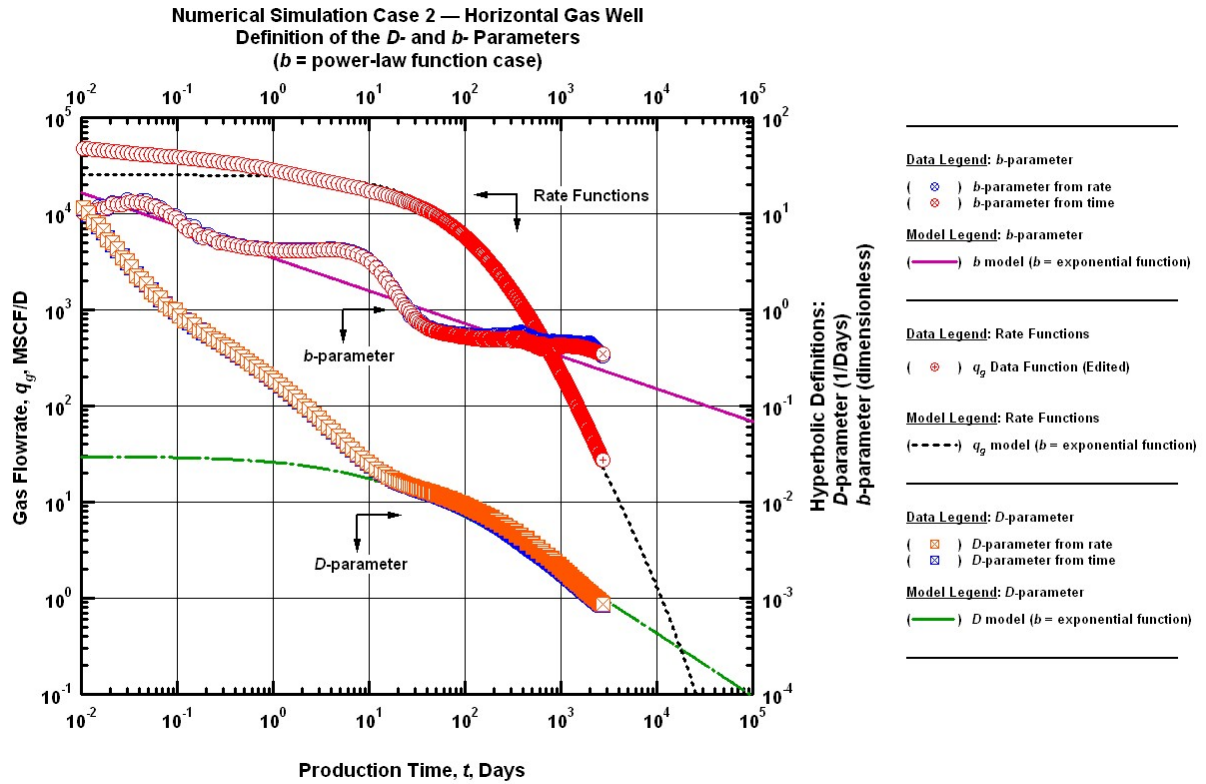


Figure 3.11 — Numerical Simulation Case 2: " q - D - b " Log-Log plot — Horizontal gas well — definition of the " D - and b -" parameters, power-law b -parameter model.

Finally we apply the rational b -parameter model. Our expectations for this case are the same with the exponential b -parameter model. Similarly we obtain the same matches of the data with the rational b -parameter model as in the case of the exponential b -parameter model (see **Fig. 3.12** for the matches). By observing the plot, we can see that this model has provided us with a good match with all the computed data. More specifically, in the case of the computed b -parameter — similarly to the exponential model — the rational function managed to capture the declining trend of the end effects at the very late times of the boundary dominated flow and has eventually yielded a better match with the computed data. However, this model as well appears to be weak at matching with the data at the early time flow regime.

Overall, for this case we can conclude that the best match of the rate data can be achieved by using an average "straight-line" trend (using the power-law b -parameter model) for the computed b -parameter data.

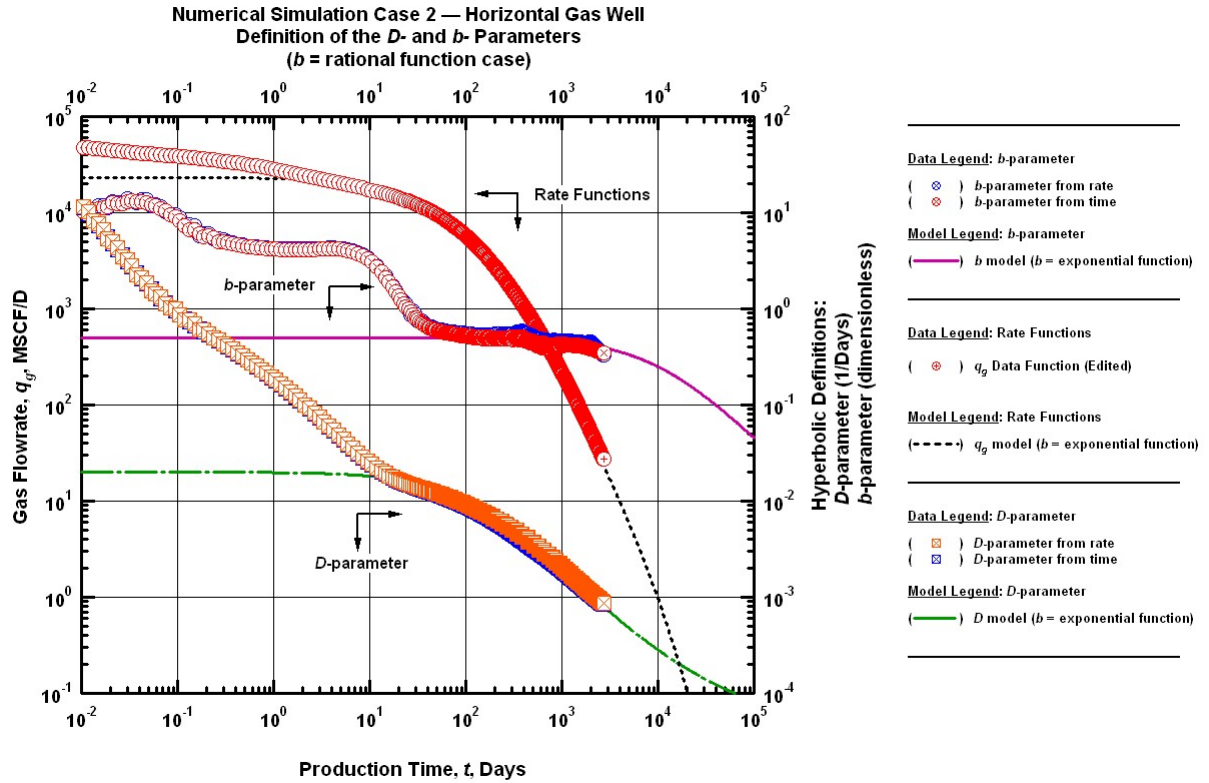


Figure 3.12 — Numerical Simulation Case 2: " q - D - b " Log-Log plot — Horizontal gas well — definition of the " D - and b - parameters, rational b -parameter model.

Application of the New Rate Decline Relations — Production Forecasts

The production forecasts for the numerical simulation case 2 are illustrated in the semi- and log-log plots with time (**Figs. 3.13** and **3.14**) respectively below. In this case as well, the cumulative production was calculated numerically.

The production forecasts for all the investigated models are shown analytically in **Table 3.4** below. It is clearly seen that all the models have achieved to forecast the same amount of reserves and more specifically the exact original gas in place ($G_{p,\max}=2.25$ BSCF). In the case of the constant model, the reserves estimate is consistent with the numerical simulator input value. This case suggests that if the complete boundary-dominated flow regime is reached, then it is possible to estimate the reserves with the hyperbolic rate-decline relation by computing the b-parameter using rate-time data.

The production forecast plots (**Figs. 3.13** and **3.14**) suggest the same reserves estimate for all the proposed models. Our concluding remarks for this case are as follows. None of the models can model the transient/transitional part of the computed b-parameter data trend successfully. This causes a mismatch with the computed b -parameter data but since the boundary-dominated flow regime is established, the reserves estimate can be obtained. However, according to the results which are illustrated in the **Fig. 3.14** the only model which can best model the behavior of the production data for all the flow regimes is the power-law model.

Table 3.4 — Production forecasts of the Numerical Simulation Case 2: Horizontal gas well.

Production Forecasts:

$b(t)=\text{constant (base)}$	=	2.25 BSCF
$b(t)=\text{exponential function}$	=	2.25 BSCF
$b(t)=\text{power law function}$	=	2.25 BSCF
$b(t)=\text{rational function}$	=	2.25 BSCF

Original Gas In Place (OGIP): 2.25 BSCF

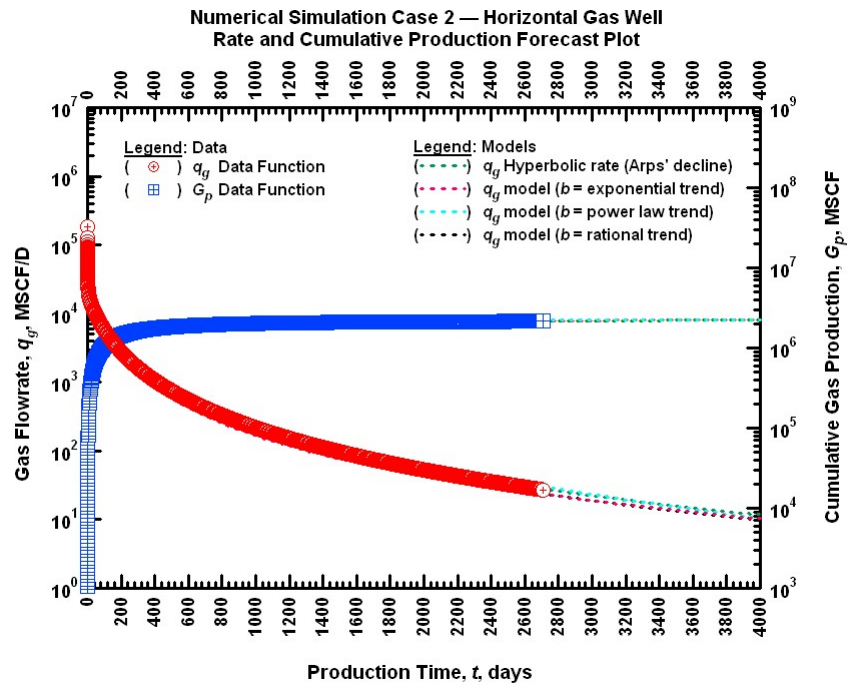


Figure 3.13 — Numerical Simulation Case 2: Production forecast (Semi-Log) plot — Horizontal gas well (all models are shown).

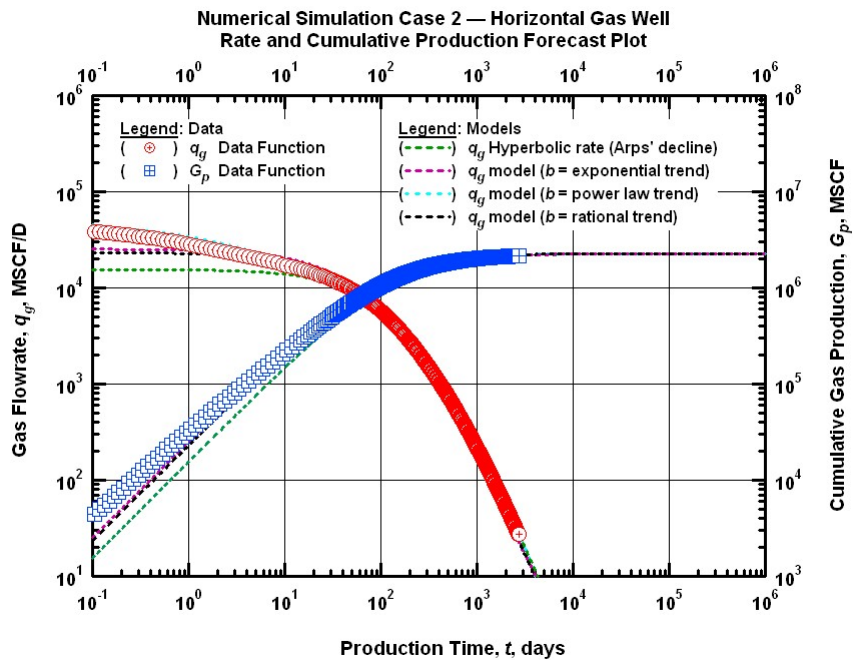


Figure 3.14 — Numerical Simulation Case 2: Production forecast (Log-Log) plot — Horizontal gas well (all models are shown).

Case 3: Vertical Unfractured Gas Well in a Cylindrical Bounded Reservoir — True Radial Flow

In this section we will investigate the behavior of our models on set of data taken from a synthetic case where we have a vertical fractured gas well. The case was generated by using commercial simulator and the production data history is illustrated in the following figure (see **Fig. 3.15** for rate and cumulative gas production versus time). In this case the grids build up in the simulator were not rectangular (as it happened to the rest of the simulation cases) but cylindrical. Therefore, there is only radial flow justifying the "True Radial Flow" title.

The model parameters and reservoir/fluid properties are provided in **Table 3.5**. It should be noted that this well is producing in a (bounded) cylindrical reservoir and boundary effects are clearly distinguished during the late times of the production.

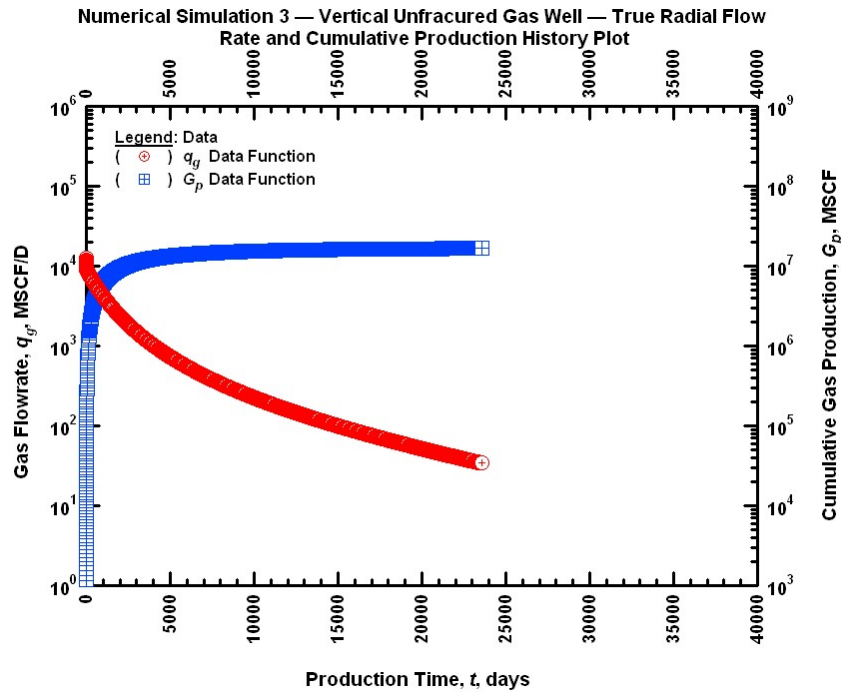


Figure 3.15 — Numerical Simulation Case 3: History (Semi-Log) plot — Vertical unfractured gas well in a cylindrical bounded reservoir — True Radial Flow.

Table 3.5 — Reservoir and fluid properties for the Numerical Simulation Case 3 — Vertical unfractured gas well in a cylindrical bounded reservoir — True Radial Flow.

<i>Reservoir Properties:</i>	
Net pay thickness, h	= 3.28 ft
Permeability in x-direction, k_x	= 100 md
Permeability in y-direction, k_y	= 100 md
Permeability in z-direction, k_z	= 100 md
Wellbore radius, r_w	= 0.30 ft
Formation compressibility, c_f	= 4×10^{-6} 1/psi
Porosity, ϕ	= 0.1 (fraction)
Initial reservoir pressure, p_i	= 1000 psia
Wellbore storage coefficient, C_D	= 0 (dimensionless)
Gas saturation, S_g	= 1.0 (fraction)
Skin factor, s	= 0 (dimensionless)
Reservoir temperature, T_r	= 212 °F
Drainage area (2x1 Rect.), A	= 4851 acres
<i>Fluid Properties:</i>	
Gas specific gravity, γ_g	= 0.65 (air = 1)
<i>Production Parameters:</i>	
Flowing pressure, p_{wf}	= 100 psia
Producing time, t	= 10474 days

In this case, the end-point effects caused by the numerical differentiation algorithm at late times seem not to affect the general stabilized trend of the computed data at the late times of the boundary dominated flow and we can conclude that they are limited. Moreover, it is clear that this is another case where we can also note that the computed b -parameter data trend exhibits a declining behavior (as opposed to constant) and the computed D -parameter trend exhibits a straight line behavior (on log-log scale). We begin the validation of the models by initially applying the hyperbolic rate-decline relation to data (Arps' equation, b =constant model).

Following the procedure and the steps that have developed and applied in the previous examples, in this case as well our main goal is not to find the "best-fit" of the proposed models with the data. But, rather we force our models to yield the same maximum cumulative production value for each case. For the hyperbolic rate-decline case the value of b is usually set to the average value of the data trend at the boundary dominated flow regime (for this case, this value is set to 0.6 as depicted by data trend at late times, see **Fig. 3.16**).

For this case we set $b=0.6$, this gives us a fair match with the rate data and the hyperbolic rate-decline relation. **Fig. 3.16** below presents the q - D - b plot for the constant b case. According to the graph by applying the constant b -parameter model we have managed to capture the stabilized behavior of the computed b -parameter at the boundary dominated flow regime. However, the model seems to be weak at modeling the trend of the data at the transient/transitional flow regime. Similar matches to the b -parameter are obtained for the case of the D -parameter (see **Fig. 3.16**). In the case of the production rate the model has successfully matched with the computed data in all the flow regimes. We proceed to our work and we apply the exponential b -parameter trend to the computed b -parameter data.

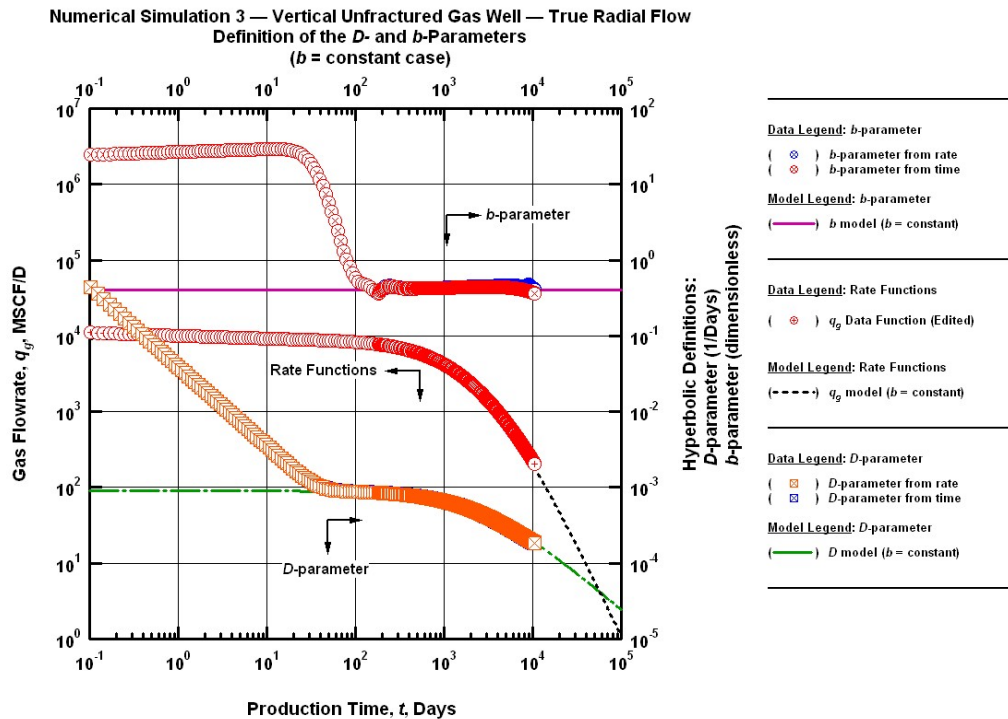


Figure 3.16 — Numerical Simulation Case 3: " q - D - b " Log-Log plot — Vertical unfractured gas well in a cylindrical bounded reservoir — True Radial Flow — definition of the " D - and b -" parameters, b -constant case (Arps' hyperbolic rate-decline relation).

As we have seen so far in the models that have been analyzed previously, the exponential b -parameter model can be more useful than the constant b model as the model indicates that at late times the decline trend is exponential, mainly because of the numerical differentiation "end effects". In this case, the "end effects" are limited and the computed data appears to follow a slightly declining trend at the very late times of the boundary dominated flow. The issue with the exponential b -parameter model is that cannot yield satisfactory matches for all the cases in the transient/transitional flow. **Fig. 3.17** presents the q - D - b plot for the exponential b -parameter model case. We note that the transient/transitional flow data is not modeled by the relation. However, we achieved to obtain a very good match of the rate data with the model for all the flow regimes. The next task is to apply the power-law model to the computed data.

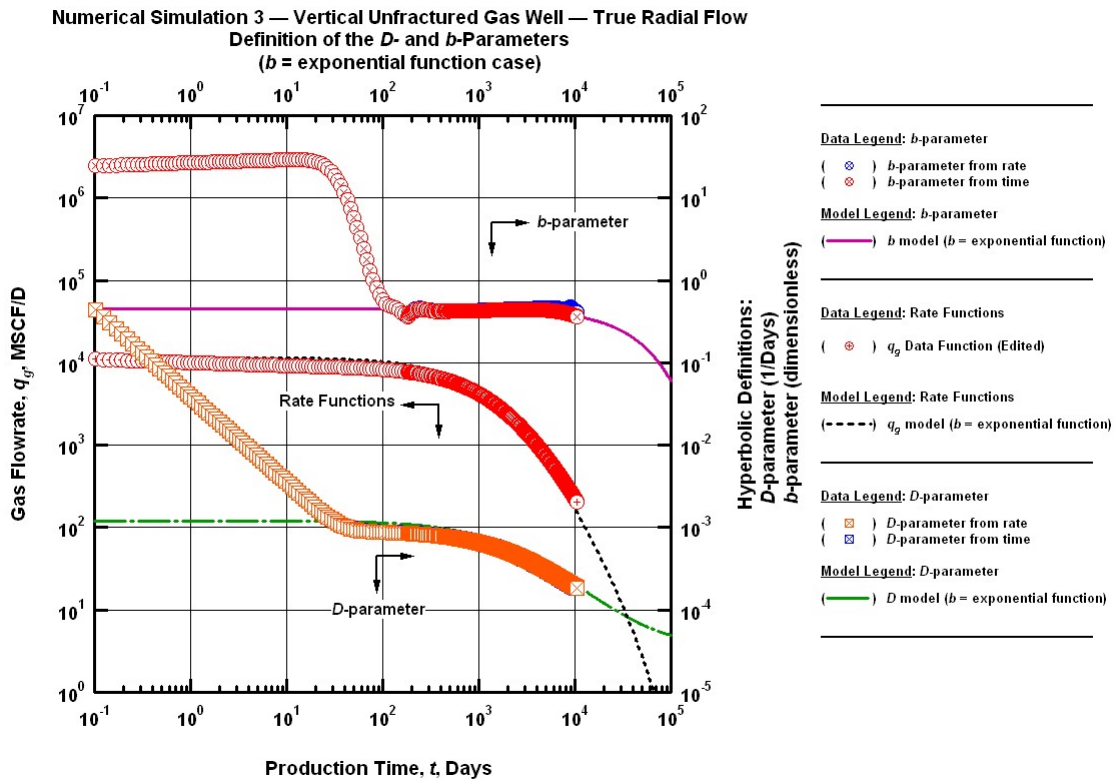


Figure 3.17 — Numerical Simulation Case 3: " q - D - b " Log-Log plot — Vertical unfractured gas well in a cylindrical bounded reservoir — True Radial Flow — definition of the " D - and b -" parameters, exponential b -parameter model.

For the power-law b -parameter model, by observing the trend of the computed b -parameter data we can understand that the application of this model could possibly yield poor matches with the computed data. In this case our main objective of the application of the b -power-law model is to find an average straight line which passes through the computed b -parameter data trend. By doing so, we obtain the matches in **Fig. 3.18**. We note that the matches with the computed data in all the cases are weak especially for the transient/transitional flow regimes. However, we have achieved to model the behavior of the rate data and the D -parameter at the boundary dominated flow regime. In this case we can clearly see the importance of the development of more than one b -parameter models, where each proposed model might give better results for a specific case.

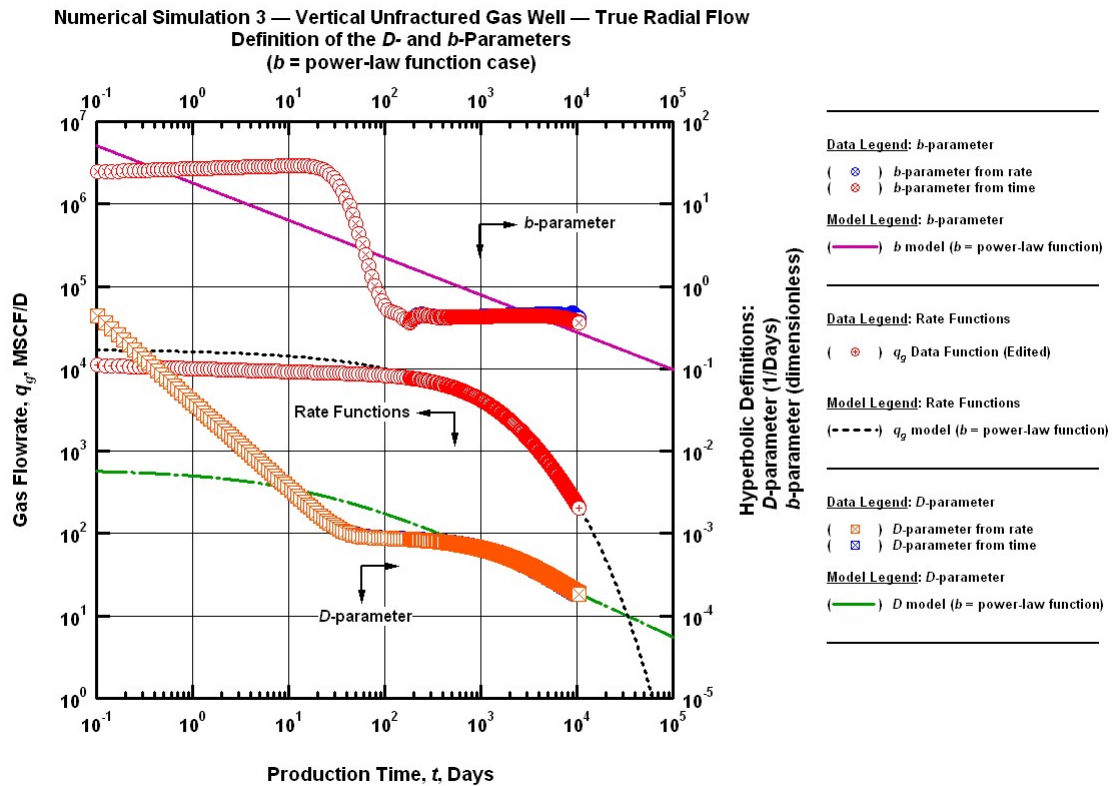


Figure 3.18 — Numerical Simulation Case 3: " q - D - b " Log-Log plot — Vertical unfractured gas well in a cylindrical bounded reservoir — True Radial Flow— definition of the " D - and b -" parameters, power-law b -parameter model.

Finally we apply the rational b -parameter model to the computed b -parameter data trend. As we have mentioned before, the behavior of the rational b -parameter model is similar to the exponential b -parameter model in terms of flexibility and modeling the b -parameter data (*i.e.*, both of them can capture the declining trend at the very late times at the boundary dominated flow of the b -parameter data). However, both of these models appear to be weak at modeling the computed data at the transient flow regime, mainly due to the nature of their equation. **Fig. 3.19** illustrates the application of the rational b -parameter model for this case. According to that, we obtained a fair match of the computed D - and b -parameter data trend with the model, by capturing the late time data trend. However, in the case of the rate data we achieved to match the model with the data throughout the flow regimes, getting outstanding results. Finally, we can conclude that the overall matches with data appear to be similar to those that we obtained in exponential b -parameter case.

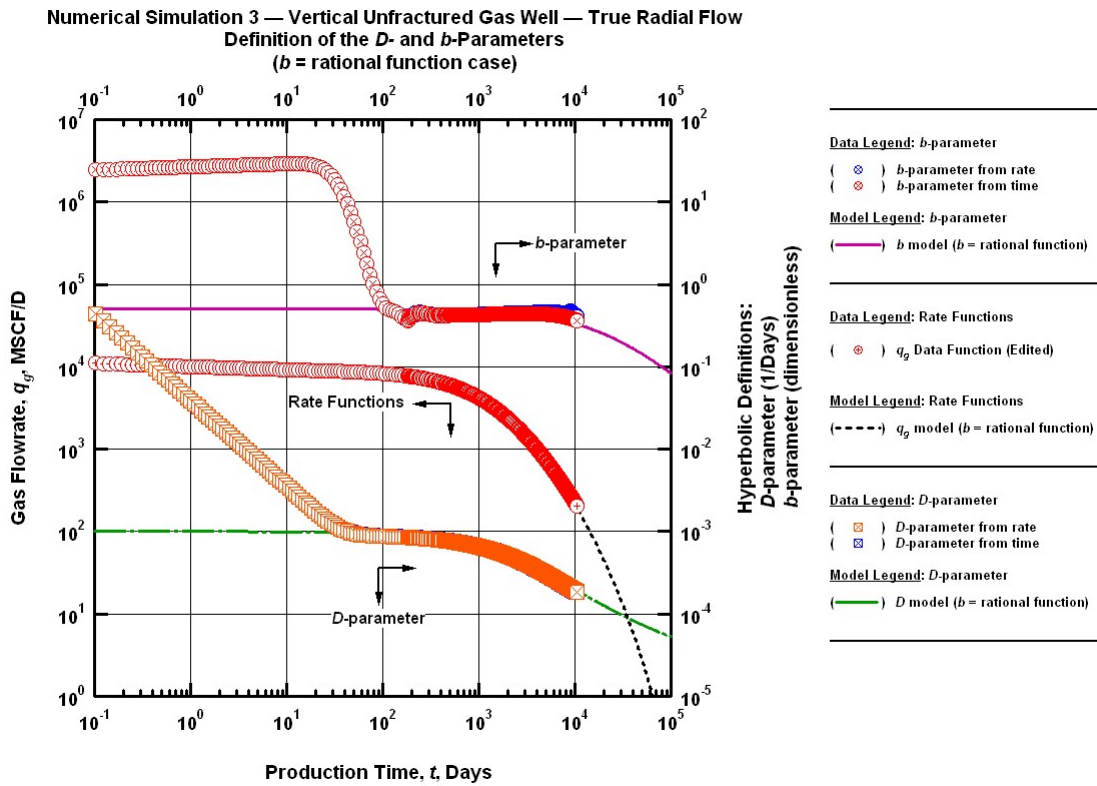


Figure 3.19 — Numerical Simulation Case 3: " q - D - b " Log-Log plot — Vertical unfractured gas well in a cylindrical bounded reservoir — True Radial Flow — definition of the " D - and b -" parameters, rational b -parameter model.

Application of the New Rate Decline Relations — Production Forecasts

In the following section, we validate the new rate decline relations that we have demonstrated above in terms of production forecasts. The two graphs which are provided below represent the production rate/cumulative forecasts presented in log- and semi-log plots. The cumulative production was calculated numerically.

In **Figs. 3.20** and **3.21** below we present the schematic plots of the production rate (q) and the cumulative production (G_p) with time in a log-log and semi-log plot respectively for the numerical simulation case 3 (Vertical unfractured gas well). The dotted lines represent the performance of the newly proposed models as well as the classical Arps' hyperbolic rate decline relation. According to the log-log plot (see **Fig. 3.21**) we observe that all of the applied models have successfully forecasted the exact amount of the original gas in place ($G_{pmax} = 16.8$ BSCF). In fact, the numerical illustration of the forecasts of the models in **Table 3.6** confirms the previous observation. In this case it is clear that the application of any of the models can eventually give us a correct forecast. Moreover, as it can be seen from **Fig. 3.21** we achieved to obtain excellent matches with the computed production data for almost all the models for all the flow regimes. On the other hand, the power-law model seems to be weak at capturing the early time trend of the computed production data.

Table 3.6 — Production forecasts of the Numerical Simulation Case 3: Vertical unfractured gas well in a cylindrical bounded reservoir — True Radial Flow.

Production Forecasts:

$b(t)=\text{constant (base)}$	=	16.8 BSCF
$b(t)=\text{exponential function}$	=	16.8 BSCF
$b(t)=\text{power law function}$	=	16.8 BSCF
$b(t)=\text{rational function}$	=	16.8 BSCF

Original Gas In Place (OGIP): 16.8 BSCF

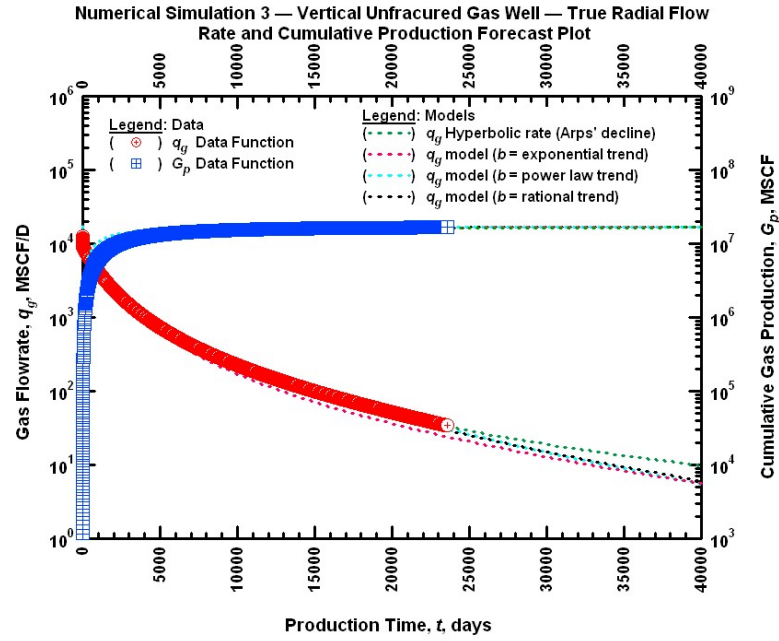


Figure 3.20 — Numerical Simulation Case 3: Production forecast (Semi-Log) plot — Vertical unfractured gas well in a cylindrical bounded reservoir — True Radial Flow (all models are shown).

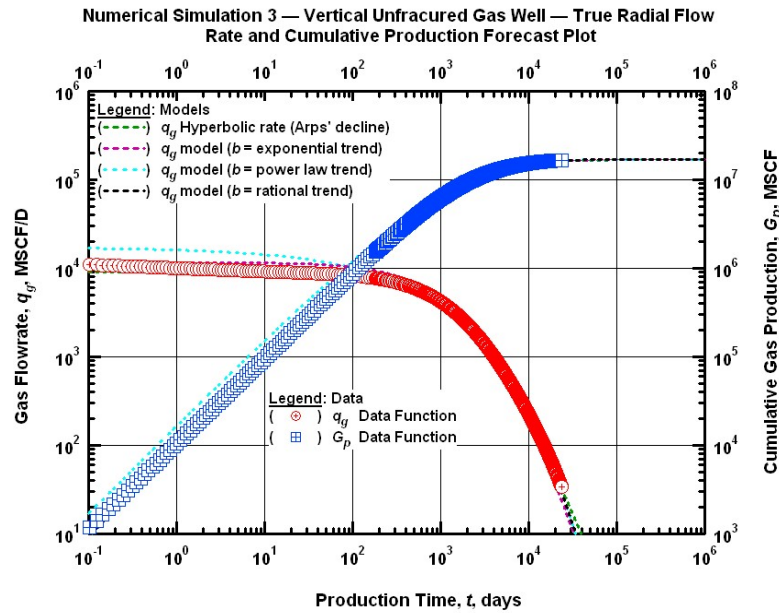


Figure 3.21 — Numerical Simulation Case 3: Production forecast (Log-Log) plot — Vertical unfractured gas well in a cylindrical bounded reservoir — True Radial Flow (all models are shown).

Case 4: Vertical Fractured Tight Gas Well (East TX) (Ilk *et.al* [2008b])

This synthetic case is derived from the classical field example of a tight gas well performance behavior that has been previously presented (Pratikno *et.al* [2003] for the early production data, and Ilk *et.al* [2008b] for the near current production data). The investigated well includes a vertical fracture with finite conductivity and we assume a constant flowing wellbore pressure to generate the synthetic flowrate performance. The illustration of the production history for this case is shown in **Fig. 3.22** that follows.

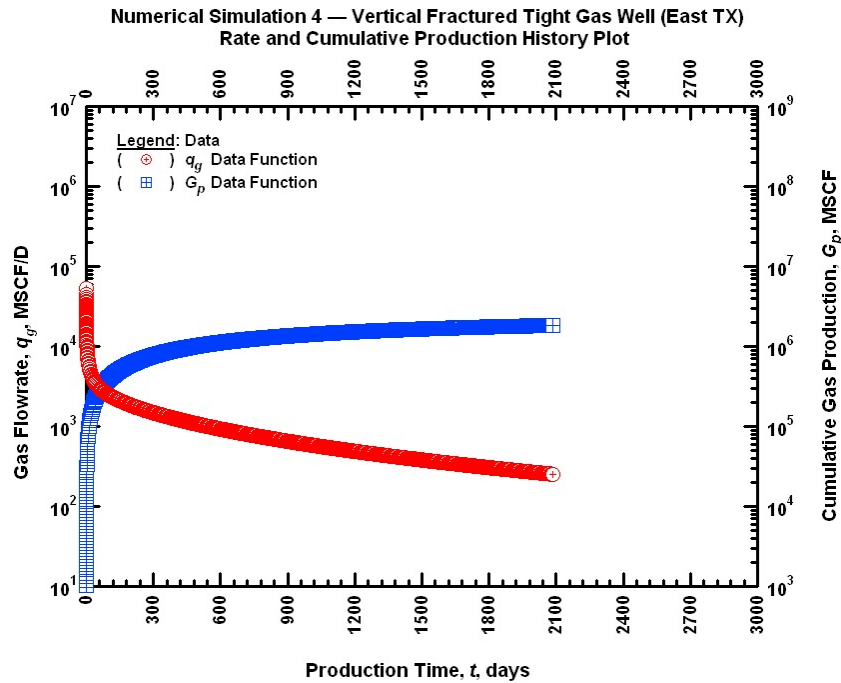


Figure 3.22 — Numerical Simulation Case 4: History (Semi-Log) plot — Vertical fractured tight gas Well (East TX).

The model parameters and reservoir/fluid properties are provided in **Table 3.7**. It should be noted that this well is producing in a (bounded) rectangular reservoir and boundary effects are observed during late times of the production.

Table 3.7 — Reservoir and fluid properties for the Numerical Simulation Case 4 — Vertical fractured tight gas well (East TX).

Reservoir Properties:

Net pay thickness, h	=	177 ft
Permeability in x-direction, k_x	=	0.005 md
Permeability in y-direction, k_y	=	0.005 md
Permeability in z-direction, k_z	=	0.005 md
Wellbore radius, r_w	=	0.333 ft
Formation compressibility, c_f	=	1×10^{-7} 1/psi
Porosity, ϕ	=	0.088 (fraction)
Initial reservoir pressure, p_i	=	9330 psia
Wellbore storage coefficient, C_D	=	0 (dimensionless)
Gas saturation, S_g	=	1.0 (fraction)
Skin factor, s	=	0 (dimensionless)
Reservoir temperature, T_r	=	300 °F
Drainage area (2x1 Rect.), A	=	13.9 acres

Fluid Properties:

Gas specific gravity, γ_g	=	0.7 (air = 1)
----------------------------------	---	---------------

Production Parameters:

Flowing pressure, p_{wf}	=	500 psia
Producing time, t	=	2088 days

We firstly apply the hyperbolic rate-decline relation to data (Arps' equation, b =constant model). In this case we have to mention that the end-point effects caused by the numerical differentiation algorithm at late times are limited, and the actual stabilized trend of the computed b -parameter at the boundary dominated flow can be observed (very late times). In additional to the previous studies, in this case as well, the computed b -parameter data trend exhibits a declining behavior and the computed D -parameter trend exhibits a straight line behavior.

Similarly to the previous application processes, we use all the investigated models in conjunction and force the same maximum cumulative production value for each case. More specifically, for the hyperbolic rate-decline case we usually set the b value equal to the value where the trend of the computed b -parameter seems to be stabilized (boundary dominated flow).

For this case we set $b=0.5$, this yields poor matches with the computed data and the hyperbolic rate-decline relation. According to **Fig. 3.23**, which presents the q - D - b plot for the constant b case, we can clearly see that the application of this model has provided us with extremely poor matches especially for the transient and transitional flow regimes. Fair matches are obtaining for the case of the D -parameter and the production rate in the boundary dominated flow regime. Overall, this model seems weak at modeling the behavior of the computed data for all the cases at the transient/transitional flow regime. It can be applicable only when the boundary dominated flow is reached.

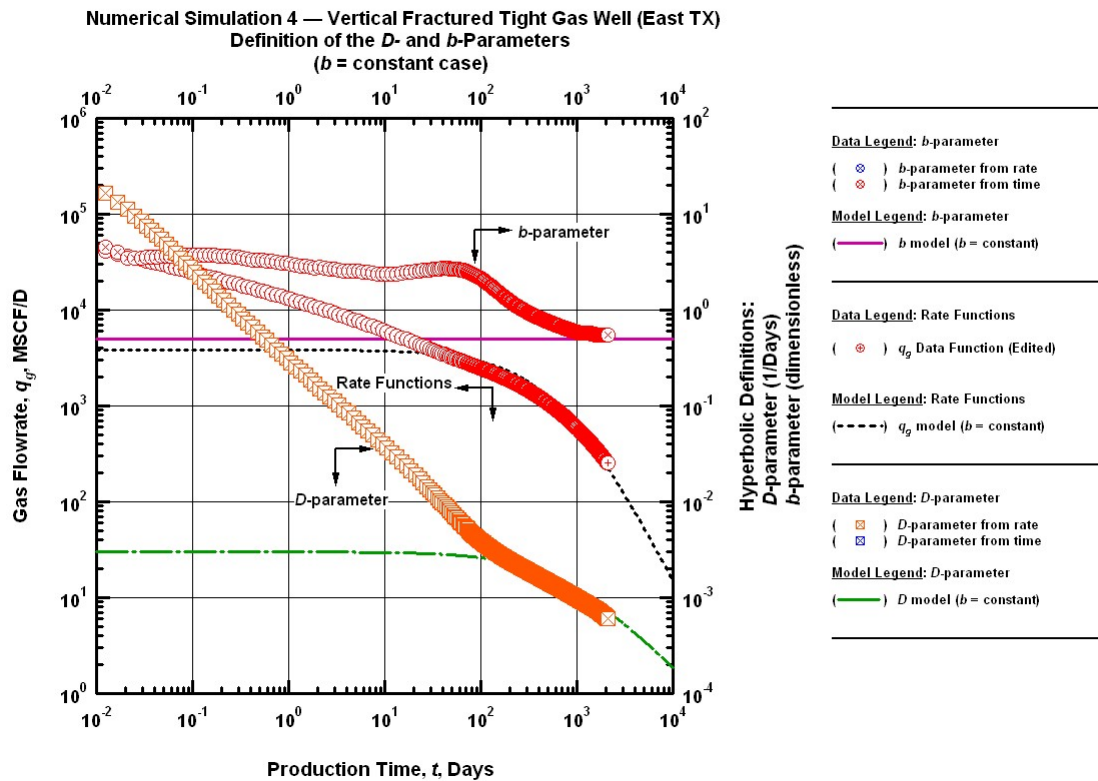


Figure 3.23 — Numerical Simulation Case 4: " q - D - b " Log-Log plot — Vertical fractured tight gas well (East TX) — definition of the " D - and b -" parameters, b -constant case (Arps' hyperbolic rate-decline relation).

The next model of the series of the proposed b -parameter models that we apply is the exponential b -parameter model. This model is expected to yield better matches than the b -constant model since the declining trend of the computed b -parameter data, which is indicated at the late times, can be captured by the exponential function. In this case, in contrast to the previous applications of the b -exponential model, our main objective is to analyze the behavior of the model at the early transient flow regime. Therefore, we try to match the model with the computed data at the transient flow regime. The results of this application are shown in **Fig. 3.24** (q - D - b plot for the exponential b -parameter model case). We note that the model has yielded poor matches with the computed b -data throughout the flow regimes, capturing a small part of the trend of the data at the transient flow regime as well as the overall declining trend of the data at the transitional part. However, this model has successfully matched with the computed rate data at the boundary dominated flow and has provided us an excellent match for the case of the D -parameter for all the flow regimes. The next model that we applied is the power-law model.

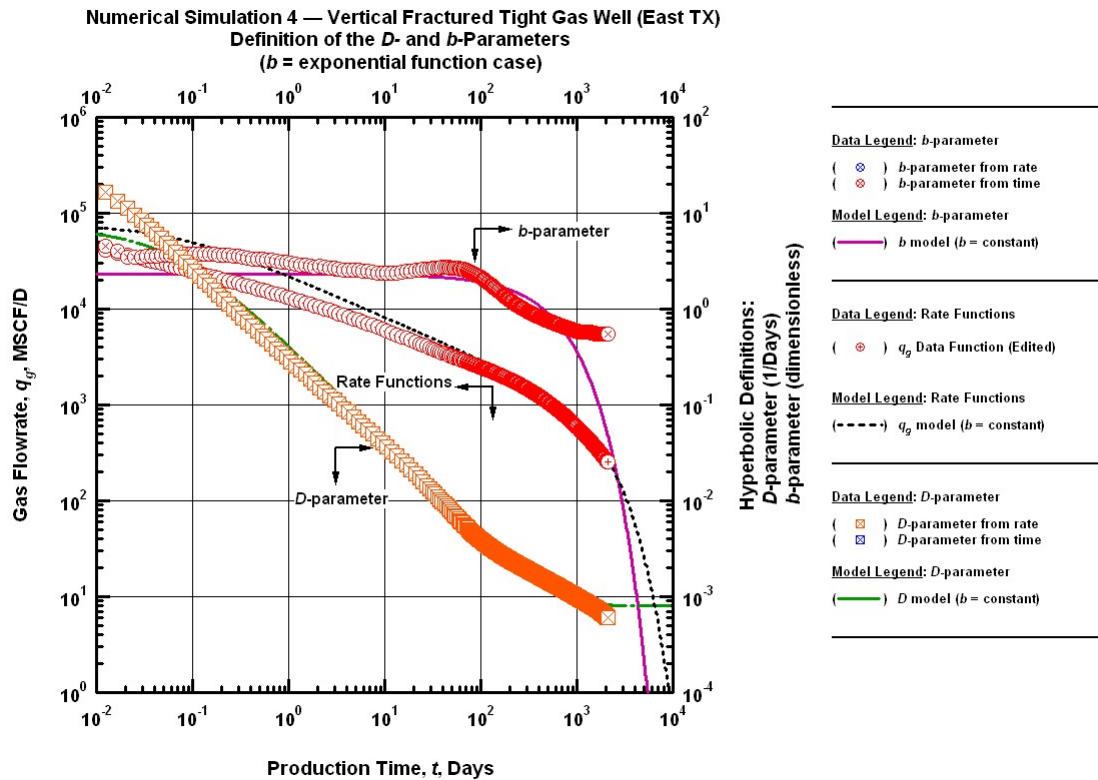


Figure 3.24 — Numerical Simulation Case 4: " q - D - b " Log-Log plot — Vertical fractured tight gas well (East TX) — definition of the " D - and b -" parameters, exponential b -parameter model.

Our next step is to apply the power-law b -parameter model. The computed b -parameter data trend indicates a declining straight behavior on the log-log scale (see the q - D - b plot, **Fig. 3.25**). Having that in mind the application of the power-law b -parameter model should eventually provided us with some satisfactory matches and accurate forecasts. We match the computed b -parameter data with the power-law model and observe a good match for the boundary dominated flow regime. Consequently, we expect to obtain similar matches for the cases of the D -parameter and rate. In fact, the b -power law model seems to fairly capture the trend of the D -parameter at the boundary dominated flow. In the case of the rate, the model appears to be modeling not only the boundary dominated flow behavior but also the transitional part and a part of the transient flow regime.

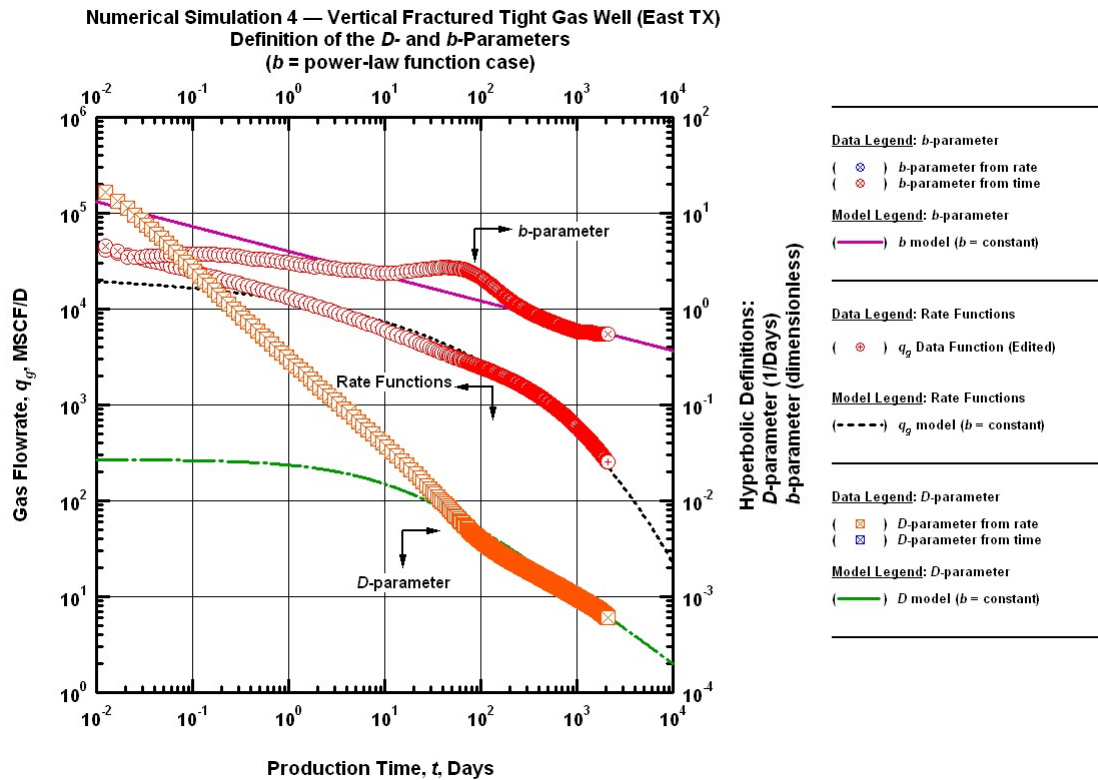


Figure 3.25 — Numerical Simulation Case 4: " q - D - b " Log-Log plot — Vertical fractured tight gas well (East TX) — definition of the " D - and b -" parameters, power-law b -parameter model.

The last model of the series of the proposed b -parameter models that we apply to the computed b -parameter data trend is the rational b -parameter model. As we have noticed previously the rational b -parameter model is similar to the exponential b -parameter model in terms of modeling the b -parameter data. Moreover, the slightly decreasing behavior of the computed b -parameter (almost straight line) at the boundary dominated flow as well as the declining trend of the transitional part allow us to expect satisfactory matches when we apply the rational b -parameter model. Indeed according to the q - D - b plot which is presented in **Fig. 3.26**, the application of the model to the computed data has yielded outstanding results for all the cases and all the flow regimes.

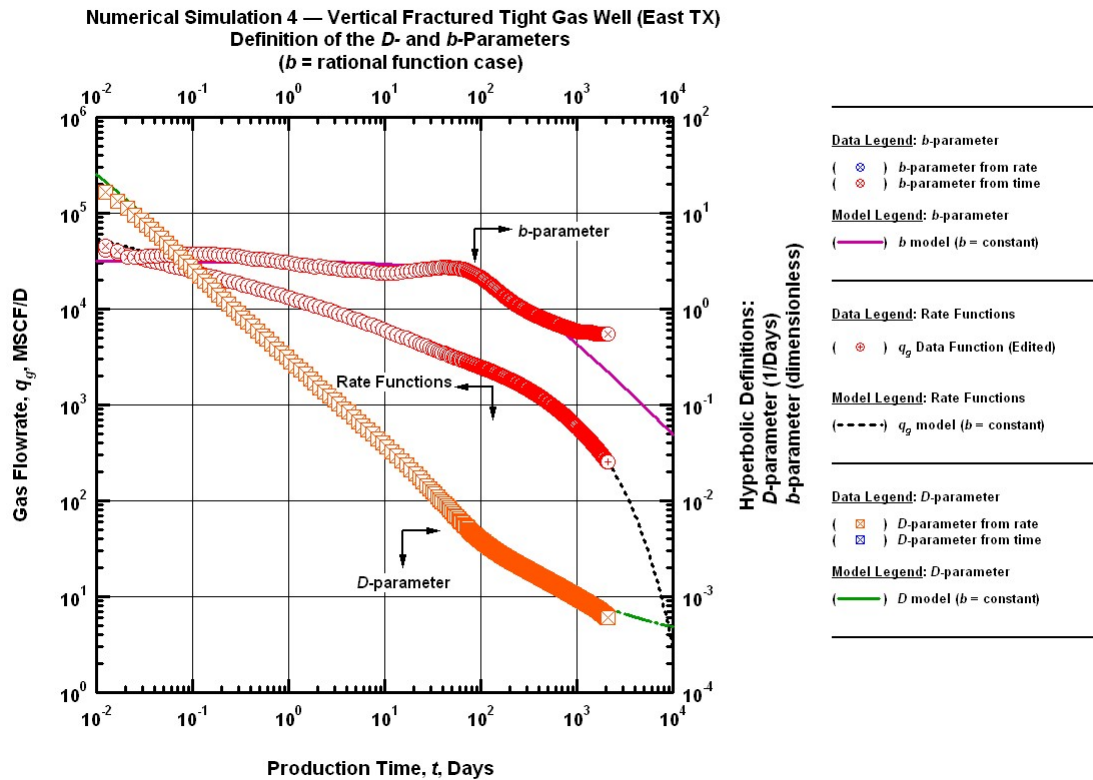


Figure 3.26 — Numerical Simulation Case 4: " q - D - b " Log-Log plot — Vertical fractured tight gas well (East TX) — definition of the " D - and b -" parameters, rational b -parameter model.

Application of the New Rate Decline Relations — Production Forecasts

In this section, we validate the proposed rate-decline relations in terms of production forecasts. The two illustrative examples which are provided below represent the production rate/cumulative forecasts presented in log- and semi-log plots. The cumulative production was calculated numerically in this case as well.

Figs. 3.27 and **3.28** represent the schematic plots of the production rate (q) and the cumulative production (G_p) with time in a log-log and semi-log plot respectively for the numerical simulation case 4 (Vertical fractured tight gas well — East TX). The dotted lines represent the performance of the newly proposed models as well as the classical Arps' hyperbolic rate decline relation. By observing the log-log plot (**Fig. 3.28**), we immediately note that all the models have successfully forecasted the correct amount of gas reserves. This can be also seen in the numerical illustration of the forecasts in the **Table 3.8** that follows. Although all of the models seem to be working perfectly, a more careful evaluation of the models according to the **Fig. 3.28** can show us that most of the models have failed at capturing the trend of rate/cumulative production data at the early time transient flow regime. On the other hand, the rational b-parameter model — as expected — is the only model which has provided us with such excellent matches with the computed production data for all the flow regimes.

Table 3.8 — Production forecasts of the Numerical Simulation Case 4: Vertical fractured tight gas well (East TX).

Production Forecasts:

$b(t)$ =constant (base)	=	2.55 BSCF
$b(t)$ =exponential function	=	2.55 BSCF
$b(t)$ =power law function	=	2.55 BSCF
$b(t)$ =rational function	=	2.55 BSCF

Original Gas In Place (OGIP): 2.55 BSCF

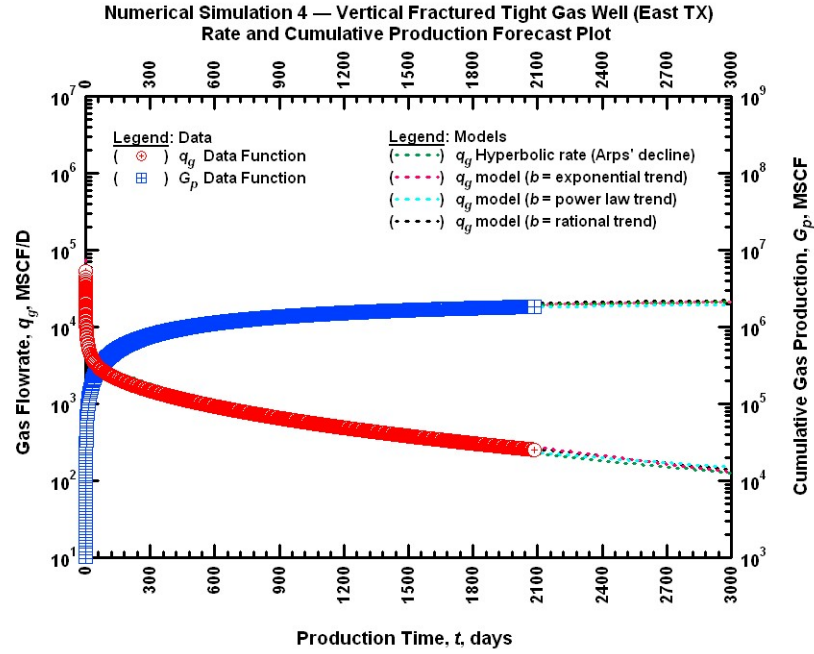


Figure 3.27 — Numerical Simulation Case 4: " q - D - b " Semi-Log plot — Vertical fractured tight gas well (East TX) — (all models are shown).

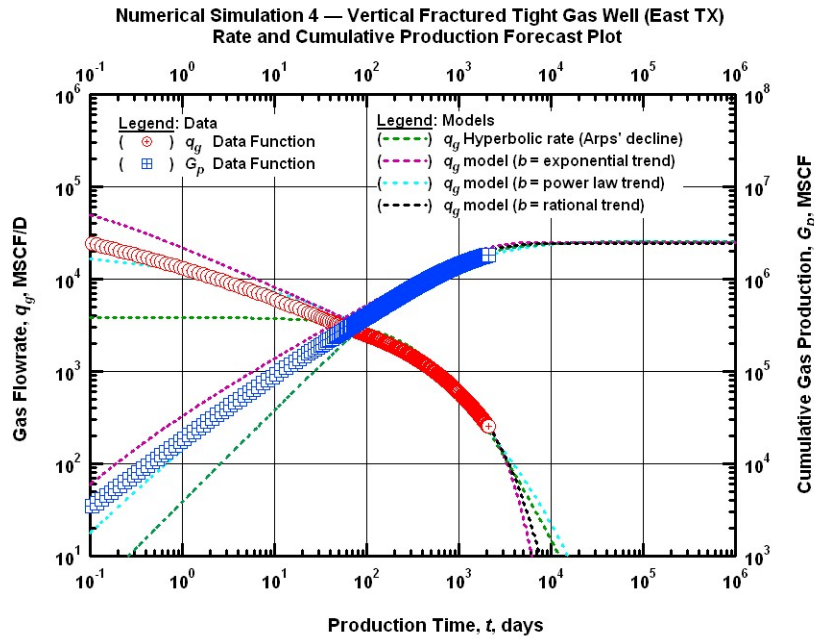


Figure 3.28 — Numerical Simulation Case 4: " q - D - b " Log-Log plot — Vertical fractured tight gas well (East TX) — (all models are shown).

Field Case Demonstration Examples

Field Case 1: Fractured Gas Well in a Tight Gas Sand Reservoir (LWF1 – 20/40 Proppant) (Ilk *et al* [2008c])

Our first example is taken from the work by Ilk *et al* (Ilk *et al* [2008c]). This is a hydraulically fractured gas well producing in a tight gas sand reservoir (this well corresponds to well LWF1 in the work by Ilk *et al*). **Fig. 3.29** presents the summary history plot for this case. Daily surface pressure and flowrate data are available for this well. Data quality seems good in general except for the liquid loading effects reflected in the flowrate data. The pressure data are not shown in this work. Model based analysis (ref. Ilk *et al* [2008c]) yielded 3.0 BSCF for the contacted gas-in-place estimate. In this case we will try to find the same value using the new rate-decline relations as obtained by the model based analysis.

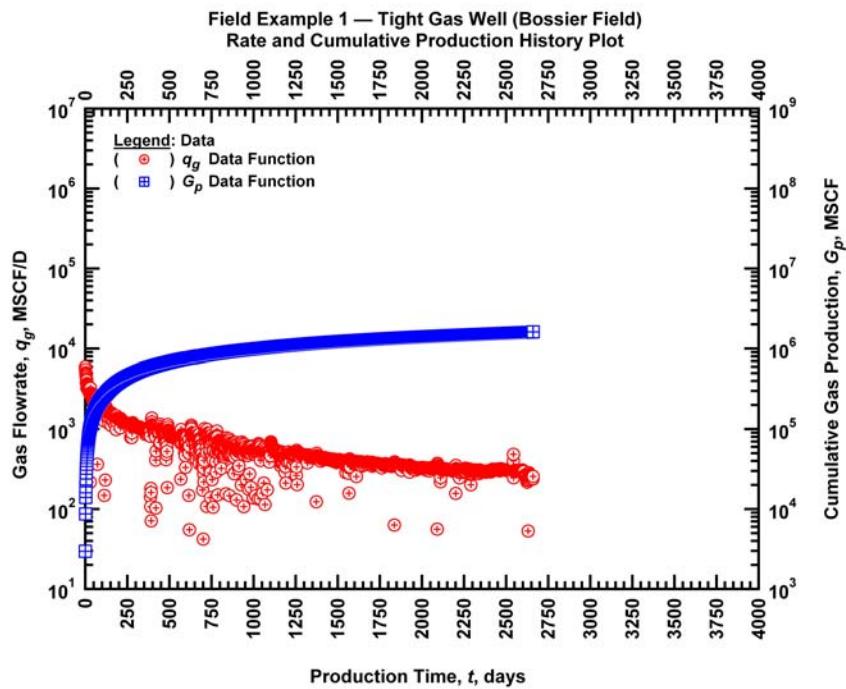


Figure 3.29 — Field Example Case 1: History (Semi-Log) plot — Fractured well in a tight gas reservoir (LWF1 – 20/40 Proppant) (ref. Ilk *et al* [2008c]).

We follow our step by step procedure for the application of the rate-decline relations. First of all, we edit/delete the spurious rate data prior to numerical differentiation. Once editing is complete, the numerical differentiation can be performed.

Fig. 3.30 illustrates the application of the Arps' rate-decline equation to this case. We set the b -parameter value to 0.9 and obtain the best matches. The rationale for the b -parameter value equals to 0.9 is that the computed b -parameter trend stabilizes at 0.9 at late times. However, by setting the b -parameter equal to 0.9, we manage to obtain a satisfactory match only for the boundary dominated flow. Consequently, we anticipate the same results for the case of the D -parameter and the production rate. This model continues to be inadequate at modeling the early time flow data trend and it is only applicable for the boundary dominated flow. As we will analytically see below, the b -constant model will eventually over-estimate the actual reserves.

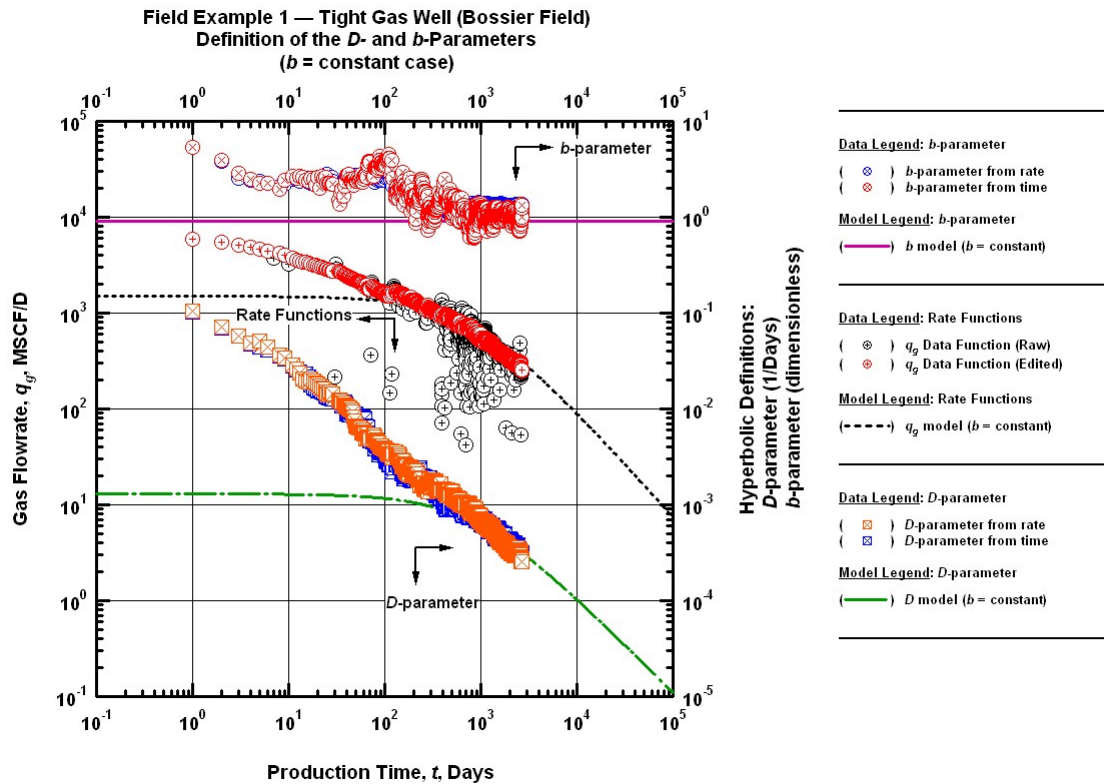


Figure 3.30 — Field Example Case 1: " q - D - b " Log-Log plot — Fractured well in a tight gas reservoir (LWF1 – 20/40 Proppant) (ref. Ilk *et al* [2008c]). — definition of the " D and b " parameters, b -constant case (Arps' hyperbolic rate-decline relation).

In the next attempt, we use the exponential b -parameter model. In some sense, the exponential b -parameter model is a way to constrain the Arps' hyperbolic rate decline relation by introducing the exponential decline at late times. We use the same value for the model parameter, b_0 , as in the case of the hyperbolic rate-decline relation (in other words we set $b_0=b$). We obtain the optimum match by changing the value of the remaining model parameters. **Fig. 3.31** presents our matches for this case. By applying the exponential model we have achieved to match the declining trend of the computed b -parameter at the late times of the boundary dominated flow. Nevertheless, the nature of the equation does not allow us to further obtain a better match with the data in the transient flow regime.

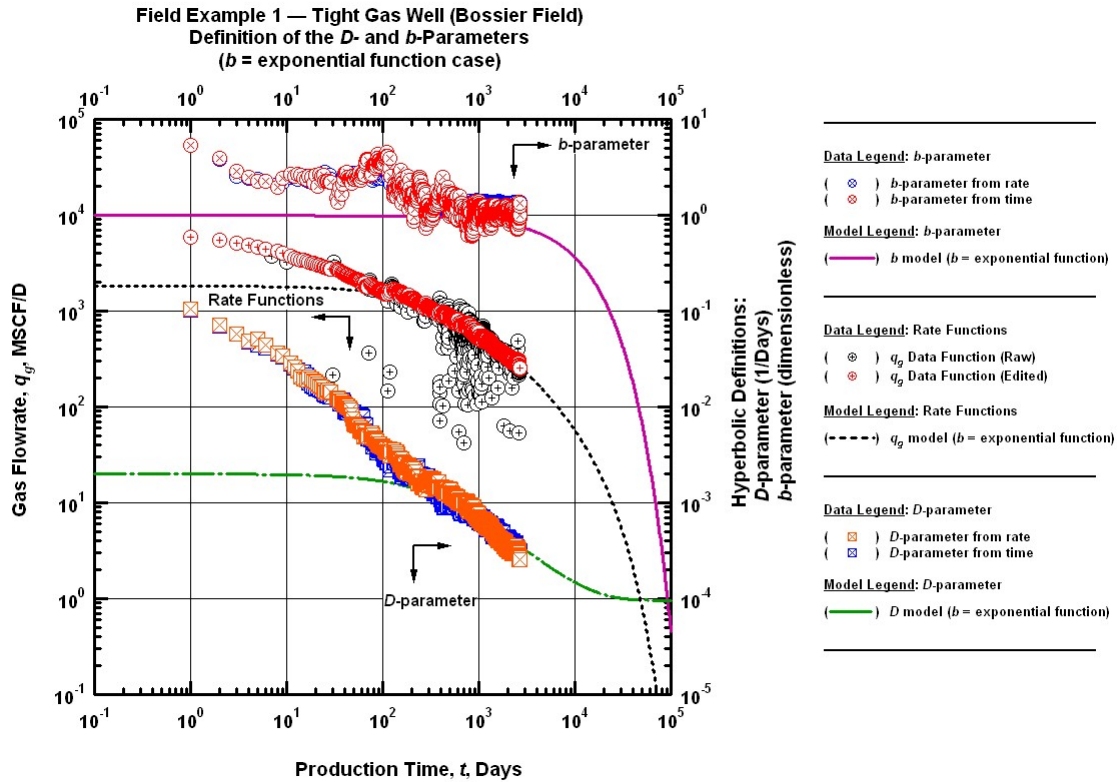


Figure 3.31 — Field Example Case 1: " q - D - b " Log-Log plot — Fractured well in a tight gas reservoir (LWF1 – 20/40 Proppant) (ref. Ilk *et al* [2008c]). — definition of the " D and b " parameters, exponential b -parameter model.

The computed b -parameter data trend indicates a power-law behavior. Therefore, we expect that for this case power-law b -parameter model should perform very well. **Fig. 3.32** presents the " q - D - b " plot for this case. As expected we obtain outstanding matches of all the data with the power-law b -parameter model and its associated relations. In particular, the match of the rate data with the model is excellent. The mismatch that appears in the case of the b -parameter at with the computed data at the very early times of the transient flow is mainly because of the nature of the power-law model equation.

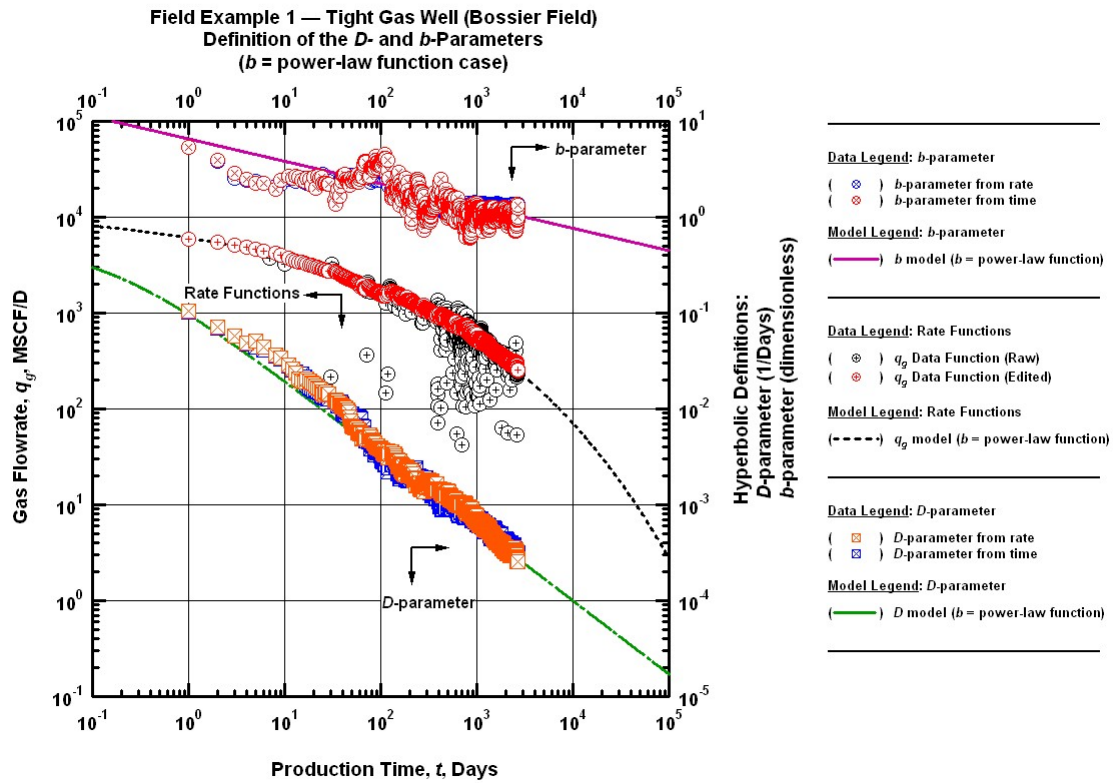


Figure 3.32 — Field Example Case 1: " q - D - b " Log-Log plot — Fractured well in a tight gas reservoir (LWF1 – 20/40 Proppant) (ref. Ilk *et al* [2008c]). — definition of the " D and b " parameters, power-law b -parameter model.

Finally we apply the rational b -parameter model to the data set. We believe the rational b -parameter model is the most flexible among the proposed models in terms of modeling the computed b -parameter data trend. We present the model matches with the data in **Fig. 3.33**. We observe extraordinary matches of the data with the models. The data are matched to the model across all flow regimes.

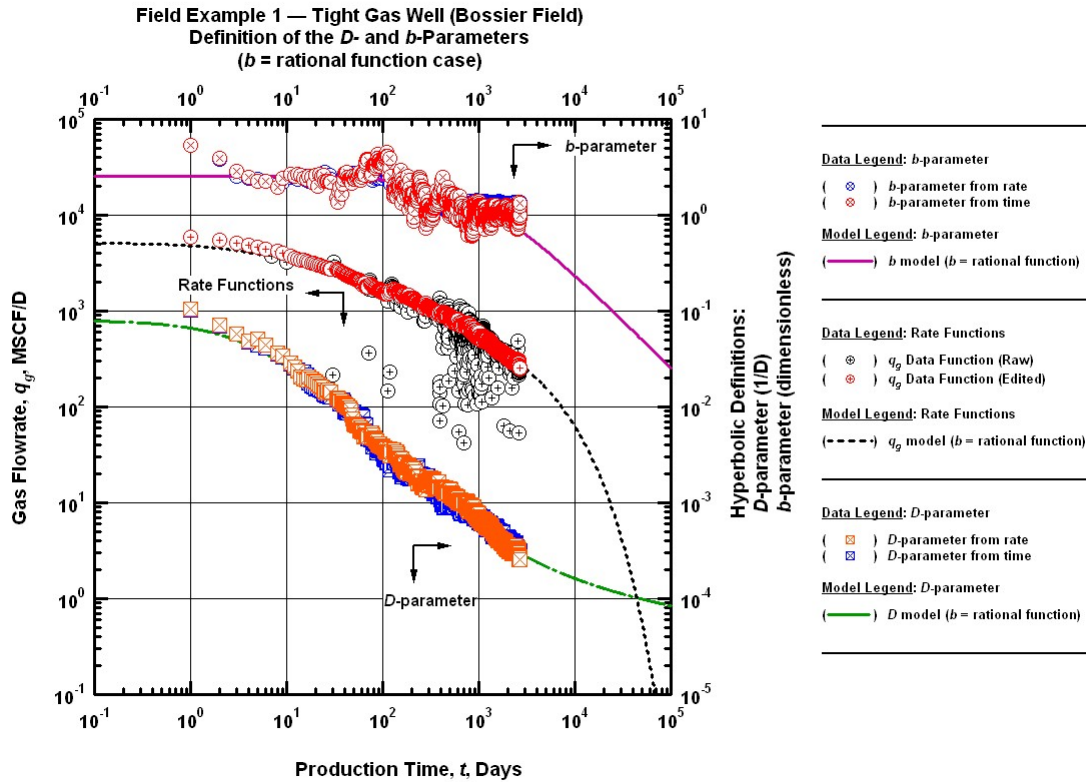


Figure 3.33 — Field Example Case 1: " q - D - b " Log-Log plot — Fractured well in a tight gas reservoir (LWF1 – 20/40 Proppant) (ref. Ilk *et al* [2008c]). — definition of the " D and b " parameters, rational b -parameter model.

Application of the New Rate Decline Relations — Production Forecasts

Our next step is to use the new rate decline relations in estimating the reserves for specific field data cases. The following semi- and log-log plots (**Figs. 3.34** and **3.35**) represent the performance of the new models on forecasting gas reserves for the first field case.

The results of the application of all the models are represented in the **Table 3.9** that follows. The b -constant model gives clearly an over-estimate and from the data it can be seen that the complete boundary-dominated flow has not been established yet. The performance of the new models remains remarkable and therefore they have successfully forecasted the original gas in place. However, according to **Fig. 3.35**, we can conclude that only the power-law and rational model can adequately model the early time behavior of the production data.

Table 3.9 — Production forecasts of the Field Case 1: Fractured well in a tight gas reservoir (LWF1 – 20/40 Proppant) (ref. Ilk *et al* [2008c]).

Production Forecasts:

$b(t)$ =constant (base)	=	8.40 BSCF
$b(t)$ =exponential function	=	3.00 BSCF
$b(t)$ =power law function	=	3.00 BSCF
$b(t)$ =rational function	=	3.00 BSCF

Original Gas In Place (OGIP): 3.00 BSCF

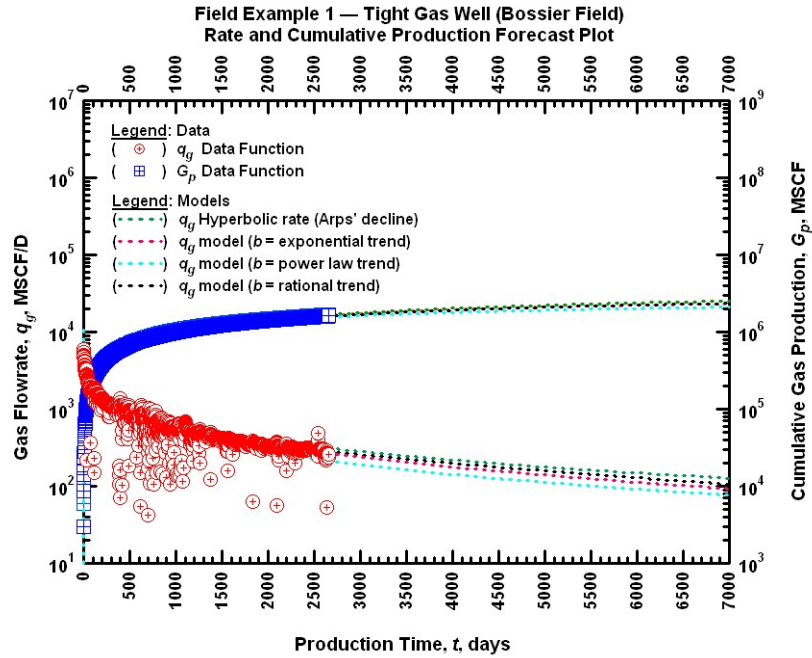


Figure 3.34 — Field Example Case 1: Production forecast (Semi-Log) plot — Fractured well in a tight gas reservoir (LWF1 – 20/40 Proppant) (ref. Ilk *et al* [2008c]) — (all models are shown).

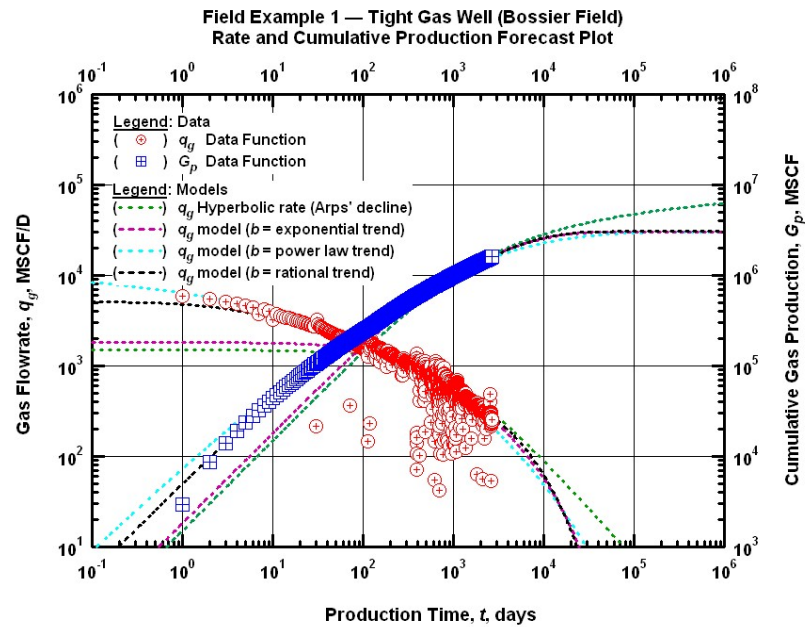


Figure 3.35 — Field Example Case 1: Production forecast (Log-Log) plot — Fractured well in a tight gas reservoir (LWF1 – 20/40 Proppant) (ref. Ilk *et al* [2008c]) — (all models are shown).

Field Case 2: Shale Gas Well (Gas Well 1 — Barnett Shale) (Mattar *et al* [2008])

The second example includes the monthly production data acquired from a shale gas well (Gas Well 1 — Barnett Shale). The production data was earlier analyzed in the work by Mattar *et al* [2008] using the "power-law exponential" rate-decline model (Ilk *et al* [2008a] and [2008b]). Our objective in this work is to get a consistent reserves estimate with the "power-law exponential" model using the new rate-decline relations. As mentioned before, almost 6.5 years of monthly production data are available via public records (see **Fig. 3.36**). For this case we note that boundary-dominated flow regime has been established by visual inspection.

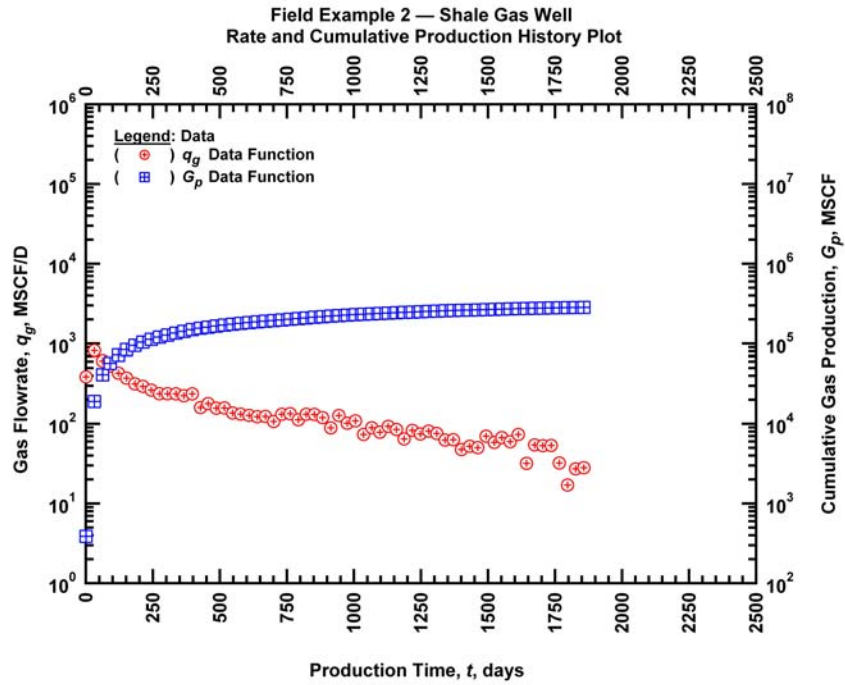


Figure 3.36 — Field Example Case 2: History (Semi-Log) plot — Shale gas well 1 — (ref. Mattar *et al* [2008]).

We first apply the hyperbolic rate-decline relation by setting b equal to 0.9 as suggested by the computed b -parameter data trend. The matches in **Fig. 3.37** are good, especially for the D -parameter and production rate cases, but we note that most of the transient/transitional data are missing. In the case of the b -parameter the model fails to capture the declining trend of the data at the boundary dominated flow and the very early times of the existing transient flow regime. Consequently, the reserves estimate by the hyperbolic rate-decline relation over-estimates the reserves estimate using the "power-law exponential" rate-decline model.

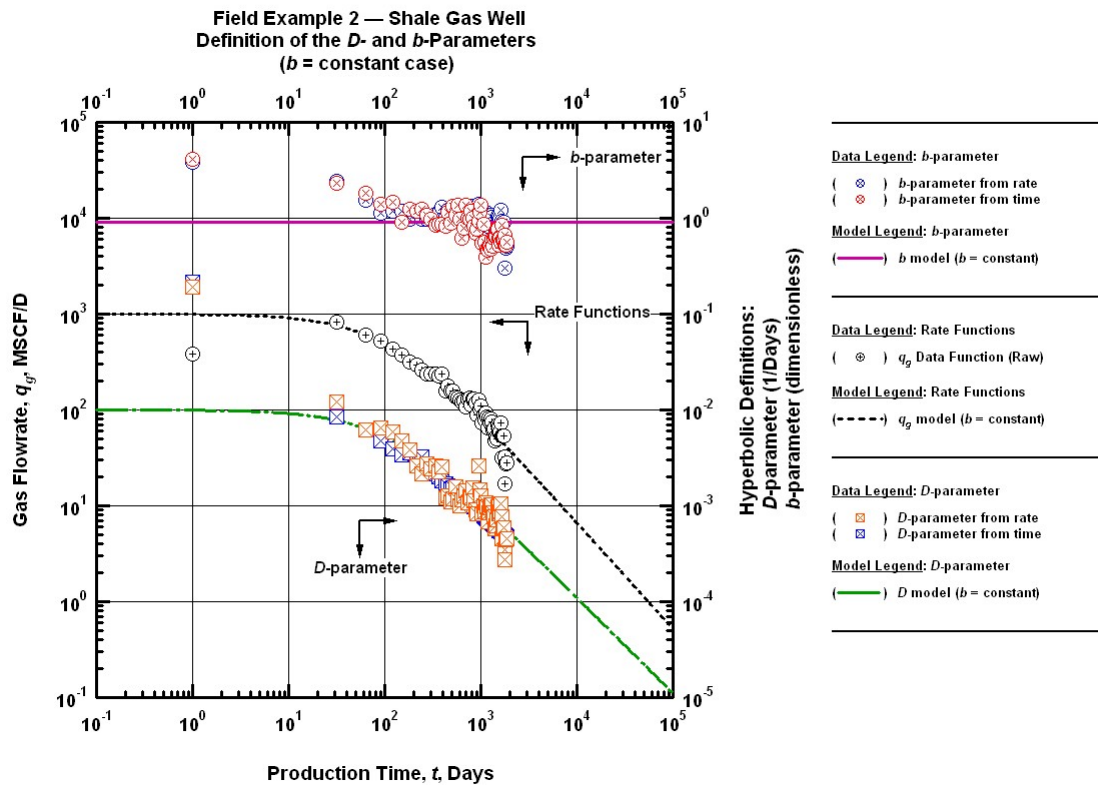


Figure 3.37 — Field Example Case 2: " q - D - b " Log-Log plot — Shale gas well 1 — (ref. Mattar *et al* [2008]) — definition of the " D and b " parameters, b -constant case (Arps' hyperbolic rate-decline relation).

We use the same rationale in the exponential b -parameter model but as mentioned earlier the exponential b -parameter model constrains the reserves estimate. **Fig. 3.38** presents the matches of the data with exponential b -parameter model and its associated relations. We can conclude from **Fig. 3.38** that all the matches are good and the reserves estimates are expected to be very accurate. However, it should be noted that most of the transient/transitional data are missing — preventing the actual performance of the model.

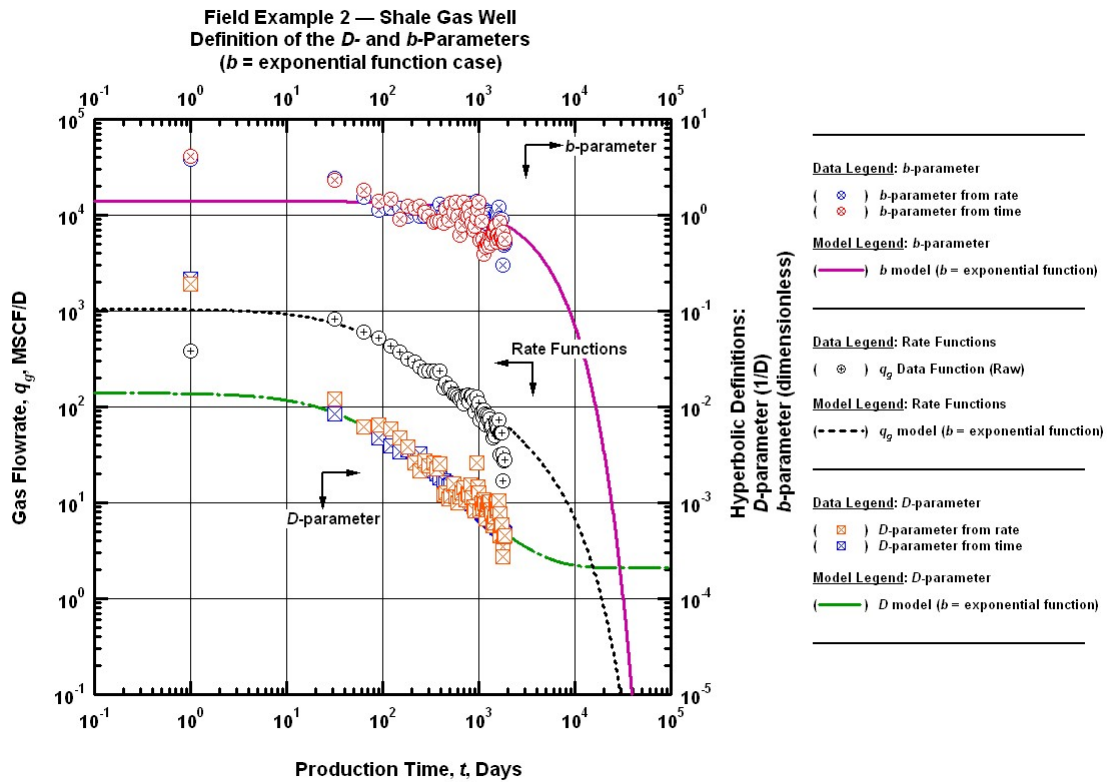


Figure 3.38 — Field Example Case 2: " q - D - b " Log-Log plot — Shale gas well 1 — (ref. Mattar *et al* [2008]) — definition of the " D and b " parameters, exponential b -parameter model.

Similarly for the power-law b -parameter model, we obtain good matches (see Fig. 3.39). In fact, the computed b -parameter data trend is not clear enough to exhibit an obvious behavior. Nevertheless, we can obtain consistent results by using all the proposed models in conjunction with each other. For example, the power-law b -parameter model is applied and forced to yield the same reserves estimate with the other models. The matches in Fig. 3.39 confirm the methodology and — as it will be shown below — the reserves estimate.

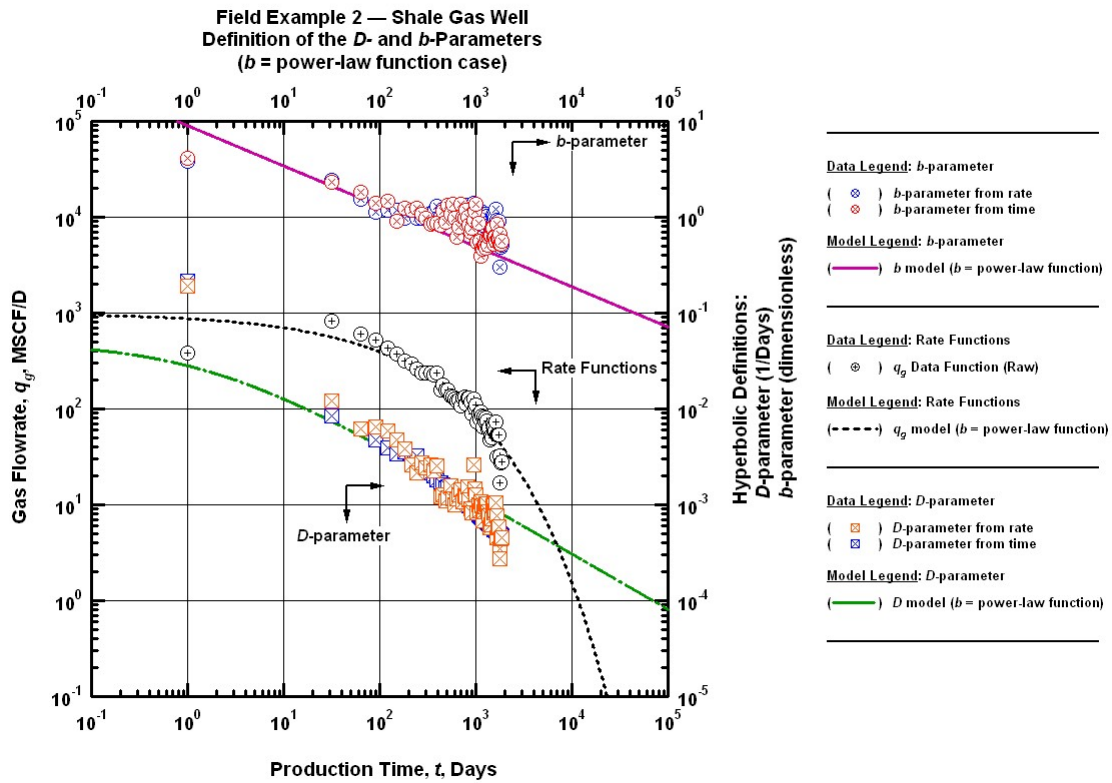


Figure 3.39 — Field Example Case 2: " q - D - b " Log-Log plot — Shale gas well 1 — (ref. Mattar *et al* [2008]) — definition of the " D and b " parameters, power-law b -parameter model.

Finally, we apply the rational b -parameter model for this case. **Fig. 3.40** presents the results — we can conclude that the best matches of the data with the model are obtained for this case. We believe this is due to the flexibility of the rational b -parameter model. We note that all the data are matched across all flow regimes. Consequently, we expect analogous matches with the production cumulative/rate data and eventually very accurate reserves estimate.

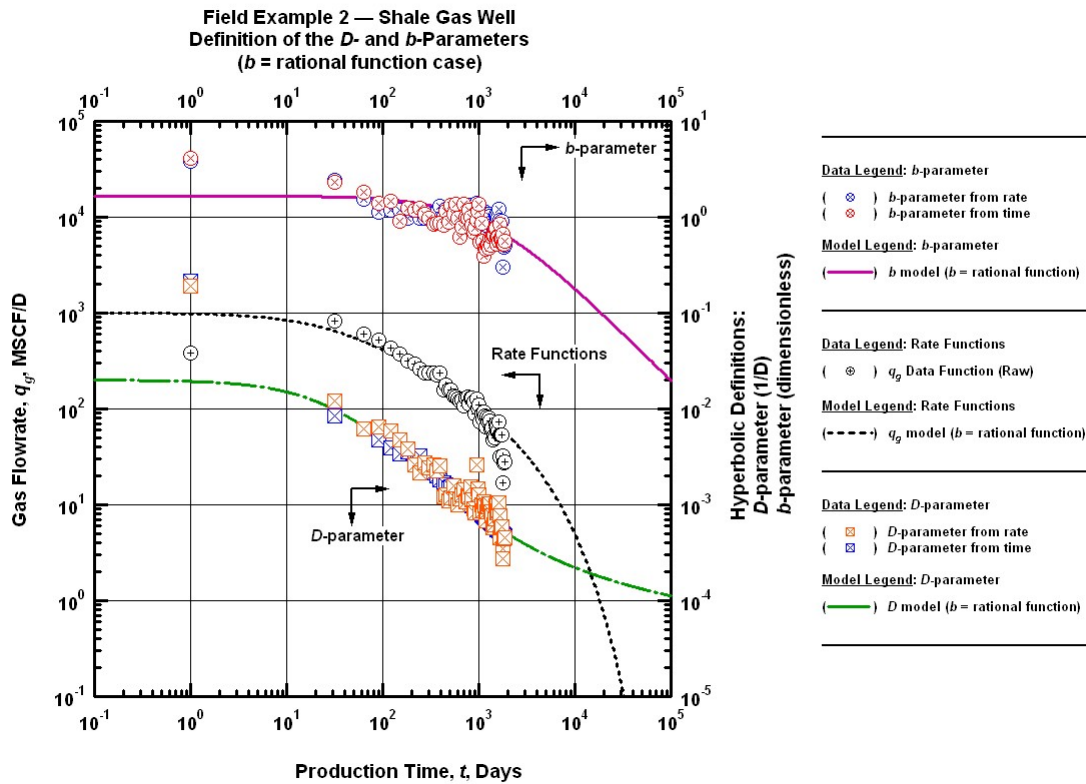


Figure 3.40 — Field Example Case 2: " q - D - b " Log-Log plot — Shale gas well 1 — (ref. Mattar *et al* [2008]) — definition of the " D and b " parameters, rational b -parameter model.

Application of the New Rate Decline Relations — Production Forecasts

The production forecasts for the shale gas well (Field Case 2) are illustrated in the semi- and log-log plots with time (**Figs. 3.41** and **3.42**) respectively below. In this case as well, the cumulative production was calculated numerically.

The performance of all the models is represented with the dotted lines in the following plots (**Figs. 3.41** and **3.42**) and their numerical illustration is shown in the **Table 3.10** below. In the case of the b -constant model, the model continues to over-estimate the original gas in place. The value of the reserves that we obtain is 0.73 BSCF, which is more than 2 times than the actual gas reserves (see **Table 3.10**). However, because of the lack of data for the transient/transitional part of the flow regimes we cannot clearly evaluate the behavior of the model at the early/middle times. The newly proposed models have successfully forecasted the original gas in place yielded for one more time remarkable results (see **Table 3.10**).

Table 3.10 — Production forecasts of the Field Case 2: Shale gas well 1 — (ref. Mattar *et al* [2008]).

Production Forecasts:

$b(t)$ =constant (base)	=	0.78 BSCF
$b(t)$ =exponential function	=	0.33 BSCF
$b(t)$ =power law function	=	0.33 BSCF
$b(t)$ =rational function	=	0.33 BSCF

Original Gas In Place (OGIP): 0.33 BSCF

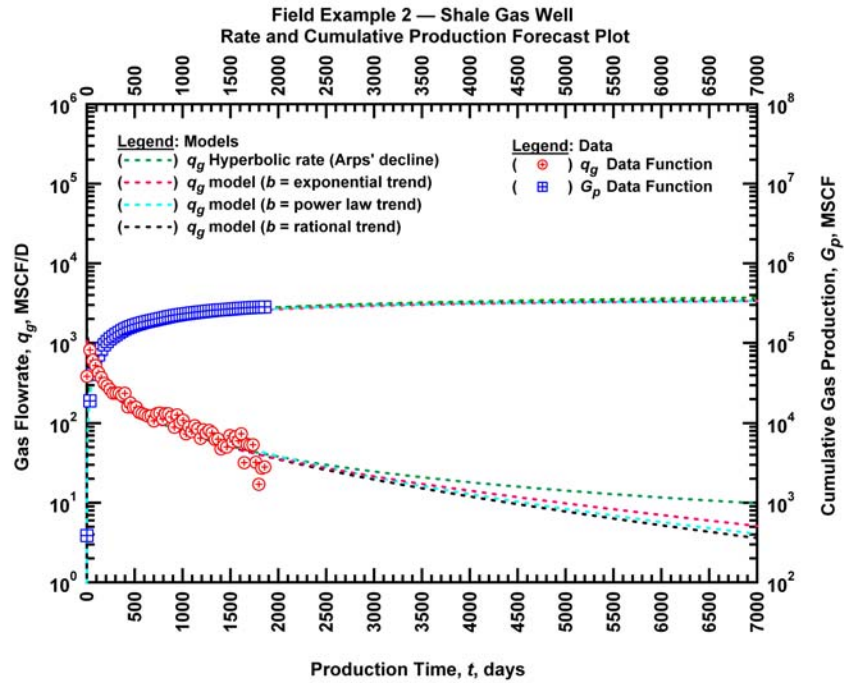


Figure 3.41 — Field Example Case 2: Production forecast (Semi-Log) plot — Shale gas well 1 — (ref. Mattar *et al* [2008]) — (all models are shown).

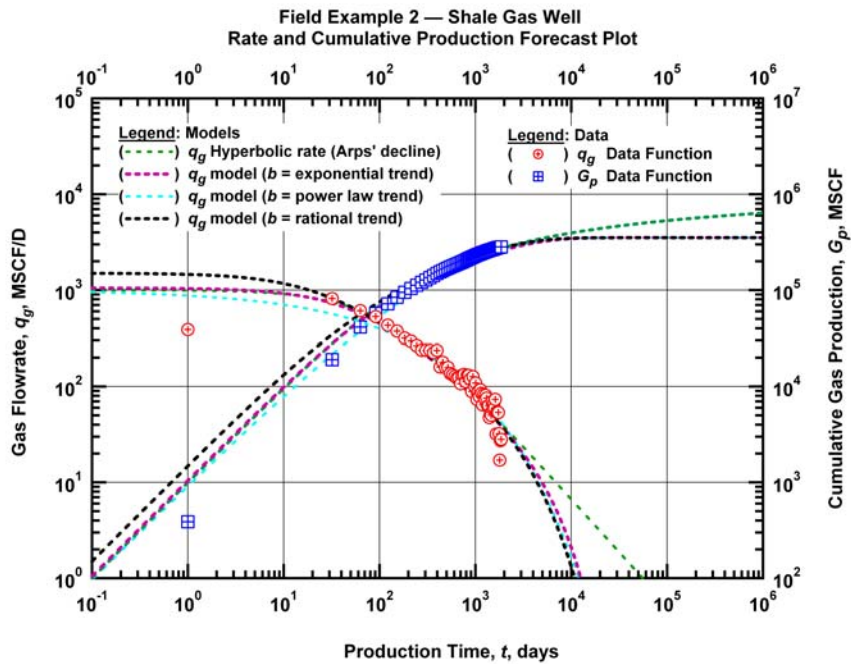


Figure 3.42 — Field Example Case 2: Production forecast (Log-Log) plot — Shale gas well 1 — (ref. Mattar *et al* [2008]) — (all models are shown).

Field Case 3: Fractured Gas Well in a Tight Gas Sand Reservoir (LWF2 – 40/70 Proppant) (Ilk *et al* [2008c])

This example is taken from the work by Ilk *et al* (Ilk *et al* [2008c]) as the first field example. It refers to a hydraulically fractured gas well producing in a tight gas sand reservoir from the Bossier field (this well corresponds to well LWF2 in the work by Ilk *et al*). **Fig. 3.43** illustrates the summary history plot for this case. Daily surface pressure and flowrate data are available for this well as well. Similarly to the first case the data quality seems to be good in general except for the involving liquid effects depicted as a "noise" in the flowrate data. The pressure data are available but are not shown in this work. Model based analysis (ref. Ilk *et al* [2008c]) yielded 6.0 BSCF for the contacted gas-in-place estimate. Our main goal in this work is to force the new rate-decline relations to obtain the same number with the model based analysis.

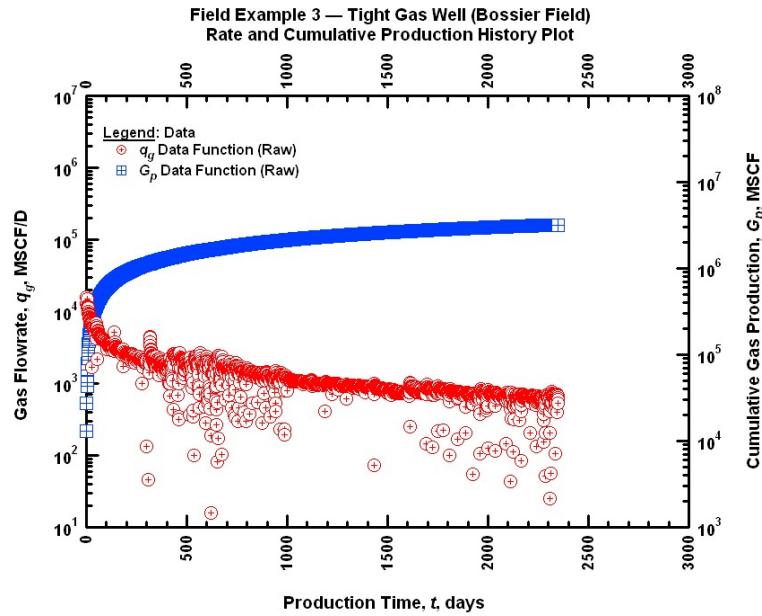


Figure 3.43 — Field Example Case 3: History (Semi-Log) plot — Fractured well in a tight gas reservoir (LWF2 – 40/70 Proppant) (ref. Ilk *et al* [2008c]).

First of all, we have to edit/delete the spurious rate data (remove the "noise") prior to numerical differentiation. Once editing is complete, the numerical differentiation can be performed. The next step is to apply the step by step procedure that we have proposed above for the application of the proposed rate-decline relations.

In **Fig. 3.44** below is illustrated the application of the Arps' rate-decline equation to this case. The value of the b -parameter is set to 0.9 in order to obtain the best matches with the computed data. As it can be seen from the graph the computed b -parameter seems to be stabilized at a value equals to 0.9 in the boundary dominated flow. However, by setting the b -parameter equal to 0.9, we manage to obtain a satisfactory match only for the boundary dominated flow. Consequently, we anticipate the same results for the case of the D -parameter and the production rate. On the other hand, this model continues not to capable of modeling the early time flow data trend therefore it is only applicable for the boundary dominated flow. Moreover, as we will analytically see in the application part below, the b -constant model will eventually over-estimate the actual reserves.

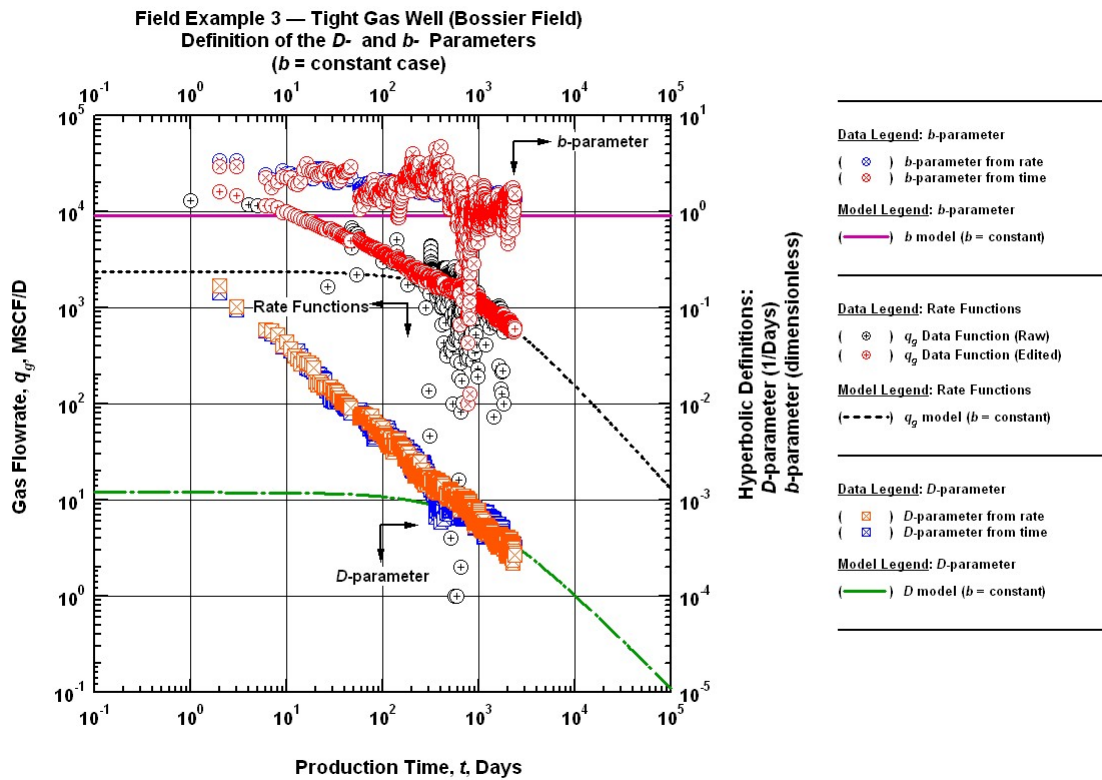


Figure 3.44 — Field Example Case 3: " q - D - b " Log-Log plot — Fractured well in a tight gas reservoir (LWF2 – 40/70 Proppant) (ref. Ilk *et al* [2008c]). — definition of the " D and b " parameters, b -constant case (Arps' hyperbolic rate-decline relation).

The next model that we apply from the series of the newly proposed rate-decline relations is the exponential b -parameter model. As we have mentioned before, this model can work as a constraining model for the Arps' hyperbolic rate decline relation by inserting the exponential declining trend at late times. We use the same value for the model parameter, b_0 , as in the case of the hyperbolic rate-decline relation (in other words we set $b_0=b$). In order to obtain the optimum match with the computed data, q_w change the value of the remaining model parameters accordingly. **Fig. 3.45** presents our matches for this case. By applying the exponential model we have achieved to match the declining trend of the computed b -parameter at the late times of the boundary dominated flow. Nevertheless, we can observe that this model cannot totally model the behavior of the computed b -parameter data at the very early times of the transient flow regime.

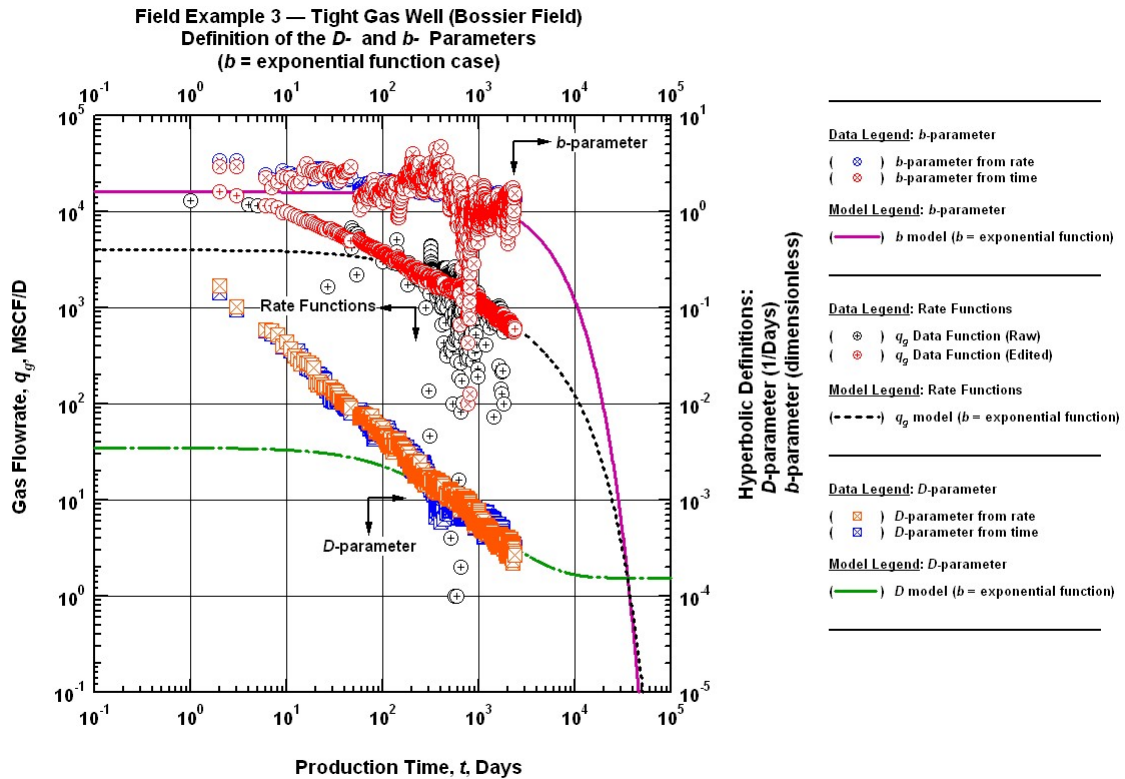


Figure 3.45 — Field Example Case 3: " q - D - b " Log-Log plot — Fractured well in a tight gas reservoir (LWF2 – 40/70 Proppant) (ref. Ilk *et al* [2008c]). — definition of the " D and b " parameters, exponential b -parameter model.

Our observations for the trend of the computed b -parameter indicate a power-law behavior. Therefore, the application of the power-law b -parameter model should yield very impressive results. **Fig. 3.46** presents the " q - D - b " plot for this case. As expected we obtain very good matches of all the data with the power-law model and its associated relations especially for the boundary dominated flow regime. In particular, the matches of the power-law model with the computed rate and b -parameter data in the boundary dominated flow as well as in the transition part are remarkably good. However, there appears to be a mismatch in all the cases with the computed data at the very early times of the transient flow. This failure of the model to capture the computed data trend at the early times is mainly because of the nature of the power-law model equation.

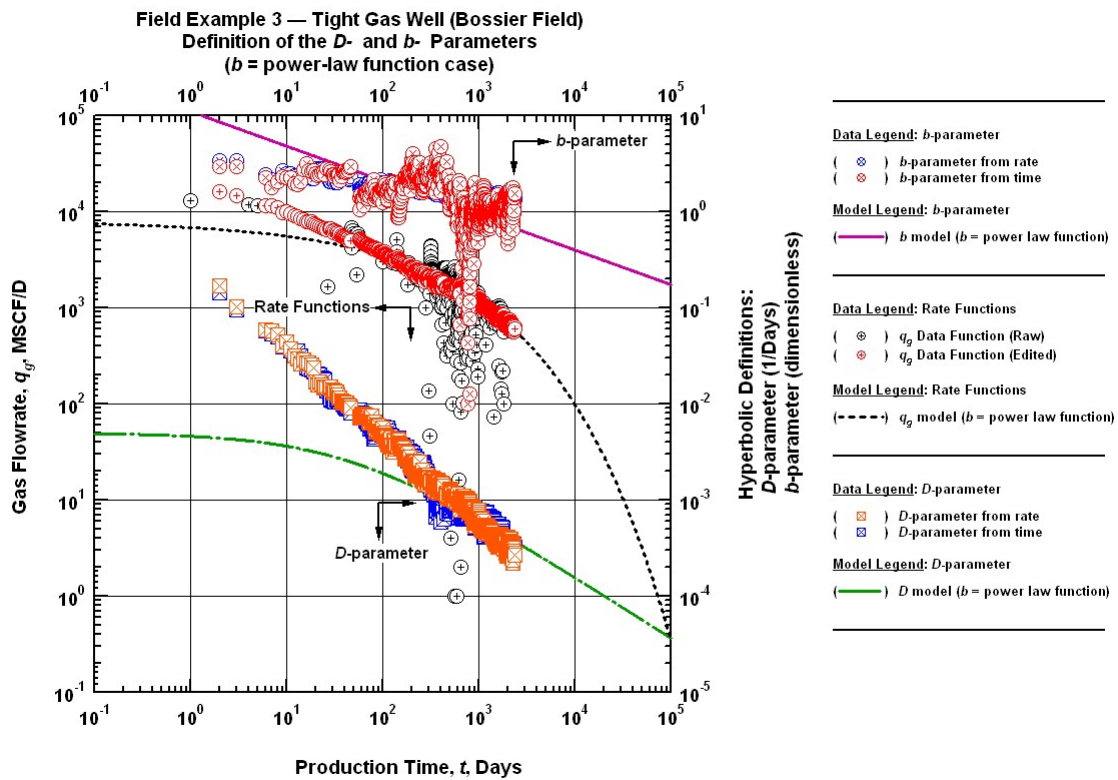


Figure 3.46 — Field Example Case 3: " q - D - b " Log-Log plot — Fractured well in a tight gas reservoir (LWF2 – 40/70 Proppant) (ref. Ilk *et al* [2008c]). — definition of the " D and b " parameters, power-law b -parameter model.

Finally we apply the rational b -parameter model to the data set. The behavior of this model is similar to the exponential b -parameter model. However, the results are expected to be better than all the other proposed models mainly due to of the flexibility that this model appears to have among the proposed models in terms of modeling the computed b -parameter data trend. We present the model matches with the data in **Fig. 3.47**. We observe extraordinary matches of the data with the model in the case of the production rate. The data are matched to the model across all flow regimes. Nevertheless, the model seems to fail at fully capturing the trend of the of the computed b - and D - parameters at the very early times of the transient flow regime.

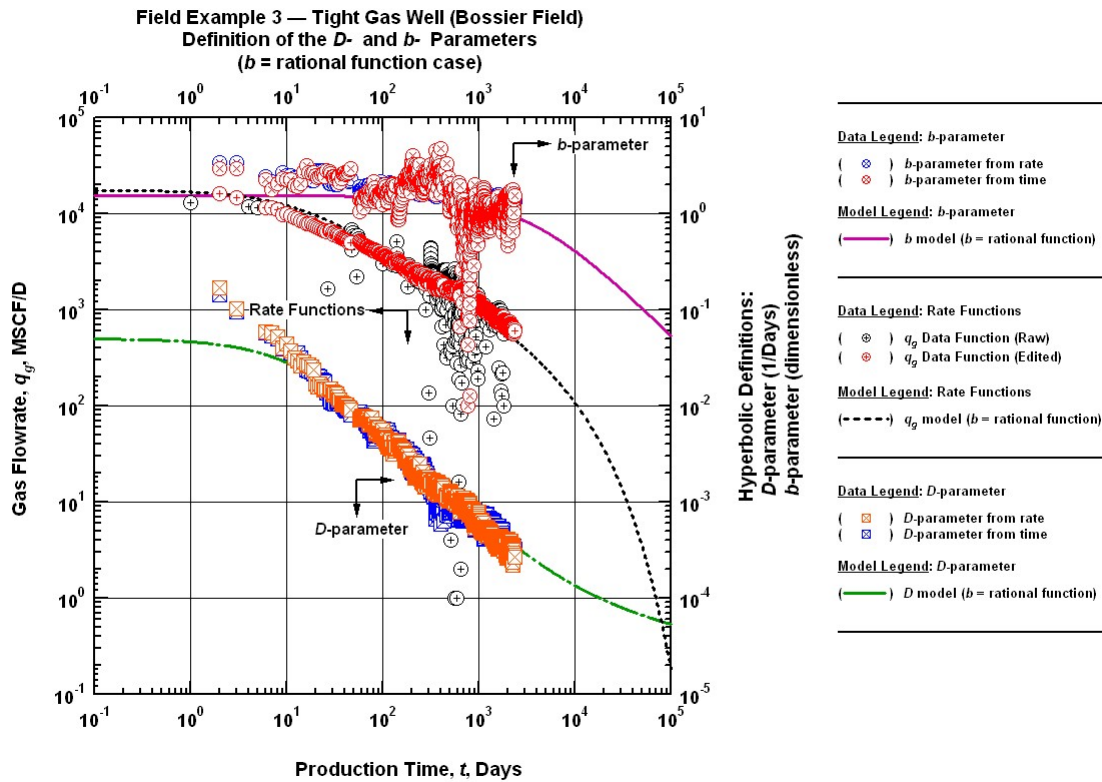


Figure 3.47 — Field Example Case 3: " q - D - b " Log-Log plot — Fractured well in a tight gas reservoir (LWF2 — 40/70 Proppant) (ref. Ilk *et al* [2008c]). — definition of the " D and b " parameters, rational b -parameter model.

Application of the New Rate Decline Relations — Production Forecasts

In the next section we will provide the results of the application of the new rate decline relations in estimating the reserves for the tight gas sand field case. The following semi- and log-log plots (**Figs. 3.48** and **3.49**) represent the performance of the new models on forecasting gas reserves for the third field case.

The results of the application of all the models are represented in the **Table 3.11** that follows. The b -constant model gives clearly an over-estimate and from the data it can be seen that the complete boundary-dominated flow has not been established yet. In particular the Arps' hyperbolic rate-decline relation gives an estimate of 14.0 BSCF overestimating the actual gas in place by more than 2 times ($G_{p,\max}=6.00$ BSCF). The performance of the new models remains remarkable and therefore they have successfully forecasted the original gas in place. However, according to the **Fig. 3.49** below, we can conclude that only the rational model can adequately model the early time behavior of the production data, while the rest of the proposed models appear to be capable of capturing only the boundary dominated flow.

Table 3.11 — Production forecasts of the Field Case 3: Fractured well in a tight gas reservoir (LWF2 – 40/70 Proppant) (ref. Ilk *et al* [2008c]).

Production Forecasts:

$b(t)=\text{constant (base)}$	=	14.5 BSCF
$b(t)=\text{exponential function}$	=	6.00 BSCF
$b(t)=\text{power law function}$	=	6.00 BSCF
$b(t)=\text{rational function}$	=	6.00 BSCF

Original Gas In Place (OGIP): 6.00 BSCF

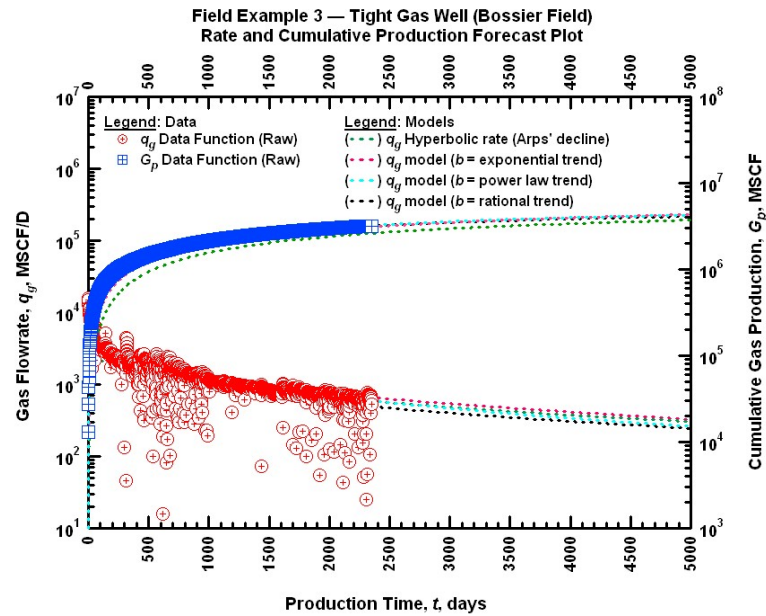


Figure 3.48 — Field Example Case 3: Production forecast (Semi-Log) plot — Fractured well in a tight gas reservoir (LWF2 – 40/70 Proppant) (ref. Ilk *et al* [2008c]) — (all models are shown).

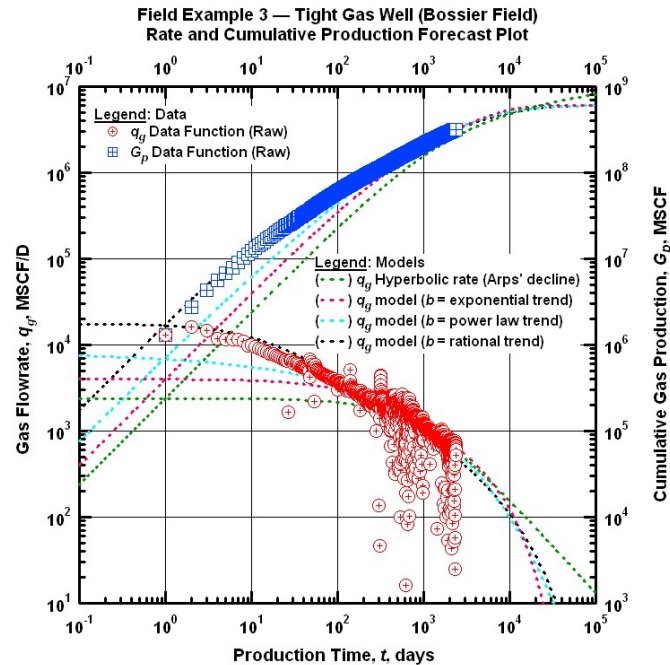


Figure 3.49 — Field Example Case 3: Production forecast (Log-Log) plot — Fractured well in a tight gas reservoir (LWF2 – 40/70 Proppant) (ref. Ilk *et al* [2008c]) — (all models are shown).

Field Case 4: Shale Gas Well (Gas Well 2 — Barnett Shale) (Mattar *et al* [2008])

The second shale gas example that we investigate includes the monthly production data obtained from shale gas well 2 from Barnett shale (Texas, USA). The production data, which is used to validate our models, was previously analyzed in the work by Mattar *et al* [2008] using the "power-law exponential" rate-decline model (Ilk *et al* [2008a] and [2008b]). By applying the newly proposed models we will try to obtain more consistent forecasts with "Power-Law Exponential" rate-decline relation. Similarly to the first shale gas well that we analyzed previously, almost 6.5 years of monthly production data are available via public records (see **Fig. 3.50**). In this case as well we visually distinguished the different flow regimes.

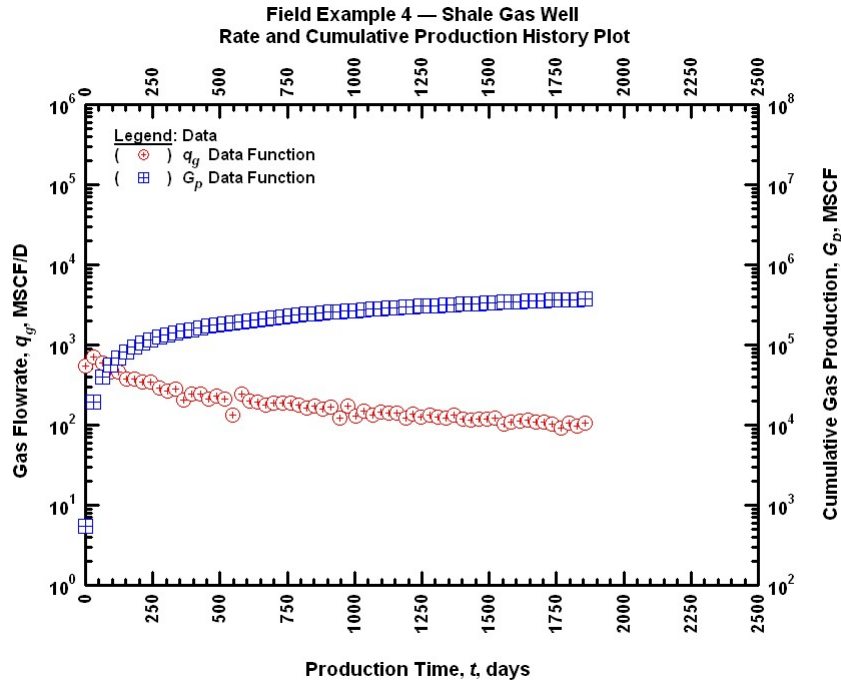


Figure 3.50 — Field Example Case 4: History (Semi-Log) plot — Shale gas well 2 — (ref. Mattar *et al* [2008]).

The first b -parameter model that we apply is the hyperbolic Arps' b -constant model. The value of b for this case is equal to 1.0 as suggested by the computed b -parameter data trend. The matches with the computed data, which are illustrated in **Fig. 3.51**, are satisfactory, especially for the D -parameter and production rate cases, but we note that most of the transient/transitional data are missing in this case as well. Therefore, no important conclusions can be drawn regarding the behavior of the model in those two cases for all the flow regimes. In the case of the b -parameter the model fails to capture the declining trend of the data at the boundary dominated flow and the very early times of the existing transient flow regime. Consequently, the reserves estimate by the hyperbolic rate-decline relation over-estimates the reserves estimate using the "power-law exponential" rate-decline model.

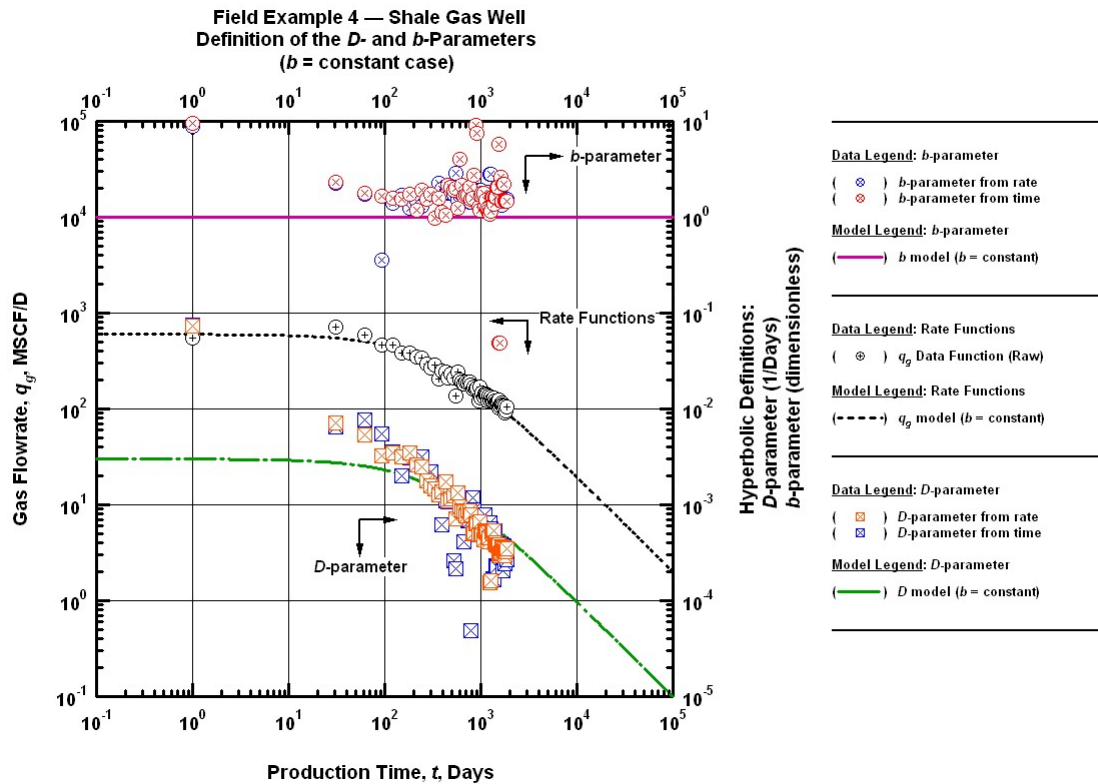


Figure 3.51 — Field Example Case 4: " q - D - b " Log-Log plot — Shale gas well 2 — (ref. Mattar *et al* [2008]) — definition of the " D and b " parameters, b -constant case (Arps' hyperbolic rate-decline relation).

The rationale for using the exponential b -parameter model is to capture the declining trend of the computed b -parameter which appears at the late times of the boundary dominated flow. Moreover, as mentioned earlier the exponential b -parameter model plays a constraining role to the reserves estimate, yielding less reserves estimate than the traditional hyperbolic rate-decline relation of Arps. In **Fig. 3.52** we present the matches of the data with exponential b -parameter model and its associated relations. According to the graph, we conclude from that all the matches are very good and the reserves estimates are expected to be very accurate. Nevertheless, because of the fact that most of the transient/transitional data are missing, we cannot adequately evaluate the behavior of the model at this flow regime.

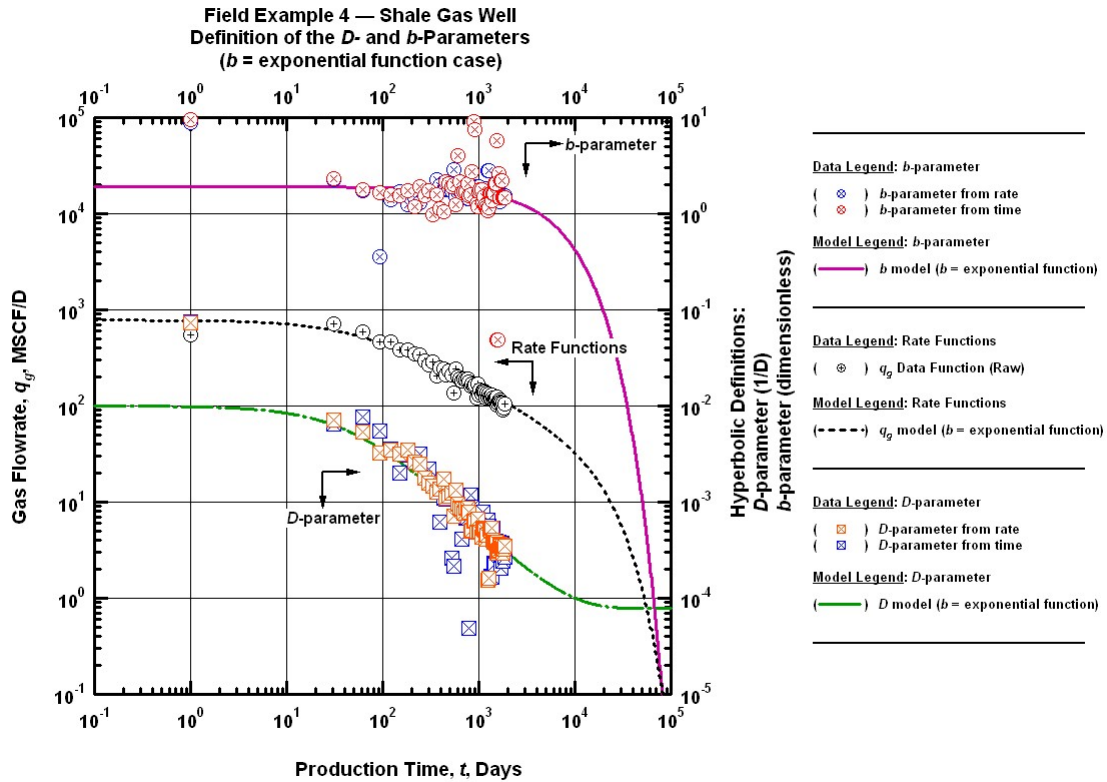


Figure 3.52 — Field Example Case 4: " q - D - b " Log-Log plot — Shale gas well 2 — (ref. Mattar *et al* [2008]) — definition of the " D and b " parameters, exponential b -parameter model.

In the case of the power-law b -parameter model, we obtain outstanding matches (see **Fig. 3.53**) with the computed data for all the cases. Although, the computed b -parameter data trend is not clear enough to exhibit an obvious behavior, however the b -parameter power-law model appears to fully capture the general declining trend of the computed b -parameter. Furthermore, we achieved very satisfactory matches in the case of the D -parameter and outstanding for the case of the production rate. Nevertheless, we can obtain consistent results by using all the proposed models in conjunction with each other. For example, the power-law b -parameter model is applied and forced to yield the same reserves estimate with the other models. The matches in **Fig. 3.53** confirm the methodology and — as it will be shown below — the reserves estimate.

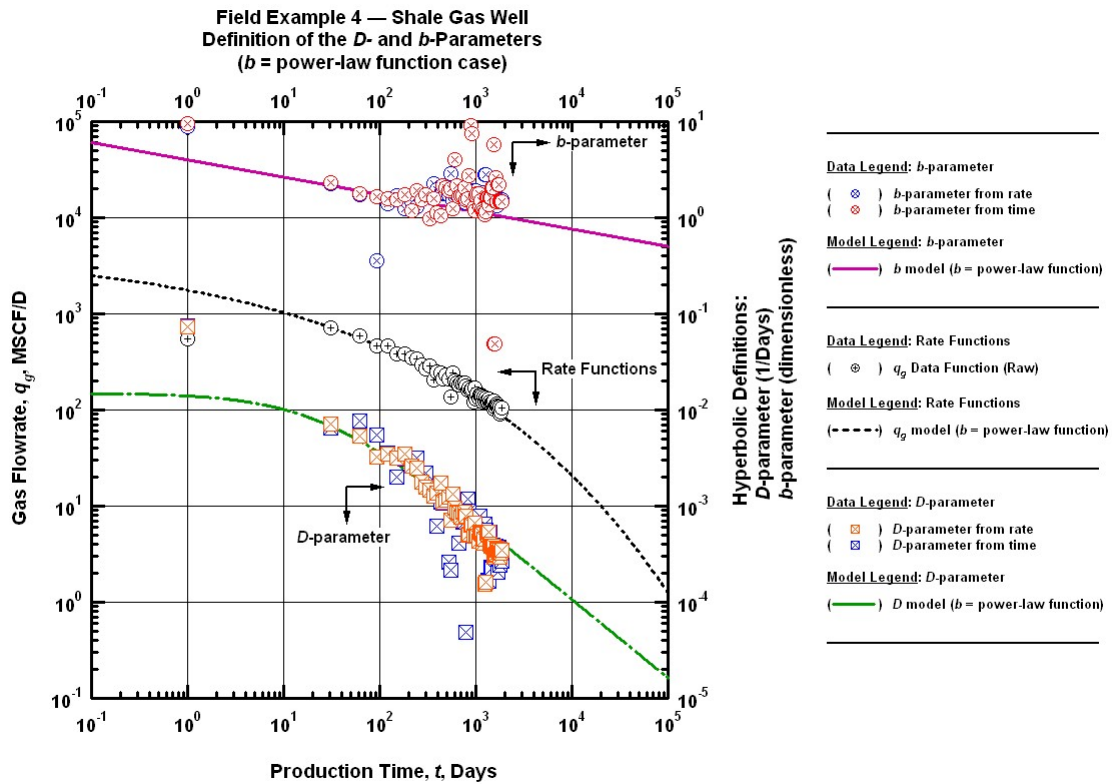


Figure 3.53 — Field Example Case 4: " q - D - b " Log-Log plot — Shale gas well 2 — (ref. Mattar *et al* [2008]) — definition of the " D and b " parameters, power-law b -parameter model.

The last model of the series of the proposed b -parameters that we applied is the rational b -parameter model. In **Fig. 3.54** below we present the results of this application. It is obvious that this model yields the best matches with the computed data so far. In general as we have mentioned earlier the nature of the equation of this model gives an extremely flexibility to it and consequently the model can be applicable to many different sets of data and wells/reservoirs by providing us excellent results. We note that all the data are matched across all flow regimes. Therefore, we expect analogous matches with the production cumulative/rate data and eventually very accurate reserves estimate.

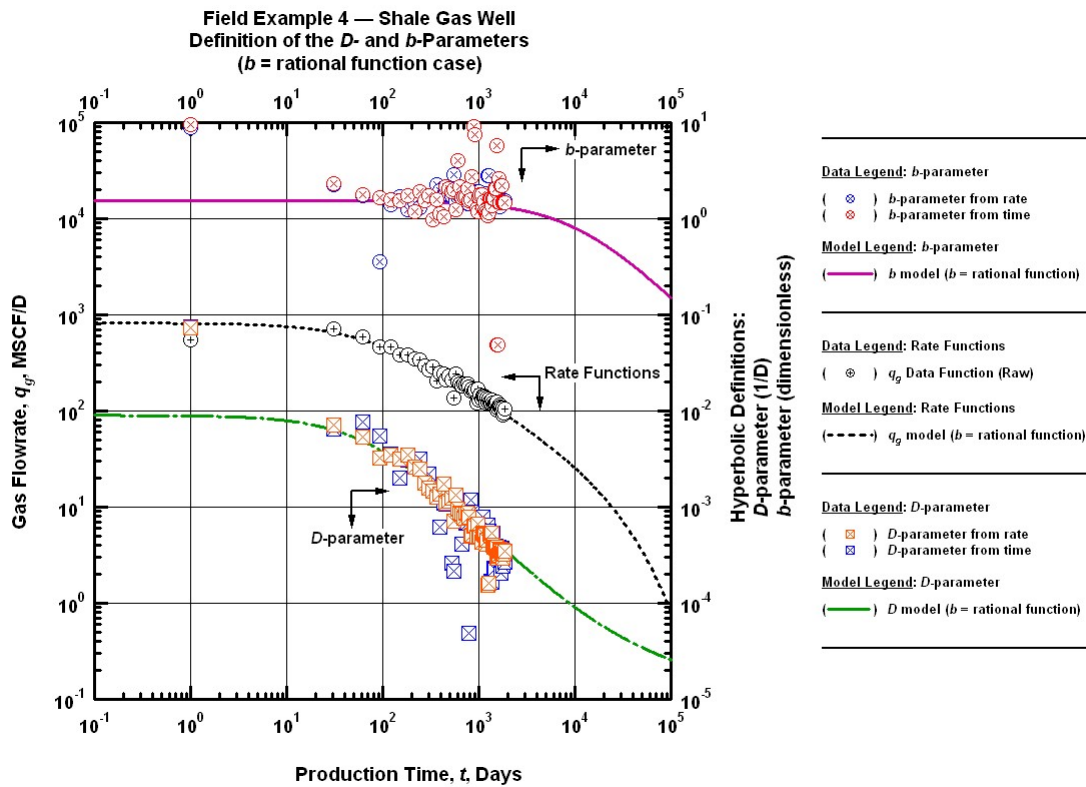


Figure 3.54 — Field Example Case 4: " q - D - b " Log-Log plot — Shale gas well 2 — (ref. Mattar *et al* [2008]) — definition of the " D and b " parameters, rational b -parameter model.

Application of the New Rate Decline Relations — Production Forecasts

In the following **Figs. 3.55** and **3.56** are illustrated the production forecasts for the shale gas well in a semi- and a log-log plot with time respectively. The cumulative production was calculated numerically by using the trapezoidal method.

The dotted colored lines represent the performance of each applied model (**Figs. 3.55** and **3.56**). The **Table 3.12** shows the numerical production forecast for each model. In the case of the b -constant model, the model continues to over-estimate the original gas in place. The value of the reserves that we obtain is 2.52 BSCF, which implies that this model has forecasted more than 1 BSCF the actual gas reserves (see **Table 3.12**). Nevertheless, we have to note that the lack of data for the transient/transitional part of the flow regimes in this case as well, does not allow us to clearly and analytically evaluate the behavior of the model at the early/middle times. The new models that we propose continue to yield excellent results and extremely accurate forecasts (see **Table 3.12**).

Table 3.12 — Production forecasts of the Field Case 4: Shale gas well 2 (Mattar *et al* [2008]).

Production Forecasts:

$b(t)$ =constant (base)	=	2.52 BSCF
$b(t)$ =exponential function	=	1.20 BSCF
$b(t)$ =power law function	=	1.20 BSCF
$b(t)$ =rational function	=	1.20 BSCF

Original Gas In Place (OGIP): 1.20 BSCF

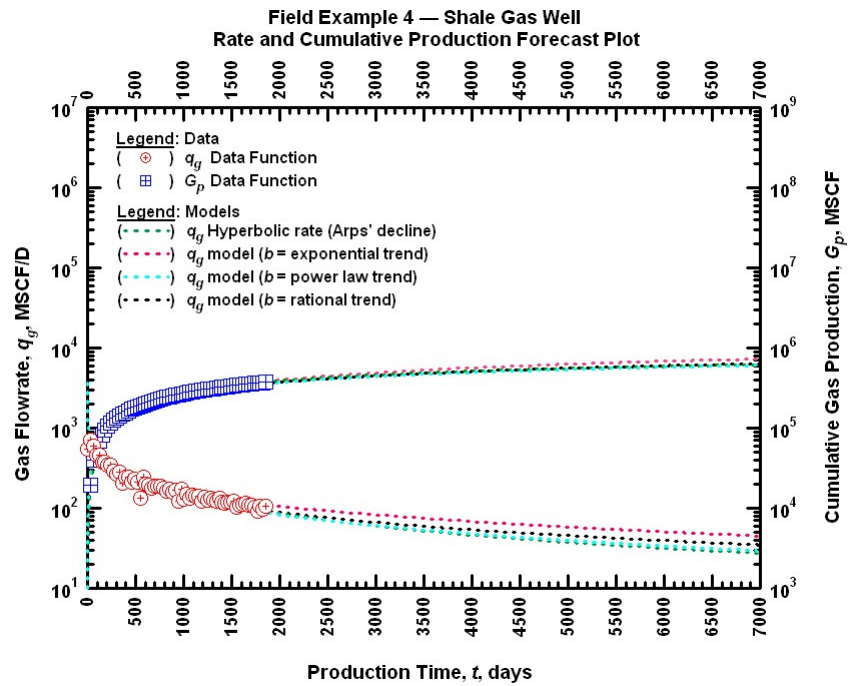


Figure 3.55 — Field Example Case 4: Production forecast (Semi-Log) plot — Shale gas well 2 — (ref. Mattar *et al* [2008]) — (all models are shown).

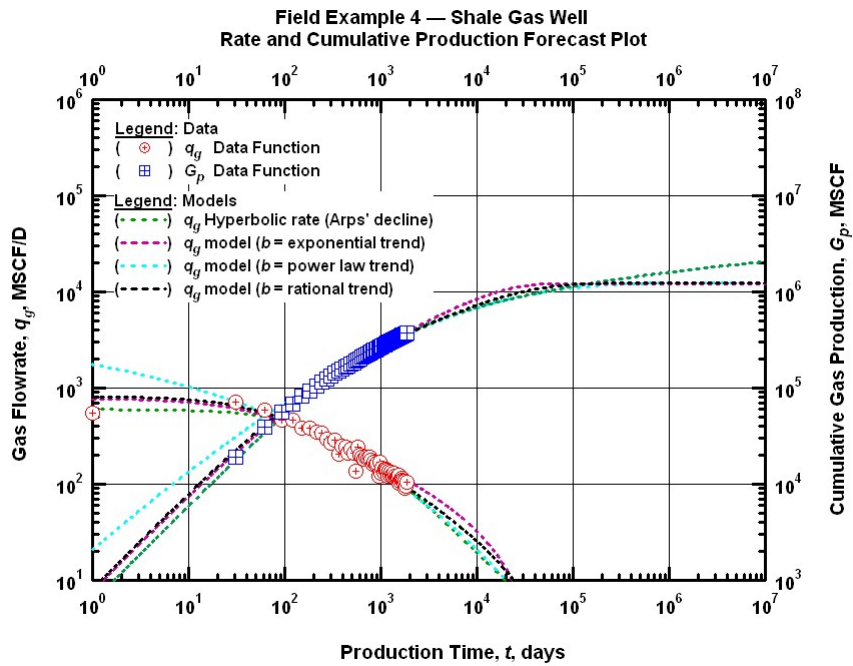


Figure 3.56 — Field Example Case 4: Production forecast (Log-Log) plot — Shale gas well 2 — (ref. Mattar *et al* [2008]) — (all models are shown).

CHAPTER IV

SUMMARY, CONCLUSIONS, AND RECOMMENDATIONS FOR FUTURE WORK

4.1 Summary

In this work we have proposed the following models for characterizing the b -parameter in addition to the Arps' hyperbolic rate decline relation (constant b -parameter case):

- Constant $b(t)$ case:
 $b(t) = \text{constant}$ (Arps' hyperbolic rate-decline relation)
- Exponential $b(t)$ case:
 $b(t) = b_0 \exp[-b_1 t]$ (exponential function)
- Power-law $b(t)$ case:
 $b(t) = b_0 t^{-b_1}$ (power-law function)
- Rational $b(t)$ case:
 $b(t) = 1/(b_0 + b_1 t)$ (rational function)

The proposed functions (models) are empirical and based on our observations. We derive the corresponding rate-decline relation for each b -parameter model by using **Eqs. 1.1** and **1.2** and solving the differential equation related with each b -parameter model. We apply the new rate-decline models to four numerical simulation cases, two tight gas sand reservoir cases, and two shale gas reservoir cases. Our results indicate that the new rate-decline models could be a useful addition to reserve estimate methods using only rate-time data.

4.2 Conclusions

1. The continuous evaluation/interpretation of the computed b -parameter data trend enhances the diagnostic understanding of the b -parameter. The behavior of the computed b -parameter data trend varies for different well/reservoir configurations (see numerical simulation cases in this work for clarity). Therefore, new rate-decline relations are required to obtain better estimates for reserves.
2. The performance of the new rate-decline relations corresponding to each b -parameter model:
 - $b(t) = \text{constant}$: This case corresponds to classical Arps' hyperbolic relation. Our experience so far has suggested that the computed b -parameter trend is *never* constant. Also, this relation is only applicable for the boundary-dominated flow regime. If the data do not exhibit boundary-dominated flow, this relation significantly over-estimates the reserves.

- $b(t)$ = exponential function: The exponential function indicates that the b -parameter is essentially constant for early and middle times, but exhibits an exponential decline for late times (boundary-dominated flow). Hence, this model can represent the boundary-dominated flow regime behavior, but not the transient flow regime(s). This model yields conservative estimates of reserves.
 - $b(t)$ = power-law function: The power-law function models the computed b -parameter trend as a straight line trend on log-log scale. For a number of field cases we have observed that the computed b -parameter trend exhibits a power-law behavior. For those particular cases the matches are typically outstanding and the reserves estimates are considered reliable.
 - $b(t)$ = rational function: We believe that the rational function for the b -parameter is the most flexible model among all the proposed models. Early time behavior is dominated by a constant, middle and late time behavior is dominated by the other model parameters causing a decline behavior. With this model, it is possible to match the computed D -parameter data trend over the entire data range. However, the rate-decline relation is tedious and it includes a special function (*i.e.*, the exponential integral) to be evaluated — on the other hand, this rate-decline relation can easily be programmed in a spreadsheet.
3. We emphasize that we do not favor a specific b -parameter model proposed in this work. We believe that each model has advantages and disadvantages — and the performance of the models can vary under different conditions. Under these circumstances we suggest the use of all the b -parameter models in conjunction to yield better resolution and to decrease the uncertainty in reserves estimates.
 4. We have also observed in some cases that the computed b -parameter trend varies according to the well/reservoir configuration (*i.e.*, different flow regimes). Numerical simulation cases 1 and 2 are examples of this situation.

4.3 Recommendations, Comments and Future Work

This work should be continued as follows:

1. For better understanding of the character of the computed b -parameter data, more models in addition to the ones proposed in this work need to be developed.
2. These models need to be applied to more cases including a variety of field data. Also, more numerical simulation cases for complex well/reservoir configurations need to be investigated.
3. Comparison with the analytical solutions can also be performed to validate the proposed models from a theoretical stand point.

NOMENCLATURE

Variables:

${}_2F_1(x)$	= Hypergeometric series (Gauss' hypergeometric functions)
A	= Drainage area, acres
b	= Arps' decline exponent
b_0	= model parameter
b_1	= model parameter
c_f	= Formation compressibility, psi ⁻¹
D	= Decline parameter defined by Eq. 1
D_i	= Initial decline parameter ($t=0$)
$E_i(x)$	= Exponential integral
G_p	= Cumulative gas production, MSCF
$G_{p,max}$	= Maximum gas production, MSCF
q	= Gas production rate, MSCF/D
q_i	= Initial Gas production rate, MSCF/D or STB/D
h	= Net Pay thickness, ft
k	= Average reservoir permeability, md
L_h	= Horizontal well length, ft
p_{wf}	= Average reservoir pressure, psia
r_e	= Reservoir drainage radius, ft
r_w	= Wellbore radius, ft
s	= Skin factor, dimensionless
S_g	= Gas saturation, fraction
t	= Time, days
T	= Reservoir temperature, °F
w_f	= Fracture width, inches
z_w	= Position of the horizontal well, ft

Dimensionless Variables:

F_{cD}	= Dimensionless fracture conductivity
----------	---------------------------------------

Greek Symbols:

γ_g	= Reservoir gas specific gravity (air = 1)
------------	--

ϕ = Porosity, fraction

Subscripts:

i = Integral function or initial value

REFERENCES

Abramowitz, M. and Stegun, I.A. 1972. *Handbook of Mathematical Functions*. New York: Dover.

Agarwal, R.G., Gardner, D.C., Kleinsteinber, S.W. and Fussell, D.D. 1999. Analyzing Well Production Data Using Combined Type-Curve and Decline-Curve Analysis Concepts. *SPEEE*. **2** (5): 478-486.

Amini, S., Ilk, D., and Blasingame, T.A. 2007. Evaluation of the Elliptical Flow Period for Hydraulically-Fractured Wells in Tight Gas Sands — Theoretical Aspects and Practical Considerations. Paper SPE 106308 presented at the SPE Hydraulic Fracturing Technology Conference, College Station, Texas, 29–31 January.

Arps J.J. 1945. Analysis of Decline Curves. *Trans. AIME*: **160**, 228-247.

Bourdet, D., Ayoub, J.A., and Pirad, Y.M. 1989. Use of Pressure Derivative in Well-Test Interpretation. *SPEFE*. **4** (2): 293-302.

Doublet, L.E., Pande, P.K, McCollum, T.J., and Blasingame, T.A. 1994. Decline Curve Analysis Using Type Curves—Analysis of Oil Well Production Data Using Material Balance Time: Application to Field Cases. Paper SPE 28688 presented at the International Petroleum Conference and Exhibition of Mexico, Veracruz, Mexico, 10-13 October.

Ecrin Software, Kappa Engineering Software, www.kappaengineering.com . Accessed on 26 June 2009.

Fetkovich, M.J. 1980. Decline Curve Analysis Using Type Curves. *JPT*. **32** (6): 1065-1077.

Fetkovich, M.J., Fetkovich, E.J., and Fetkovich, M.D. 1996. Useful Concepts for Decline-Curve Forecasting, Reserve Estimation and Analysis. *SPEEE*. **11** (1): 13-22.

Gradshteyn, I.S., and Ryzhik, I.M. 1996. *Table of Integrals, Series, and Products*. San Diego: Academic Press.

Ilk, D., Rushing, J.A., and Blasingame, T.A. 2008a. Estimating Reserves Using the Arps Hyperbolic Rate-Time Relation — Theory, Practice and Pitfalls. Paper CIM 2008-108 presented at the 59th Annual Technical Meeting of the Petroleum Society, Calgary, Alberta, Canada, 17-19 June.

Ilk, D., Perego, A.D., Rushing, J.A., and Blasingame, T.A. 2008b. Exponential vs. Hyperbolic Decline in Tight Gas Sands — Understanding the Origin and Implications for Reserve Estimates Using Arps' Decline Curves. Paper SPE 116731 presented at the SPE Annual Technical Conference and Exhibition, Denver, Colorado, 21-24 September.

Ilk, D., Perego, A.D., Rushing, J.A., and Blasingame, T.A. 2008c. Integrating Multiple Production Analysis Techniques To Assess Tight Gas Sand Reserves: Defining a New Paradigm for Industry Best Practices. Paper SPE 114947 presented at the SPE Gas Technology Symposium, Calgary, Alberta, Canada, 17-19 June.

Johnson, R.H. and Bollens, A.L. 1927. The Loss Ratio Method of Extrapolating Oil Well Decline Curves. Trans. AIME **77**: 771.

Kupchenko, C.L., Gault, B.W., and Mattar, L. 2008. Tight Gas Production Performance Using Decline Curves. Paper SPE 114991 presented at the SPE Gas Technology Symposium, Calgary, Alberta, Canada, 17-19 June.

Maley, S. 1985. The Use of Conventional Decline Curve Analysis in Tight Gas Sands. Paper SPE 13898 presented at the SPE Low Permeability Gas Reservoirs Symposium, Denver, CO, May 19-22.

Mathematica. 2007. <http://www.wolfram.com>

Mattar, L., Gault, B.W., Morad, K., Clarkson, C.R., Freeman, C.M., Ilk, D., and Blasingame, T.A. 2008. Production Analysis and Forecasting of Shale Gas Reservoirs: Case History-Based Approach. Paper SPE 119897 presented at the SPE Shale Gas Production Conference, Fort Worth, TX, 16-18 November.

Rushing, J.A., Perego, A.D., Sullivan, R.B., and Blasingame, T.A. 2007. Estimating Reserves in Tight Gas Sands at HP/HT Reservoir Conditions: Use and Misuse of an Arps Decline Curve Methodology.

Paper SPE 109625 presented at the 2007 Annual SPE Technical Conference and Exhibition, Anaheim, CA., 11-14 November.

Valko, P.P. 2009. Assigning Value to Stimulation in the Barnett Shale: A Simultaneous Analysis of 7000 Plus Production Histories and Well Completion Records. Paper SPE 119369 presented at the SPE Hydraulic Fracturing Technology Conference, Woodlands, TX, January 19-21.

APPENDIX A

DERIVATION OF THE RATE DECLINE RELATIONS

The derivation of the Arps hyperbolic rate relation (Arps [1945]) is provided earlier in the work by Blasingame and Rushing [2006]. This derivation is provided for the purpose of orienting the analyst in the application of the Arps hyperbolic rate decline relation. Although there is no theoretical basis to force the "*b*-parameter" in the range between 0 and 1 ($0 < b < 1$), we suggest the use of the hyperbolic rate relation as a *starting point* for "modern" methods to correlate and extrapolate rate performance behavior by limiting the *b*-parameter between 0 and 1.

Arps defined the so-called "loss-ratio" and the "derivative of the loss-ratio" functions as:

Definition of the Loss-Ratio:

$$\frac{1}{D} \equiv -\frac{q}{dq/dt} \dots\dots\dots (A-1)$$

Derivative of the Loss-Ratio:

$$b \equiv \frac{d}{dt} \left[\frac{1}{D} \right] \equiv -\frac{d}{dt} \left[\frac{q}{dq/dt} \right] \dots\dots\dots (A-2)$$

As mentioned earlier, our primary objective in this work is to characterize the behavior of the "*b*-parameter" and consequently obtain the corresponding rate-time relation. In this appendix we derive the rate relations for the proposed characterizations for the "*b*-parameter".

Exponential Rate Decline Case (*b*=0)

This case corresponds to the special condition where the "*b*-parameter" is equal to zero. Using this condition we have

$$\frac{1}{D} = -\frac{q}{dq/dt} \dots\dots\dots (A-3)$$

Equation A-3 implies that the *D*-parameter is constant and can be defined as D_i (*i.e.*, initial decline). Consequently, Eq. A-3 becomes

$$\frac{1}{q} \frac{dq}{dt} = -D_i \dots\dots\dots (A-4)$$

Separation of variables yields

$$\frac{dq}{q} = -D_i dt \dots\dots\dots (A-5)$$

Integrating Eq A-5, we obtain:

$$\int_{q_i}^q \frac{dq}{q} = -D_i \int_0^t dt \dots\dots\dots (A-6)$$

Completing the integration gives us the following result:

$$\ln \left[\frac{q}{q_i} \right] = -D_i t \dots\dots\dots (A-7)$$

In order to solve for the rate function, we exponentiate and rearrange both sides, this yields the exponential rate decline relation:

$$q = q_i \exp(-D_i t) \dots\dots\dots (A-8)$$

Hyperbolic Rate Decline Case ($b=\text{constant}$)

The starting point for this case is Eq. A-2 where we assume that the b -parameter is constant.

$$b = -\frac{d}{dt} \left[\frac{q}{dq/dt} \right] \dots\dots\dots (A-9)$$

Separating the variables we have:

$$d \left[\frac{q}{dq/dt} \right] = -b dt \dots\dots\dots (A-10)$$

Taking the indefinite integration yields

$$\frac{q}{dq/dt} = -bt - c \dots\dots\dots (A-11)$$

where c is defined as the constant of integration. Recalling the definition of the loss-ratio (Eq. A-1):

$$\frac{1}{D} = bt + c \dots\dots\dots (A-12)$$

The definition for the initial decline term states that D_i is defined as t goes to zero (*i.e.*, $D \approx D_i$, $t \rightarrow 0$). By using this definition we obtain the value for the constant of integration.

$$\frac{1}{D_i} = c \dots\dots\dots (A-13)$$

Substituting the constant of integration in Eq. A-11 gives us:

$$\frac{q}{dq/dt} = -bt - \frac{1}{D_i} \dots\dots\dots (A-14)$$

Taking the reciprocal of Eq. A-14 we have:

$$\frac{1}{q} \frac{dq}{dt} = \frac{1}{-bt - \frac{1}{D_i}} = -D_i \frac{1}{1 + bD_i t} \dots\dots\dots (A-15)$$

By integrating Eq. A-21 we have:

$$\int_{q_i}^q \frac{1}{q} dq = \ln \left[\frac{q}{q_i} \right] = -D_i \int_0^t \frac{1}{1 + bD_i t} dt \dots\dots\dots (A-16)$$

To solve the integral in the right-hand-side of Eq A-16, a variable of substitution is defined as shown below:

$$z = 1 + bD_i t \quad (\text{at } t = 0; z = 1 \text{ and at } t = t; z = 1 + bD_i t) \dots\dots\dots (A-17)$$

Therefore:

$$dz = 1 + bD_i dt \quad \text{or} \quad dt = \frac{1}{bD_i} dz \dots\dots\dots (A-18)$$

By using the transformation, the right-hand-side of the equation becomes:

$$\begin{aligned} RHS &= -D_i \int_0^t \frac{1}{1 + bD_i t} dt \\ &= -D_i \int_0^{1+bD_i t} \left[\frac{1}{z} \right] \left[\frac{1}{bD_i} \right] dz \\ &= -\frac{1}{b} D_i \int_0^{1+bD_i t} \left[\frac{1}{z} \right] dz \dots\dots\dots (A-19) \\ &= -\frac{1}{b} \ln[1 + bD_i t] \\ &= \ln \left[(1 + bD_i t)^{-\frac{1}{b}} \right] \end{aligned}$$

Substituting the solution of the right-hand-side into Eq. A-16, we finally have:

$$\ln \left[\frac{q}{q_i} \right] = \ln \left[(1 + bD_i t)^{-\frac{1}{b}} \right] \dots\dots\dots (A-20)$$

Exponentiating the both sides of Eq. A-20, we have:

$$\frac{q}{q_i} = (1 + bD_i t)^{-\frac{1}{b}} \dots\dots\dots (A-21)$$

Solving for the rate term yields the hyperbolic rate decline relation:

$$q = \frac{q_i}{(1 + bD_i t)^{1/b}} \dots\dots\dots (A-22)$$

The special case for Eq. A-22 is defined when the b -parameter is equal to one. This condition refers to the "harmonic" rate-decline relation (as shown below).

$$q = \frac{q_i}{(1 + D_i t)} \dots\dots\dots (A-23)$$

Characterization of the b -parameter — Derivation of the New Rate Decline Relations

• Exponential b -parameter model — $b(t)=b_0 \exp[-b_1 t]$

This case presents the derivation of the rate relation based on characterizing the b -parameter as an exponential function. We propose the following equation to model the b -parameter.

$$b(t) = b_0 \exp[-b_1 t] \dots\dots\dots (A-24)$$

Recalling the definition of the derivative of the loss-ratio (Eq. A-2) and inserting Eq. A-24 for the b -parameter term, we have:

$$-\frac{d}{dt} \left[\frac{q}{dq/dt} \right] = b_0 \exp[-b_1 t] \dots\dots\dots (A-25)$$

Separating the terms and integrating indefinitely yields:

$$-\int d \left[\frac{q}{dq/dt} \right] = b_0 \int \exp[-b_1 t] dt \dots\dots\dots (A-26)$$

Completing the integration we have:

$$-\frac{q}{dq/dt} = -\frac{b_0 \exp[-b_1 t]}{b_1} + c \dots\dots\dots (A-27)$$

Where c is defined as the constant of integration. Recalling the definition for the D -parameter, we have:

$$\frac{1}{D} = -\frac{b_0 \exp[-b_1 t]}{b_1} + c \dots\dots\dots (A-28)$$

We set $t=0$ ($D=D_i$) and solve for the constant of integration. This gives:

$$c = \frac{1}{D_i} + \frac{b_0}{b_1} \dots\dots\dots (A-29)$$

Substituting Eq. A-29 into Eq. A-27 we obtain:

$$-\frac{q}{dq/dt} = -\frac{b_0 \exp[-b_1 t]}{b_1} + \frac{1}{D_i} + \frac{b_0}{b_1} \dots\dots\dots (A-30)$$

Taking the reciprocal of Eq. A-30 gives us:

$$-\frac{1}{q} \frac{dq}{dt} = \frac{1}{\left[-\frac{b_0 \exp[-b_1 t]}{b_1} + \frac{1}{D_i} + \frac{b_0}{b_1} \right]} \dots\dots\dots (A-31)$$

Separating the rate (q) and time (t) variables, we have:

$$-\frac{dq}{q} = \frac{dt}{\left[-\frac{b_0 \exp[-b_1 t]}{b_1} + \frac{1}{D_i} + \frac{b_0}{b_1} \right]} \dots\dots\dots (A-32)$$

Taking the integral of both sides yields:

$$-\int \frac{dq}{q} = \int \frac{dt}{\left[-\frac{b_0 \exp[-b_1 t]}{b_1} + \frac{1}{D_i} + \frac{b_0}{b_1} \right]} \dots\dots\dots (A-33)$$

Completing the integration, we obtain:

$$-\ln[q] = \frac{D_i}{b_1 + b_0 D_i} \ln[b_1 \exp[b_1 t] + b_0 D_i (-1 + \exp[b_1 t])] c \dots\dots\dots (A-34)$$

Where c is defined as the integration constant. We use the following condition to find the integration constant, c .

$$q = q_i, \quad t \rightarrow 0 \dots\dots\dots (A-35)$$

As $t \rightarrow 0$, Eq. A-34 becomes:

$$-\ln[q_i] = \frac{D_i}{b_1 + b_0 D_i} \ln[b_1] c \dots\dots\dots (A-36)$$

Solving for the integration constant, c , we obtain:

$$\frac{q_i}{b_1^{-D_i/(b_1+b_0 D_i)}} = c \dots\dots\dots (A-37)$$

Substituting Eq. A-37 into Eq. A-34 yields:

$$\ln[q] = \frac{-D_i}{b_1 + b_0 D_i} \ln[b_1 \exp[b_1 t] + b_0 D_i (-1 + \exp[b_1 t])] \frac{q_i}{b_1^{-D_i/(b_1+b_0 D_i)}} \dots\dots\dots (A-38)$$

Finally, rearranging Eq. A-38 for the rate term, we obtain the following relation for the case where the b -parameter is characterized as an exponential function:

$$q = q_i (b_1 \exp[b_1 t] + b_0 D_i (-1 + \exp[b_1 t]))^{-D_i/(b_1+b_0 D_i)} b_1^{D_i/(b_1+b_0 D_i)} \dots\dots\dots (A-39)$$

Eq. A-39 can be represented in a simpler form as:

$$q = A + (B + C \exp[-Dt]) \dots\dots\dots (A-40)$$

• **Power-law b -parameter model** — $b(t) = b_0 t^{-b_1}$

For this case we model the b -parameter trend as a power-law function. This formulation is given as:

$$b(t) = b_0 t^{-b_1} \dots\dots\dots (A-41)$$

Recalling the definition of the derivative of the loss-ratio (Eq. A-2) and inserting Eq. A-41 for the b -parameter term, we have:

$$-\frac{d}{dt} \left[\frac{q}{dq/dt} \right] = b_0 t^{-b_1} \dots\dots\dots (A-42)$$

Separating the terms and integrating indefinitely yields:

$$-\int d \left[\frac{q}{dq/dt} \right] = b_0 \int t^{-b_1} dt \dots\dots\dots (A-43)$$

Completing the integration we have:

$$-\frac{q}{dq/dt} = -\frac{b_0 t^{1-b_1}}{1-b_1} + c \dots\dots\dots (A-44)$$

Where c is defined as the integration constant. We obtain the value of c similarly as before.

$$c = -\frac{1}{D_i} + \frac{1}{b_1} \dots\dots\dots (A-45)$$

Substituting Eq. A-45 into Eq. A-44, we have:

$$-\frac{q}{dq/dt} = -\frac{b_0 t^{1-b_1}}{1-b_1} - \frac{1}{D_i} + \frac{1}{b_1} \dots\dots\dots (A-46)$$

Taking the reciprocal of both sides we obtain the following:

$$\frac{dq}{q} = \frac{dt}{\left[\frac{b_0 t^{1-b_1}}{1-b_1} + \frac{1}{D_i} - \frac{1}{b_1} \right]} \dots\dots\dots (A-47)$$

Separating and integrating yields:

$$\int \frac{dq}{q} = \int \frac{dt}{\left[\frac{b_0 t^{1-b_1}}{1-b_1} + \frac{1}{D_i} - \frac{1}{b_1} \right]} \dots\dots\dots (A-48)$$

The integration on the right-hand-side is performed using a symbolic computer language (Mathematica [2007]): The result is given as:

$$\ln[q] = \frac{b_1 D_i}{b_1 - D_i} t {}_2F_1 \left[\frac{1}{1-b_1}, 1, 1 + \frac{1}{1-b_1}, \frac{b_0 b_1 D_i t^{1-b_1}}{(1-b_1)(b_1 - D_i)} \right] c \dots\dots\dots (A-49)$$

Where c is defined as the integration constant and ${}_2F_1$ is the hypergeometric function (Gradshteyn and Ryzhik [1980]). Solving for the integration constant ($t=0$), we obtain:

$$c = q_i \dots\dots\dots (A-50)$$

For our purposes we perform a two-term series expansion for the hypergeometric function (${}_2F_1$).

$${}_2F_1\left[\frac{1}{1-b_1}, 1, 1+\frac{1}{1-b_1}, \frac{b_0 b_1 D_i t^{1-b_1}}{(1-b_1)(b_1-D_i)}\right] \approx 1 + \frac{(b_1-1)(b_1-D_i)t^{(b_1-1)}}{b_0 b_1^2 D_i} \quad (\text{A-51})$$

Inserting A-51 into Eq. A-49 and rearranging gives us the rate-decline relation for the power-law b -parameter case:

$$q = q_i \exp\left[\frac{(b_1-1)(b_1-D_i)t^{b_1}}{b_0 b_1^2}\right] \quad (\text{A-52})$$

We note that Eq. A-52 can be written in a general form as:

$$q = A \exp[-Bt^C] \quad (\text{A-53})$$

Where A , B , and C are constants.

• **Rational b -parameter model** — $b(t)=1/(b_0 + b_1 t)$

For this case we model the b -parameter trend as a rational function given by the following equation:

$$b(t) = 1/(b_0 + b_1 t) \quad (\text{A-54})$$

Recalling the definition for the derivative of the loss-ratio (Eq. A-2), we have:

$$-\frac{d}{dt}\left[\frac{q}{dq/dt}\right] = 1/(b_0 + b_1 t) \quad (\text{A-55})$$

Separating and integrating yields:

$$-\int d\left[\frac{q}{dq/dt}\right] = \int \frac{dt}{(b_0 + b_1 t)} \quad (\text{A-56})$$

Completing the integration of both sides, we obtain:

$$-\frac{q}{dq/dt} = \frac{\ln[b_0 + b_1 t]}{b_1} + c \quad (\text{A-57})$$

c is defined as the constant of integration. We obtain the value for the constant of integration by setting $t=0$.

$$\frac{1}{D_i} = \frac{\ln[b_0]}{b_1} + c \quad (\text{A-58})$$

$$c = \frac{1}{D_i} - \frac{\ln[b_0]}{b_1} \quad (\text{A-59})$$

Substituting Eq. A-59 into Eq. A-57, we have:

$$-\frac{q}{dq/dt} = \frac{\ln[b_0 + b_1 t]}{b_1} + \frac{1}{D_i} - \frac{\ln[b_0]}{b_1} \dots\dots\dots (A-60)$$

Separating and taking the reciprocal of both sides yields:

$$-\frac{dq}{q} = dt / \left[\frac{\ln[b_0 + b_1 t]}{b_1} + \frac{1}{D_i} - \frac{\ln[b_0]}{b_1} \right] \dots\dots\dots (A-61)$$

Next we take the integral of both sides:

$$-\int \frac{dq}{q} = \int dt / \left[\frac{\ln[b_0 + b_1 t]}{b_1} + \frac{1}{D_i} - \frac{\ln[b_0]}{b_1} \right] \dots\dots\dots (A-62)$$

The integration on the right-hand-side is taken using a symbolical computer language (Mathematica [2007]). Completing the integration, we have the following relation for the right-hand-side:

$$RHS = \exp \left[\ln[b_0] - \frac{b_1}{D_i} \right] E_i \left[\frac{b_1}{D_i} - \ln[b_0] + \ln[b_0 + b_1 t] \right] c \dots\dots\dots (A-63)$$

Where c is the integration constant, and E_i is the exponential integral function and defined as (Abramowitz and Stegun [1972]):

$$E_i[z] = -\int_{-z}^{\infty} \frac{\exp[-t]}{t} dt \dots\dots\dots (A-64)$$

Solving for c , we have ($t=0$, $q=q_i$):

$$c = q_i \exp \left[-\exp \left[\ln[b_0] - \frac{b_1}{D_i} \right] E_i \left[\frac{b_1}{D_i} \right] \right] \dots\dots\dots (A-65)$$

Substituting the value for c into the solution for the integration, we obtain the rate-decline relation for the rational b -parameter case:

$$q = q_i \frac{\exp \left[-\exp \left[\ln[b_0] - \frac{b_1}{D_i} \right] E_i \left[\frac{b_1}{D_i} - \ln[b_0] + \ln[b_0 + b_1 t] \right] \right]}{\exp \left[-\exp \left[\ln[b_0] - \frac{b_1}{D_i} \right] E_i \left[\frac{b_1}{D_i} \right] \right]} \dots\dots\dots (A-66)$$

Eq. A-66 is our final form for the rate-decline relation. We can also represent Eq. A-66 in a simpler form as:

$$q = A \exp[-B E_i[C + \ln[D + Et]]] \dots\dots\dots (A-67)$$

Where A , B , C , D , and E are constants to be determined.

Nomenclature: Derivation of the Rate Decline Relations

Variables:

- ${}_2F_1(x)$ = Hypergeometric series (Gauss' hypergeometric functions)
 b = Arps' decline exponent
 b_0 = model parameter
 b_1 = model parameter
 D = Decline parameter defined by Eq. 1
 D_i = Initial decline parameter ($t=0$)
 $E_i(x)$ = Exponential integral
 q = Gas production rate, MSCF/D
 q_i = Initial Gas production rate, MSCF/D or STB/D
 t = Time, days

Subscripts:

- i = Integral function or initial value

References: Derivation of the Rate-Decline Relations

- Arps J.J. 1945. Analysis of Decline Curves. *Trans. AIME*: **160**, 228-247.
- Johnson, R.H. and Bollens, A.L. 1927. The Loss Ratio Method of Extrapolating Oil Well Decline Curves. *Trans. AIME* **77**: 771.
- Fetkovich, M.J. 1980. Decline Curve Analysis Using Type Curves. *JPT*. **32** (6): 1065-1077.
- Mathematica*. 2007. <http://www.wolfram.com>
- Rushing, J.A., Perego, A.D., Sullivan, R.B., and Blasingame, T.A. 2007. Estimating Reserves in Tight Gas Sands at HP/HT Reservoir Conditions: Use and Misuse of an Arps Decline Curve Methodology. Paper SPE 109625 presented at the 2007 Annual SPE Technical Conference and Exhibition, Anaheim, CA., 11-14 November.

APPENDIX B

BEHAVIOR OF THE COMPUTED b -PARAMETER FOR THE FIELD CASE EXAMPLES

In this Appendix we present a series of schematic plots which illustrate the behavior of the computed b -parameter as well as the application of the proposed b -parameter models with respect to the production time (days) in three different plots (*i.e.*, the log-log, semilog and Cartesian plots).

• Field Example 1 — Tight Gas Well 1 (Bossier Field)

In **Figures B.1, B.2 and B.3** we illustrate the behavior of the computed b -parameter data and the performance of all the b -parameter models using the production time in a log-log, semilog, and Cartesian plots, respectively. In the first case of the log-log plot, we can conclude that the computed b -data exhibits a power-law behavior (see **Fig. B.1**). Moreover, by carefully analyzing the behavior of the applied b -models we can see that all of the newly proposed models yield very good matches across all flow regimes with the computed b -data for this case.

In the second plot (**Fig. B.2** — *i.e.*, the semilog plot) we observe a slightly decreasing trend of the computed b -data at the early times while at middle and late times the behavior seems to be stabilizing. In contrast, the log-log plot (**Fig. B.1**) shows a more robust comparison of the data and model trend using the power-law model for the b -parameter. Specifically, in **Fig. B.2** we note that the semilog model does not match the "early" portion of the data well — which suggests that this model may be inadequate for this case.

In the Cartesian plot (**Fig. B.3**) we plot the reciprocal of all the computed b -parameter data and the b -models. From **Fig B.3** we note that the "rational" model (*i.e.*, the straight-line trend) does not match the data functions well in form or trend, except at early times. This behavior suggests that the rational model may not be appropriate for this case, and we propose that the power-law function is the most representative model for this particular data case.

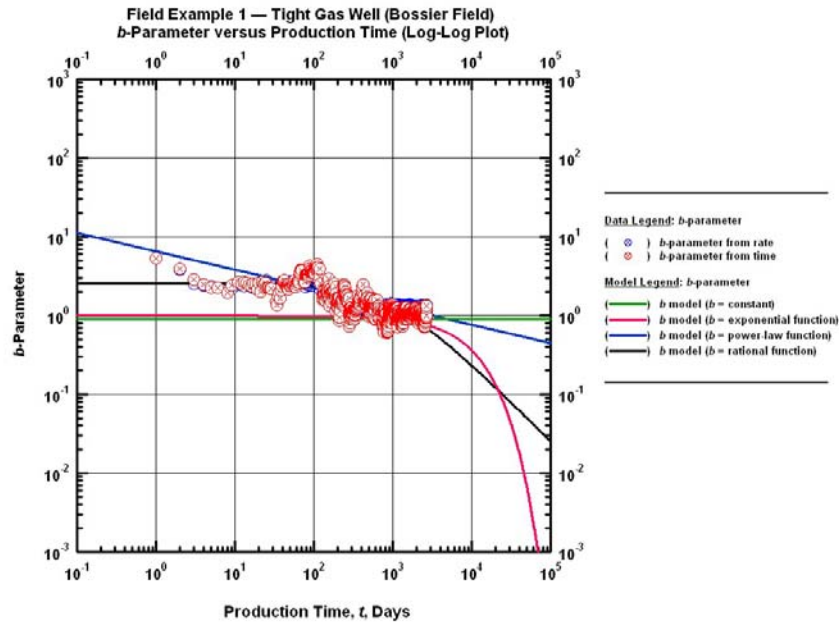


Figure B.1 — Field Example Case 1: Illustration of the behavior of the computed *b*-parameter with production time on a log-log plot [Tight Gas Well 1 — all models are shown on this plot].

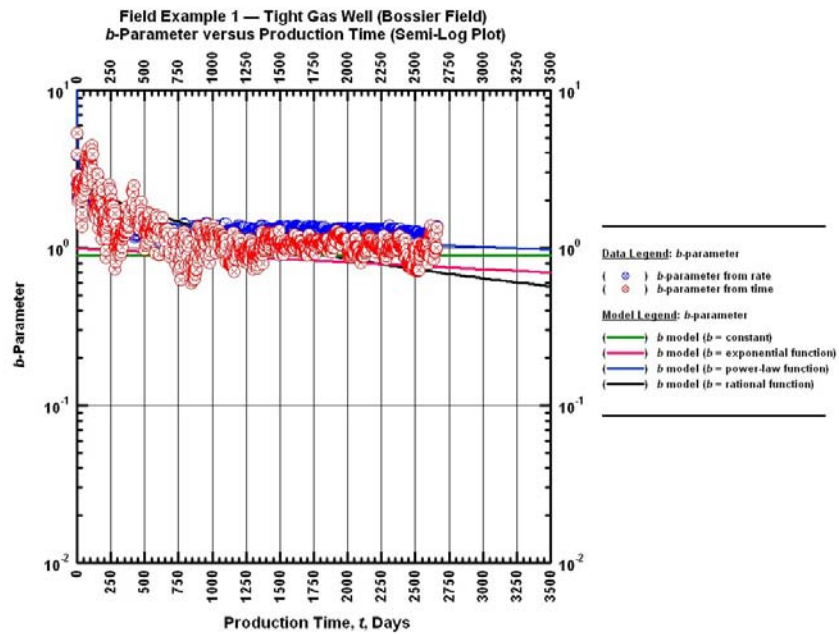


Figure B.2 — Field Example Case 1: Illustration of the behavior of the computed *b*-parameter with production time on a Semilog plot [Tight Gas Well 1 — all models are shown on this plot].

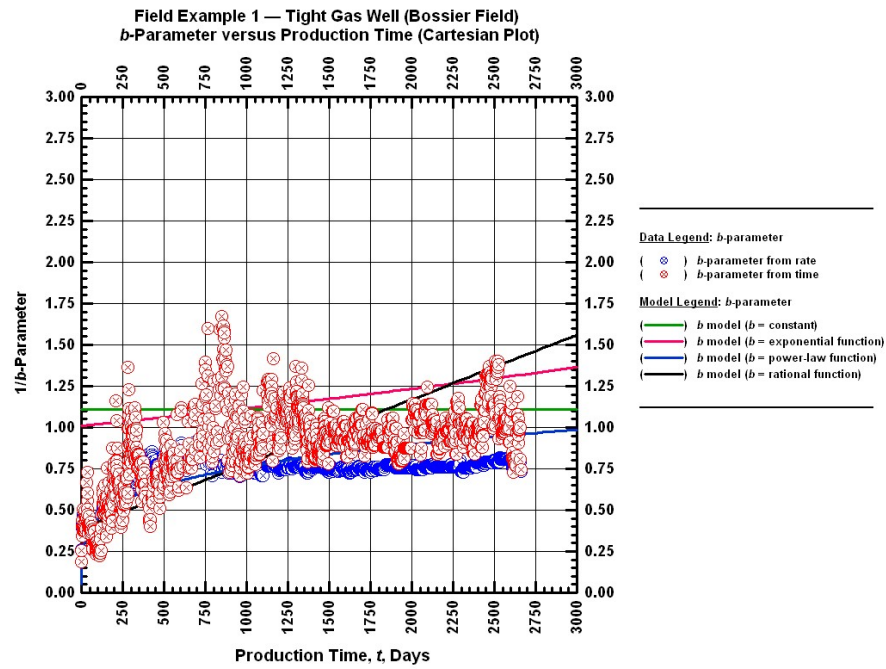


Figure B.3 — Field Example Case 1: Illustration of the behavior of the computed *b*-parameter with production time on a Cartesian plot [Tight Gas Well 1 — all models are shown on this plot].

• Field Example 2 — Shale Gas Well 1 (Barnett)

The computed b -data (and corresponding models) are plotted for the second field in **Figs. B.4, B.5 and B.6**. The lack of transient flow data at early times is due to the monthly reporting of these production data (these data were obtained from public sources). Obviously, a lack of data at early times means that we must focus on the late-time data (*i.e.*, boundary-dominated flow data). The computed b -data appears to follow a generally declining trend which cannot be seen clearly in the log-log plot (**Fig. B.4**). From **Fig. B.4** we note that the models do compare fairly well with the data functions; and we propose that any of our proposed b -models should be representative of the stabilized behavior (*i.e.*, boundary-dominated flow behavior).

The semilog plot (**Fig. B.5**) gives a somewhat better view of the models and the data. The "data noise" is again attributed to the monthly reporting of the data, but we do believe that the data functions in **Fig. B.5** (particularly the "rate" computed b -function data) exhibit a fairly distinct exponential decline behavior.

In the Cartesian plot (**Fig. B.6**) we note that the data noise is amplified by the Cartesian scale, and we cannot draw any specific conclusions about the behavior of the b -models using this plot. Nevertheless, it seems that a general inclining behavior is shown, as would be predicted by the "rational" b -function model.

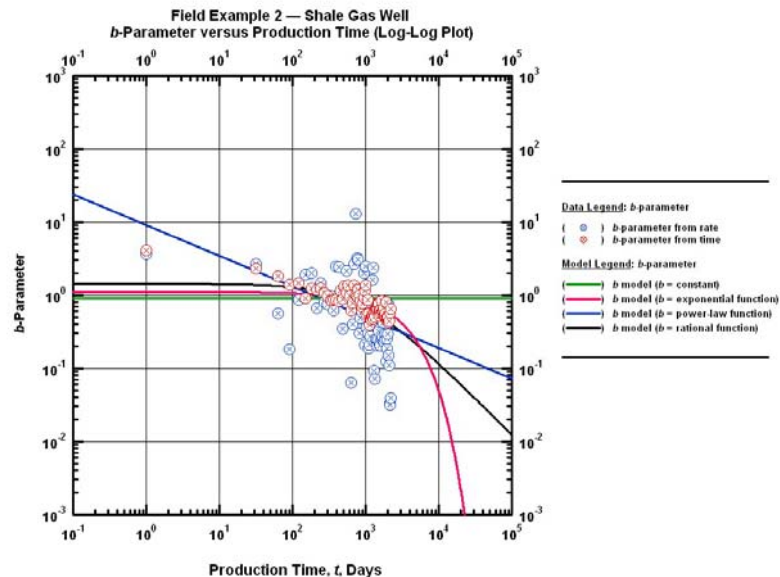


Figure B.4 — Field Example Case 2: Illustration of the behavior of the computed b -parameter with production time on a log-log plot [Shale Gas Well 1 — all models are shown on this plot].

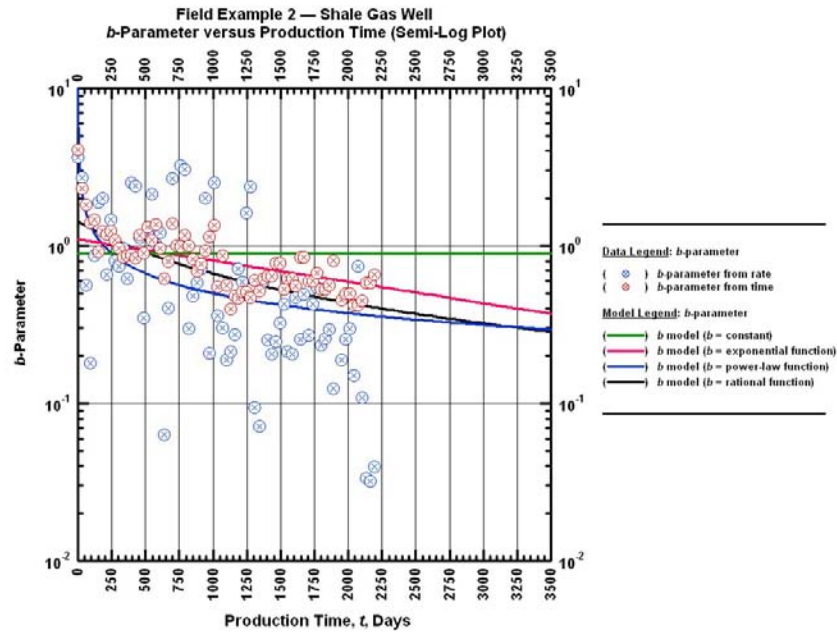


Figure B.5 — Field Example Case 2: Illustration of the behavior of the computed b -parameter with production time on a Semilog plot [Shale Gas Well 1 — all models are shown on this plot].

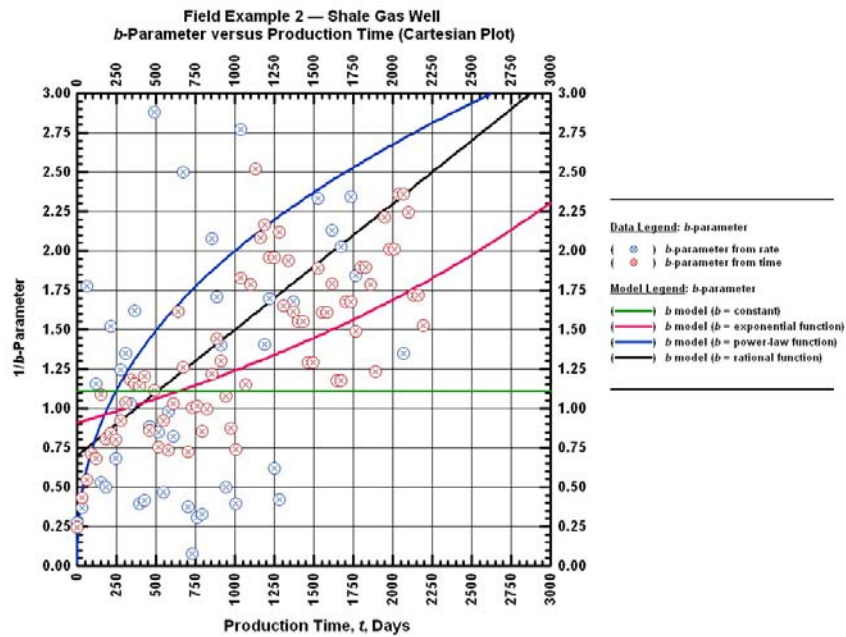


Figure B.6 — Field Example Case 2: Illustration of the behavior of the computed b -parameter with production time on a Cartesian plot [Shale Gas Well 1 — all models are shown on this plot].

• **Field Example 3 — Tight Gas Well 2 (Bossier Field)**

Our third field case refers to the Tight Gas Well 2 and the plots for this case are shown in **Figs. B.7, B.8 and B.9**. The behavior of the b -data and models is shown on the log-log plot (**Fig. B.7**) can best be described as a power-law function. Our work suggests that, for this case, the best fit can be obtained by applying the rational and power-law b -parameter models.

The semilog plot (**Fig. B.8**) shows that the computed data seem to be stabilized (*i.e.*, following a straight line trend) at middle and late times and all of our proposed models appear to capture this trend.

In the Cartesian plot (**Fig. B.9**) we find that the b -constant models fail to capture the trend of the data function. We are reluctant to suggest (or recommend) any of the models based on the behaviors exhibited in **Fig. B.9**.

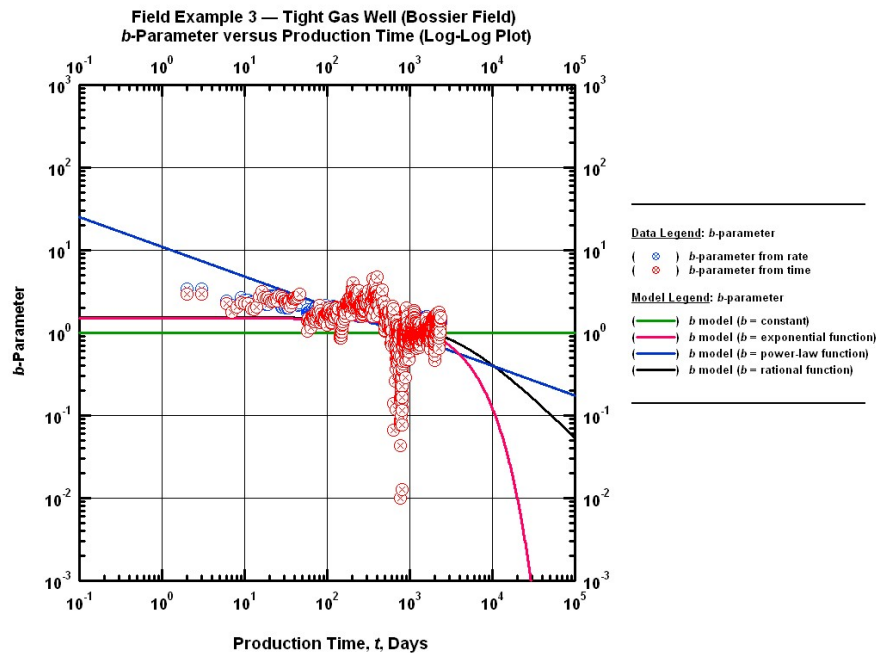


Figure B.7 — Field Example Case 3: Illustration of the behavior of the computed b -parameter with production time on a log-log plot [Tight Gas Well 2 — all models are shown on this plot].

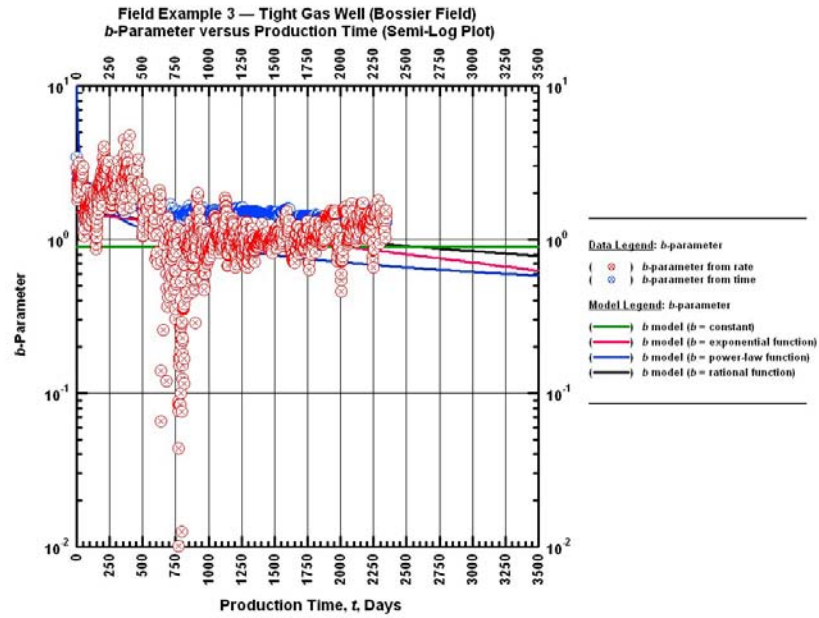


Figure B.8 — Field Example Case 3: Illustration of the behavior of the computed b -parameter with production time on a semilog plot [Tight Gas Well 2 — all models are shown on this plot].

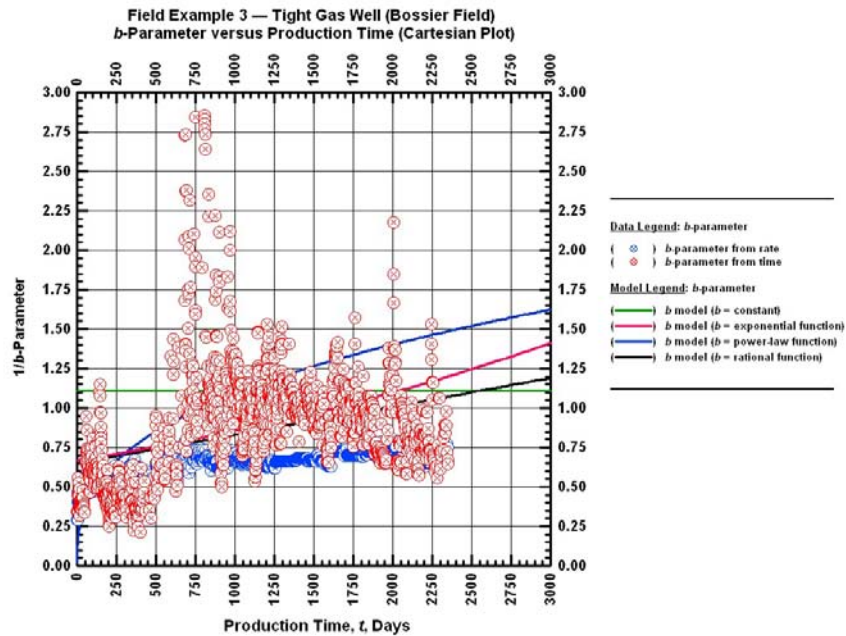


Figure B.9 — Field Example Case 3: Illustration of the behavior of the computed b -parameter with production time on a Cartesian plot [Tight Gas Well 2 — all models are shown on this plot].

• **Field Example 4 — Shale Gas Well 2 (Barnett)**

The computed b -data for the fourth field case are illustrated in **Figs. B.10, B.11 and B.12**. In this case, as with Field Example 2, we lack data at early times due to the monthly reporting of production data. As in Field Example 2, we cannot evaluate any early time flow effects.

As shown in **Fig. B.10**, the computed b -data appears to follow a stabilized (almost constant) trend, which declines slightly at late times which suggests boundary dominated flow. Due to the relatively small span of data, each of the models give "satisfactory" matches with the computed b -data. The b -constant model (forced to $b=1$) appears to be weakest of any of the proposed models.

On the semilog plot (**Fig. B.11**) we observe a fairly unique straight-line trend in the b -data function. This observation confirms our exponential (or semilog) model for the b -parameter, and at least for this case, this model seems to be the most representative when compared to the data functions. As comment, we note that the rational function model also matches the data well on **Fig. B.11**.

In **Fig. B.12** (*i.e.*, the Cartesian plot) the computed data is quite scattered and we cannot draw any specific conclusions about the behavior of the b -models, other than to suggest that the exponential model is likely the most representative model for this case.

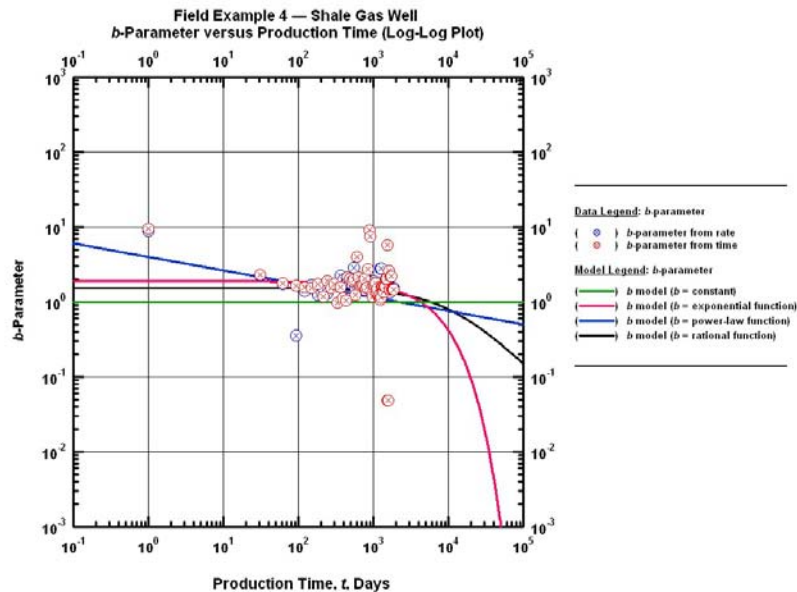


Figure B.10 — Field Example Case 4: Illustration of the behavior of the computed b -parameter with production time on a log-log plot [Shale Gas Well 2 — all models are shown on this plot].

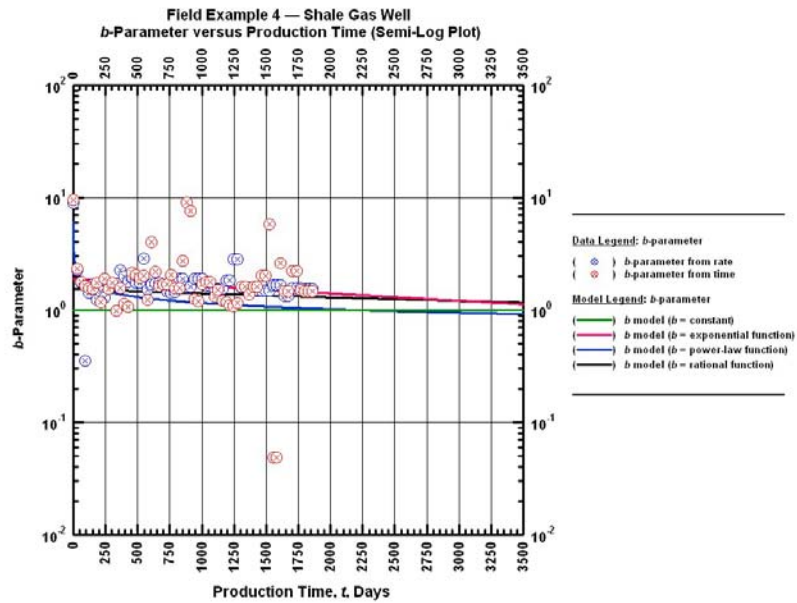


Figure B.11 — Field Example Case 4: Illustration of the behavior of the computed b -parameter with production time on a semilog plot [Shale Gas Well 2 — all models are shown on this plot].

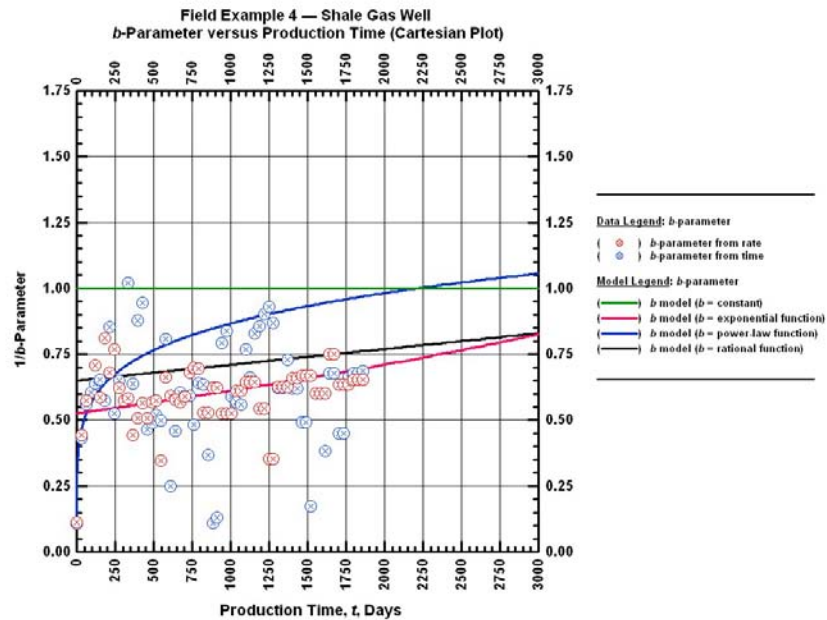


Figure B.12 — Field Example Case 4: Illustration of the behavior of the computed b -parameter with production time on a Cartesian plot [Shale Gas Well 2 — all models are shown on this plot].

APPENDIX C

SUMMARY OF THE b -PARAMETER MODEL RESULTS FOR THE FIELD CASE EXAMPLES

The values of the proposed b -models parameters (b , b_0 , b_1 , D_i) are presented in the following tables. The illustrated values provided us with the specific matches with the computed data as well as with the production forecasts for all the investigated cases above.

Table C.1 — Numerical illustration of the values of the b -models parameters — Numerical Simulation Case 1 — Horizontal gas well with multiple transverse fractures.

Model Parameters	b -constant model	b -exponential function model	b -power-law function model	b -rational function model
D_i	0.08	0.25	0.008	0.2
b	0.99	—	—	—
b_0	—	1.4	2.2	0.7
b_1	—	0.0008	0.17	0.001
q_i	38000	48000	380000	42000

Table C.2 — Numerical illustration of the values of the b -models parameters — Numerical Simulation Case 2 — Horizontal gas well.

Model Parameters	b -constant model	b -exponential function model	b -power-law function model	b -rational function model
D_i	0.0006	0.006	0.025	0.007
b	0.4	—	—	—
b_0	—	0.6	8.9	1.5
b_1	—	0.0006	0.46	0.0015
q_i	7200	6450	9200	7200

Table C.3 — Numerical illustration of the values of the b -models parameters — Numerical Simulation Case 3 — Vertical unfractured gas well — True Radial Flow.

Model Parameters	b -constant model	b -exponential function model	b -power-law function model	b -rational function model
D_i	0.0009	0.0012	0.006	0.001
b	0.4	—	—	—
b_0	—	0.45	18	2
b_1	—	0.00002	0.453	0.0001
q_i	9100	11600	17200	9450

Table C.4 — Numerical illustration of the values of the b -models parameters — Numerical Simulation Case 1 — Vertical fractured gas well (East TX).

Model Parameters	b -constant model	b -exponential function model	b -power-law function model	b -rational function model
D_i	0.003	7	0.027	123
b	0.4	—	—	—
b_0	—	2.3	4	0.32
b_1	—	0.00185	0.259	0.002
q_i	3850	75000	23500	90000

Table C.5 — Numerical illustration of the values of the b -models parameters — Field Case 1 — Tight gas well 1 (Bossier Field).

Model Parameters	b -constant model	b -exponential function model	b -power-law function model	b -rational function model
D_i	0.0013	0.002	0.532	0.08
b	0.9	—	—	—
b_0	—	0.99	6.55	0.39
b_1	—	0.0001	0.233	0.0039
q_i	1500	1820	12200	5150

Table C.6 — Numerical illustration of the values of the b -models parameters — Field Case 2 — Shale gas well 1 (Barnett).

Model Parameters	b -constant model	b -exponential function model	b -power-law function model	b -rational function model
D_i	0.001	0.01	0.015	0.03
b	0.9	—	—	—
b_0	—	1.9	4	0.7
b_1	—	0.00015	0.18	0.0008
q_i	1000	780	5000	1500

Table C.7 — Numerical illustration of the values of the b -model parameters — Field Case 3 — Tight gas well 2 (Bossier Field).

Model Parameters	b -constant model	b -exponential function model	b -power-law function model	b -rational function model
D_i	0.0012	0.0034	0.005	0.05
b	0.9	—	—	—
b_0	—	1.5	11	0.65
b_1	—	0.00025	0.56	0.00018
q_i	2400	4000	8000	17600

Table C.8 — Numerical illustration of the values of the b -model parameters — Field Case 4 — Shale gas well 2 (Barnett).

Model Parameters	b -constant model	b -exponential function model	b -power-law function model	b -rational function model
D_i	0.003	0.01	0.015	0.009
b	1.0	—	—	—
b_0	—	1.9	4	0.65
b_1	—	0.00015	0.18	0.00006
q_i	600	780	5000	820

VITA

Name: Anastasios S. Boulis

Permanent Address: Agiou Ioannou 47,
Agia Paraskevi
Athens, 15342
GREECE

E-mail Address: peteng13@hotmail.com

Education: Texas A&M University, College Station, Texas, USA
Master of Science Degree in Petroleum Engineering
August 2009

National Technical University of Athens, Greece
Bachelor of Engineering Degree in Mining & Drilling Engineering.
June 2006

Affiliations: Society of Petroleum Engineers
American Association of Drilling Engineers
Society of Mining Engineers